Autotrophic and heterotrophic food sources of copepods in the Scheldt Estuary as traced by stable C and N isotopes

Loreto De Brabandere

Vrije Universiteit Brussel

Faculteit Wetenschappen

Laboratorium voor Analytische en Milieuchemie

Autotrophic and heterotrophic food sources of copepods in the Scheldt Estuary as traced by stable N and C isotopes

Loreto De Brabandere

Proefschrift voorgedragen tot het behalen
van de graad van Doctor in de Wetenschappen

2005

Promotor: Prof. Dr. F. Dehairs
Co-promotor: Prof. Dr. M. Tackx

Contents

Een woordje van dank ...

...Aan iedereen die op zijn eigen manier bijgedragen heeft om de voorbije jaren aangenaam te maken: Frank die er nu meer dan ooit van overtuigd is dat mensen met Zuid-Amerikaans bloed omgekeerd redeneren, Natacha om de vele lachbuien tijdens de staalnames en de babbels bij de panini's in 't Complex, Marc voor de statistische back-up, Elvire om de lachkrampen, Willy, Jean-Pierre, Sandra om de hulp bij de vele kleine en grote probleempjes, en alle collega's voor de steentjes bijgedragen...

...Aan iedereen die, ondanks mijn waarschuwende blik van 'begin-er-niet-over-hé', het toch waagde om te vragen hoe 'het ermee ging', hoe het 'op het werk was', of 'het vooruit ging', 'vlot het een beetje',... allemaal manieren om het woord doctoraat niet in de mond te moeten nemen: voilà, hier ligt het voor uw neus!

...Aan al diegene die vinden dat copepoden op raketten lijken, die denken dat een isotoop eetbaar is, dat een estuarium aquarium is maar dan verkeerd gespeld, dat nitrificatie per definitie tot ontploffing leidt...voor u is dit werk verplichte lectuur!

...En slot aan al diegenen die er waren als het efkes niet meer ging of gewoon voor de vele hilarische momenten samen: ma, pa, Karin, Eva, Izaak, Jouke, Manu, Eva, Koen, Diane, Bruno: een dikke knuffel voor jullie allemaal!

SUMMARY

Estuaries draining densely populated watersheds experience significant anthropogenic pressure and sustain large autotrophic and heterotrophic production owing to an increased input of nutrients and organic matter. Polluted estuaries are often net heterotrophic systems. Our objective was to study the relative contribution of autotrophic and heterotrophic food webs in sustaining the high productivity of pelagic estuarine ecosystems along the estuarine gradient of the Scheldt estuary. We concentrated on the nature of the primary food sources of calanoid and cyclopoid copepods and on the organic substrates supporting heterotrophic production.

An extensive study of the monthly variation of $\delta^{15}N$ and $\delta^{13}C$ of suspended matter and copepods over a period of two year showed that variations in the relative contribution and isotopic signature of phytoplankton were probably the main factors controlling the seasonal and spatial variation in the $\delta^{15}N$ and $\delta^{13}C$ signature of suspended organic matter. Comparisons between the seasonal $\delta^{15}N$ and $\delta^{13}C$ patterns of suspended matter and copepods showed that the nature of the primary food sources differed between calanoid and cyclopoid copepods and between freshwater and oligohaline-mesohaline reaches. In the oligohaline and mesohaline reaches, calanoid and cyclopoid copepods were mainly supported by autotrophic and heterotrophic biomass, respectively, whereby the latter probably thrived on dissolved organic matter derived from local phytoplankton. In the freshwater section, cyclopoid copepods dominated the copepod community. The important discrepancy between $\delta^{15}N$ of cyclopoid copepods and the modeled $\delta^{15}N$ of phytoplankton in the freshwater reaches eliminated local phytoplankton or heterotrophs thriving on dissolved organic matter derived from local phytoplankton as a possible food source. This situation was explained via a scenario where bacteria thriving on phytoplankton detritus imported from the tributaries formed the main food source of local cyclopoid copepods. Our observations highlighted a very different ecosystem functioning for the freshwater part compared to the oligo- and mesohaline waters of the estuary proper.

In this work, we constructed an isotopic baseline for future studies on the diet and trophic level of planktivorous fish by calculating the annual mean $\delta^{15}N$ and $\delta^{13}C$ of copepods. However, the highly variable nature of the annual mean $\delta^{15}N$ hampers the use of stable N isotopes as a tool to study fish migration between freshwater and marine reaches. Nevertheless, mesohaline stations showed sufficiently distinct $\delta^{15}N$ signatures to allow tracing of migration between this habitat and the freshwater reaches.

GENERAL INTRODUCTION

Estuaries draining highly urbanized watersheds typically experience significant anthropogenic pressure owing to input of sewage-derived labile organic matter rendering the system net heterotrophic because of enhanced bacterial production (Hopkinson and Vallino, 1995; Abril et al., 2002). On the other hand, increased inputs of nutrients from agricultural, industrial or domestic origin or via the bacterial mineralization of organic matter increases the phytoplankton production, so that polluted estuaries also support a high autotrophic biomass (Hopkinson and Vallino, 1995). The riverine productivity model of Thorp and Delong (2002) states that, despite the net heterotrophy of a system, the primary energy source supporting higher trophic levels is autochthonous primary production entering food webs via algal-grazer and decomposer pathways. Decomposers would mainly process autochthonous organic matter with allochthonous organic matter being relatively unimportant due to its recalcitrant nature. However, if highly degradable sewage dominates allochthonous organic matter, allochthonous organic matter sources may be an important substrate for heterotrophic bacteria (Abril et al., 2002). Moreover, if net primary production (NPP) is low compared to gross primary production (GPP) due to a high respiration rate of phytoplankton, NPP may not be sufficient to sustain the large heterotrophic respiration generally observed in these heterotrophic systems. Therefore, allochthonous sources should contribute significantly to carbon metabolism of the system (Howarth et al., 1996). Hence, for polluted estuaries, the primary energy source may not necessarily be autochthonous organic matter.

The highly eutrophic Scheldt estuary is an ideal system to understand the relative importance of primary energy sources in fuelling the secondary production for polluted environments. Here, the NPP/GPP ratio is low because the high turbidity and the fact that the mixing depth exceeds the euphotic depth result in considerable losses of phytoplankton due to respiration (Soetaert et al., 1994; Soetaert and Herman, 1995b). Sewage input dominates the total carbon input to the estuary (68% compared to 12% phytoplankton and 20% soil organic matter) (Abril et al., 2002), suggesting a major importance for the heterotrophic food web in transferring energy to the higher trophic levels.

Current knowledge of the trophic structure of the Scheldt estuary

It is generally accepted that the Scheldt estuary supports two distinct food chains: a detritus based, heterotrophic food chain in the freshwater reaches (Muylaert et al. 2000b), and a photo-autotrophic one in the lower marine zone (Hummel et al., 1988; Hamerlynck et al., 1993; Soetaert and Herman, 1994). Both food chains are separated from each other by a stretch of 20 km in the upper marine zone where phytoplankton biomass is high since no zooplankton group is present in sufficiently high numbers to control phytoplankton growth (Hamerlynck et al., 1993).

In the freshwater section, the top-predators are cyclopoid copepods from spring till autumn and carnivorous ciliates during winter, when cyclopoid density is low (Muylaert et al., 2000b). Here, the cyclopoid *Acanthocyclops robustus* is the dominant species (Muylaert et al., 2000b; Tackx et al., 2004). Being top-predators, cyclopoid copepods prey on rotifers, ciliates and heterotrophic nanoflagellates. Rotifers, which are present from spring to autumn, are important predators of heterotrophic nanoflagellates, ciliates (Muylaert et al, 2000b) and phytoplankton (Muylaert, pers. comm.). Both ciliates and heterotrophic nanoflagellates are found to feed on bacteria. The amoeboid protozoan *Asterocaelum* reaches its peak abundance in summer and feeds on diatoms (genus *Cyclotella*). Since its biomass nearly equals the one of its prey at maximum population densities, it is an important potential grazer of centric diatoms (Muylaert et al., 2000b; 2001).

Before the early nineties, oxygen concentrations in the oligohaline zone were too low to allow a zooplankton community to develop (Hummel et al., 1988; Hamerlynck et al., 1993; Soetaert and Van Rijswijk, 1993; Tackx et al., *in press*). The food chain was probably very short, since rotifers, ciliates, protozoa, nematodes and oligochaetes were the only groups present in high quantities. During the nineties, the continuing improvement of the O_2 conditions following wastewater treatment resulted in an increased abundance of the calanoid copepod *Eurytemora affinis* (Tackx et al., 2004, Appeltans et al., 2003) which is replaced by the calanoid *Acartia tonsa* during summer (Soetaert and Van Rijswijk, 1993; Muylaert et al., 2000b; Tackx et al., 2004). Both *A. tonsa* and *E. affinis* are selective feeders on live phytoplankton (Tackx et al., 1995; 2003). *E. affinis* is able to feed very selectively on phytoplankton, since it is able to obtain 80% of its maximal gut pigment content when phytoplankton concentrations contribute only 5% of the total particulate organic carbon pool (Tackx et al., 2003). *A. tonsa* feeds also selectively on microzooplankton like tintinnids (ciliates) (Tackx et al., 1995), which is the only group of heterotrophic protists present in this zone although in relatively low numbers (Muylaert et al., 2000b).

Potential effects of improving water quality following wastewater treatment

Since sewage is the dominant source of organic carbon to the estuary, enhanced wastewater treatment may reduce the amount of highly degradable organic matter available to heterotrophic bacteria (Abril et al., 2002). This could subsequently lead to a decrease in the relative importance of heterotrophic food webs in the transfer of energy to higher trophic levels. Tackx et al. (2004) already mentioned that in the future, the improved water conditions will probably change the trophic structure of the ecosystem, by affecting the feeding conditions for zooplankton because of an expected increase in the phytoplankton/detritus ratio and an increase of the competition between the present eutrofication tolerant zooplankton species and some more sensitive ones.

In order to assess the relative importance of heterotrophic and autotrophic food webs in the Scheldt estuary, more information is needed about the relative importance of allochthonous and autochthonous sources in sustaining the primary and secondary production. To date, little research has been done on the origin of organic matter fuelling primary and secondary production in the Scheldt estuary. Boschker et al. (2005) showed that heterotrophic bacteria relied mainly on phytoplankton-derived dissolved organic matter in the lower reaches of the estuary. In the upper oligohaline reaches, however, bacterial growth was mainly supported by allochthonous carbon sources. To our knowledge, information on the organic matter sources sustaining the high production in the freshwater reaches is lacking.

Objectives

The Scheldt estuary offers an ideal opportunity to investigate the effect of wastewater treatment on the relative importance of heterotrophic and autotrophic pathways in the transfer of energy. Our objective was to investigate the relative importance of heterotrophic and autotrophic primary food sources sustaining the secondary production in the estuary for a situation where sewage-derived labile organic matter still contributes significantly to the pollution of the system. Our results can then serve as a reference situation for future studies conducted in less polluted conditions. In particular, we concentrated on the nature of the primary food sources (bacteria and phytoplankton) of copepods since copepods form an important intermediate trophic level for many fish and macrocrustaceans (e.g. Fujiwara and Highsmith, 1997; Coull, 1999; Hughes et al., 2000; Maes et al., 2003). We conducted this research at different

salinity conditions along the estuarine gradient in order to investigate the longitudinal variability in the relative importance of autotrophic and heterotrophic primary sources.

Chapter outline

The Scheldt estuary has been intensively studied for more than 30 years now. One of the most prominent features of the Scheldt estuary is the high anthropogenic disturbance. The continuous efforts to reduce the human pressure on the system have resulted in a gradual improvement of the water quality, a process that has been well-documented in the literature of the past 30 years. In Chapter 1, we provide an extensive overview of the current knowledge about the hydrological characteristics and the biogeochemical functioning of the Scheldt estuary.

In this study, we used the stable isotope technique to investigate nitrogen cycling and the transfer of carbon and nitrogen to higher trophic levels in the Scheldt system. In Chapter 2, we give a detailed overview of the stable isotope technique and its application to ecological studies. In Chapter 3, we present an overview of the sampling strategy and sample treatments, together with the analytical details of the measurement of stable isotopes.

In Chapter 4 we investigate the spatial variation in the importance of autotrophic and heterotrophic primary food sources of calanoid and cyclopoid copepods by looking at the similarities between the seasonal pattern of their C and N isotopic composition and the one of the suspended matter pool.

In Chapter 5 we concentrate on the $\delta^{15}N$-signature of phytoplankton and heterotrophic bacteria at a freshwater station. We report on the seasonal variation of the $\delta^{15}N$ of NH_4^+ and calculate the fractionation factor during NH_4^+ consumption. We reconstruct the $\delta^{15}N$ signature of phytoplankton and investigate the relative importance of different N-sources of heterotrophic microorganisms in setting the $\delta^{15}N$ signature of heterotrophs decomposing organic matter.

Finally, in Chapter 6, we look at the factor controlling the spatial variation of the $\delta^{13}C$ and $\delta^{15}N$ signatures of suspended matter along the entire estuarine gradient, we calculate an isotope baseline for future research on the diet of planktivorous fish and discuss the use of stable isotopes as a tool to investigate fish migration in the Scheldt estuary.

Study area: The Scheldt Estuary

Chapter 1

1.1. Geographical description

The Scheldt River has a drainage basin that covers an area of 21,863 km² situated in the north-west of France, the west of Belgium and the south-west of Netherlands (Fig. 1.1). Its catchment area is inhabited by more than 10 million people, making it subject to high anthropogenic stress (Maeckelberghe, 1997). The Scheldt River flows into the North Sea after a course of 320 km, of which half is subject to tides (Claessens, 1988). The tidal section of the Scheldt River (160 km) is called the Scheldt estuary.

Based on geographical characteristics and salinity, the Scheldt estuary can be divided in two main zones: the Zeeschelde, on Belgian territory and the Westerschelde, on Dutch territory (Table 1.1). The former corresponds roughly with the freshwater (km 160 to km 90) and oligohaline zone (< ± 10 psu, km 90 to 57) and the latter with the mesohaline (± 10 to ± 20 psu, km 57 to 40) and marine zone (> 20 psu, km 40 to 0). On the basis of geometrical and dynamical criteria, the Scheldt estuary is frequently divided in three main zones. Zone 1 extends from km 0 (at the mouth of the estuary) to km 40 and is characterized by a complicated system of ebb and flood channels where tidal motion is large and mixing important. Zone 2 (km 40 to km 90) has a single, well-defined channel in which mixing is partial, with longitudinal and vertical salinity gradients. Zone 3 (km 150 to km 90) is the fluvial part of the Scheldt and has a network of tributaries (Regnier et al., 1998).

Figure 1.1: Map of the Scheldt estuary and its tributaries Upper Scheldt, Dender, Durme and Rupel.

Table 1.1: Geographical classification of the Scheldt estuary

	Distance (km)	Salinity (psu)	Zone	Country
Marine	0 - 40	±33 to ±20	1	The Netherlands
Mesohaline	40 - 57	±20 to ±10	2	The Netherlands
Oligohaline	57 - 90	±10 to ±0	2	Belgium
Lower freshwater	90 - 140	0	3	Belgium
Upper freshwater	140-155	0	3	Belgium
Tributaries				
Upper Scheldt	160	0	3	Belgium
Dender	128	0	3	Belgium
Durme	101	0	3	Belgium
Rupel	92	0	3	Belgium

Most studies mentioned in the following sections apply only to the 'real estuary', i.e. the section of the Scheldt estuary where freshwater mixes with seawater (< km 90), unless mentioned otherwise. Reported data in these papers roughly cover the period from 1973 till 2004.

1.2. Physico-chemical characteristics of the estuary

1.2.1. Oxygen

The Scheldt estuary has characteristic low O_2 concentrations with the most depleted values found near the mouth of the Rupel (km 92); (Fig. 1.2); (Van Damme et al., 1999). The O_2 concentration increases again in the mixing zone of freshwater and seawater downstream from the Dutch-Belgian border (Maeckelberghe, 1997, Van Damme et al., 1999). The low O_2 concentrations are the result of O_2 consuming biological processes of which heterotrophic respiration and nitrification by bacteria are the main actors (Heip and Herman, 1995; Goosen et al., 1997). Comparison of the activity of both heterotrophic and nitrifying bacteria showed that in the freshwater-oligohaline section downstream of Rupelmonde, the O_2 consumption by degradation of organic matter is much lower than O_2 uptake by nitrification making the nitrification process the main O_2 consumer (Regnier et al., 1997). From this it is clear that the low O_2 values are man-induced, since the high amounts of organic material and NH_4^+

discharged with wastewater support high activities of heterotrophic and nitrifying bacteria.

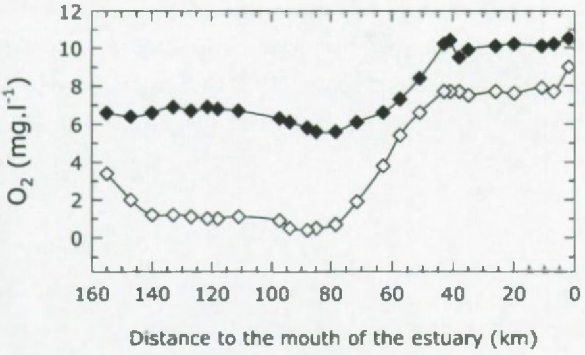

Figure 1.2: Spatial variation of mean O_2 concentrations during February (black) and July (white) in the Scheldt estuary for the period of study (1999-2003).

1.2.2. Tide

The Scheldt is a macro-tidal estuary with a tidal amplitude of 4 m at the mouth of the estuary. Due to the funnel shape of the estuary, the tidal amplitude increases to a maximum of 5.3 m at the inland station of Schelle (km 90). The tide is artificially stopped by a set of weirs near Gent, where the tidal amplitude still reaches 2 m (Claessens, 1988).

The modeled average discharge at the mouth of the estuary is approximately 50×10^3 m^3.s^{-1} for a mean freshwater discharge of 120×10^3 m^3.s^{-1} (Wollast, 1973). For an average freshwater discharge of 100 m^3.s^{-1}, Regnier et al. (1998) calculated discharge values at the mouth of the estuary ranging between 71.4×10^3 and 107.3×10^3 m^3.s^{-1} during flood and ranging between 56.7×10^3 and 83.6×10^3 m^3.s^{-1} during ebb. Due to the magnitude of the seawater mass entering the estuary and river bed, the mixing zone of fresh and salt waters extends over a distance of 70-100 km (Regnier et al., 1998), with the steepest salinity gradient found roughly between km 80 and 50 (Van Damme et al., 1999).

1.2.3. Discharge

Freshwater discharge is measured at Schelle (km 90), at the confluence of the Scheldt River and its last main tributary, the Rupel River. The mean freshwater discharge during the period of study (1999-2003) was 167 m^3.s^{-1}, with a maximum of

591 $m^3.s^{-1}$ and a minimum of 46 $m^3.s^{-1}$ (Taverniers, 1999; 2000; 2001; 2002; 2003). However, in the Scheldt estuary, river discharge (advective flow) and net flow towards the sea (residual flow) differ markedly because the input of seawater during flood creates an important dispersive flow component (Wollast, 1973; Regnier et al., 1997; 1998). The effect of inland seawater transport on the deviation of the residual flow from the discharge is more pronounced during low discharge periods. The variability and the departures of the residual flow from the discharge increase seaward due to increasing importance of dispersion and are noticeable even for high freshwater discharges (Wollast, 1973; Regnier et al., 1998).

1.2.4. Residence time

The residence time is defined as the average time needed for a parcel to leave the estuary (Wollast, 1973; Soetaert and Herman, 1995a). Wollast (1973), Soetaert and Herman (1995a) and Regnier et al. (1997) calculated the residence time of water in the Scheldt estuary at the upper limit of the mixing zone (± km 90). Wollast (1973) calculated a residence time of 74 days for a mean freshwater discharge of 80 $m^3.s^{-1}$, while the one calculated by Soetaert and Herman (1995a) varied from 50 to 70 days for a freshwater flow between ± 200 and ± 50 $m^3.s^{-1}$, respectively. The residence time calculated by Regnier et al. (1997) ranged from 2 to 3 months for a range of freshwater discharge of 100 to 40 $m^3.s^{-1}$. Summer residence time values are generally longer than winter values, since the characteristic winter river discharge is higher (Soetaert and Herman, 1995a; Regnier et al. 1998). Differences in summer and winter retention times are especially apparent in the most upstream compartments as these are mainly dominated by advective processes (Soetaert and Herman, 1995a).

1.2.5. Suspended matter dynamics

The overall suspended matter load in the Scheldt estuary is high with maximum concentrations of a few grams per liter near the bottom and up to 200 mg per liter at the surface (Chen, 2003); (Fig. 1.3). There are two zones along the estuarine transect where hydrodynamic forces and physical processes cause an increase in turbidity. The first maximum turbidity zone (MTZ) is situated at the freshwater-seawater interface and is caused by the combination of a flocculation process (small particles coagulate into larger ones) due to increasing salinities, an increased resuspension of bottom sediments due to high tidal energy and hydrodynamic trapping. Hydrodynamic trapping of particles is caused by an increased residence time due to the annihilation of the

upstream bottom current as a result of converging saline upstream directed bottom currents and downstream directed riverine currents (Wollast, 1973; Baeyens et al., 1998; Chen, 2003). The second MTZ is situated in the freshwater section of the estuary. Here the turbidity maximum originates from the tidal asymmetry, i.e. the dominance of flood tidal currents above ebb currents. The resulting enhanced resuspension and transport (tidal pumping) causes the accumulation of particulate matter (Muylaert et al., 2000a; Chen, 2003).

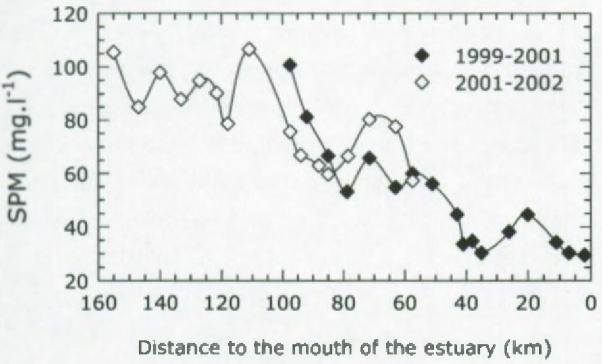

Figure 1.3: Spatial variation of mean SPM concentrations in the upper (white) and lower (black) half of the Scheldt estuary for the period 1999-2002.

The material processed by bacteria in the mixing zone is from marine and riverine origin. The fraction of marine suspended matter in the mixing zone is always higher than the seawater fraction so that their mixing curves have different shapes (Verlaan et al., 1998). This is probably due to the higher concentration of marine suspended matter compared to fluvial matter, the latter being strongly diluted by the incoming seawater. The fraction of marine suspended matter at a given location in the estuary varies strongly over the year as a result of varying discharge, i.e. a downward shift of the turbidity maximum is observed when discharge is high. For instance, at the Dutch-Belgian border, the marine fraction is 65% for a discharge of ± 100 $m^3.s^{-1}$ and decreases linearly to a fraction of 30% for a discharge of ± 200 $m^3.s^{-1}$ after which the decreasing pattern is less pronounced (Verlaan et al., 1998). Other factors influencing the percentage of marine suspended matter in the mixing zone are the variable input of riverine material to the mixing zone and the presence of resuspended matter. The input of riverine material increases when discharge is higher and depositions in the zone between Antwerp and Rupelmonde are resuspended and transported seaward with the residual current to the area downstream of Antwerp (Verlaan, 2000). However, the marine organic matter fraction at a given location is lower than the total

marine suspended matter fraction, since the organic fraction in freshwater material is higher than the one in marine material (Verlaan et al., 1998).

High discharge can also lead to the flushing out of zooplankton and in extreme cases also phytoplankton (Muylaert et al., 2001).

1.2.6. Biogeochemical processes

The nature and extent of the biogeochemical transformations which occur during transport from land to sea is governed by the residence time of the water within the estuary (Regnier et al., 1997; 1998; Regnier and Steefel, 1999). As such, the importance of the biogeochemical processes increases markedly in the mixing zone of freshwater and seawater. Here, the residence time of the freshwater masses increases quickly due to the dilution in a large body of sea water (Wollast, 1973; 1982; Herman and Heip, 1999). Moreover, the increased turbidity in this zone also enhances biogeochemical processes by the presence of large amount of suspended solids on which the bacteria can attach (Goosen, 1995; 1999; Herman and Heip, 1999).

1.2.7. Solute concentration

River discharge affects the nature of the nutrients imported to the estuary. Increasing discharge results in higher NO_3^- and lower NH_4^+ fluxes to the estuary, since NH_4^+ is mainly delivered by point sources such as inputs from domestic, industrial and agricultural activities, which are diluted as the river discharge increases (Herman and Heip, 1999; Regnier and Steefel, 1999, Vanderborght et al., 2002). On the other hand, nitrate inputs are primarily from diffuse origin due to agricultural land wash-out (fertilizers) (Wollast, 1982; Vanderborght et al., 2002) so that the flux increases during periods of higher rainfall. Due to seasonality of the discharge, NO_3^- is generally higher and NH_4^+ is generally lower during winter (Regnier and Steefel, 1999).

The tidally averaged horizontal and vertical salinity distribution is strongly dependent on the freshwater flow, the maximum gradient being shifted seaward as the river flow increases (Wollast, 1973; Claessens, 1988; Regnier et al., 1997; 1998). With increasing river discharge, the water column in the mixing zone changes from mostly well mixed to slightly partially mixed while stratification effects remain small (Wollast, 1973; Verlaan, 2000).

1.3. Important processes in the water column and the sediments

1.3.1. Heterotrophic - autotrophic balance

Most polluted north-west European estuaries are known as net heterotrophic ecosystems (Heip et al., 1995), which is also the case for the Scheldt estuary (Borges and Frankignoulle, 2002; Frankignoulle et al., 1996; 1998; Goosen et al., 1995; 1997; 1999; Hellings et al., 2001; Soetaert and Herman, 1995b). The extremely high anthropogenic organic load to the estuary leads to bacterial production rates that are among the highest reported in literature (Soetaert and Herman, 1995b; Goosen et al., 1995; 1999). Indeed, the total organic carbon input (dissolved and particulate) from the Scheldt tributaries is calculated to be around 83.10^3 $t.y^{-1}$ for an average total tributary discharge of 70 $m^3.s^{-1}$ (Abril et al., 2000). The relative contribution of particulate organic carbon (POC) and dissolved organic carbon (DOC) to the total carbon input from the boundaries is roughly equal (Regnier and Steefel, 1999; Muylaert et al., submitt.), but a large part of this DOC is refractory to bacterial degradation (e.g. 90% of the DOC for a summer condition) (Vanderborght et al., 2002; Muylaert et al., submitt.). The amount of carbon input by phytoplankton primary production is only a fraction of the amount imported from the Scheldt River at the inland border of the mixing zone and from waste discharges. Bacteria process more carbon than is produced by phytoplankton production (Soetaert and Herman, 1995b (modeled data); Goosen et al., 1997; Hellings et al., 2001). Goosen et al. (1999) report that the heterotrophic microbial biomass does not exceed the phytoplankton biomass (maximum of 35% in the turbidity zone), while the bacterial production is much larger than the primary production (Goosen et al., 1997; 1999). There is a gradient in the degree of heterotrophy, with the lowest degree found near the sea and the highest in the high turbidity region (Soetaert and Herman, 1995b; Goosen et al., 1995; 1997; 1999). This is probably due to the high amount of particles to which the micro-organisms can attach (Goosen et al., 1995; 1999) and the injection of fresh organic material resulting from increased mortality of phytoplankton due to salinity stress (Herman and Heip, 1999). In the marine part of the estuary, highly degradable marine matter is imported resulting in increased mineralization rates (Soetaert and Herman, 1995b).

As a result of the intense bacterial respiration and the long residence time the Scheldt estuary functions as a source of CO_2 to the atmosphere (Frankignoulle et al., 1996; 1998; Borges and Frankignoulle, 2002). In the freshwater zone (between km 96 and km 155) a maximum pCO_2 value of 12,900 μatm (atmospheric pCO_2 = 366 μatm)

was found during late autumn, mainly as a result of the mineralization of organic waste advected by the Rupel (Hellings et al., 2001). Frankignoulle et al. (1996) calculated that a partial pressure excess of 5,700 μatm in the water column, integrated over the surface of the estuary between km 97 and km 0, resulted in an atmospheric flux of 600 $t.d^{-1}$. These values are high compared to other European estuaries (Frankignoulle et al., 1996; 1998). Upstream of km 96 and downstream of km 78, Hellings et al. (2001) calculated a net conversion of organic carbon to dissolved inorganic carbon (DIC) (i.e. the difference between CO_2 production and consumption by uptake) as a result of the predominance of heterotrophy over autotrophy. In the upper part of the estuary (salinity <10 psu), the amount of CO_2 lost to the atmosphere exceeds the input by bacterial respiration which results in a net loss of inorganic C (Frankignoulle et al., 1998). The high efflux of CO_2 is sustained by the steady decrease of the pH due to the predominance of pH-decreasing processes such as nitrification and bacterial respiration, over pH-increasing processes such as CO_2 efflux to the atmosphere (Frankignoulle et al., 1996; 1998; Regnier et al., 1997). Also Hellings et al. (2001) observed a net consumption of DIC in the 78 to 96 km stretch, where the Rupel joins the Scheldt, which was probably due to dilution with DIC-depleted Rupel water and precipitation of $CaCO_3$.

1.3.2. N budgets

The Scheldt estuary receives high amounts of organic material and nutrients from the tributaries. The two main inorganic nitrogen species imported are nitrate and ammonium, nitrite loadings being at least one order of magnitude smaller (Regnier and Steefel, 1999; Abril and Frankignoulle, 2001); (Fig. 1.4). The main sources of nitrate are leaching of soils and surface run-off while ammonium has an anthropogenic source and its presence is more directly related to domestic wastewater discharge (Wollast, 1982).

If the fluxes of total nitrogen are calculated, the estuary acts as a sink for nitrogen (Table 1.2). Indeed, for the period 1973 to 1983 Billen et al. (1985) calculated the annual import of N (organic + inorganic) to the estuary to be 61.10^3 $t.y^{-1}$ for an average annual discharge of 115 $m^3.s^{-1}$ while the export to the sea was only 27.10^3 $t.y^{-1}$, resulting in a net removal of N of 34.10^3 $t.y^{-1}$. For a period between 1980 and 1986, Soetaert and Herman (1995c) calculated that the total nitrogen import into the estuary was around 71.10^3 $t.y^{-1}$ and net export to the sea amounted to about 56.10^3 $t.y^{-1}$ for an average discharge of 105 $m^3.s^{-1}$. For the period 1990-1999, total nitrogen import decreased to 31.10^3 $t.y^{-1}$, while the export decreased to 25.10^3 $t.y^{-1}$ (Brion,

ECSA 2002). Between 1973 and 1999, the amount of N removed during transport to the sea had thus decreased from 34.10^3 to 15 - 16.10^3 t.y^{-1}.

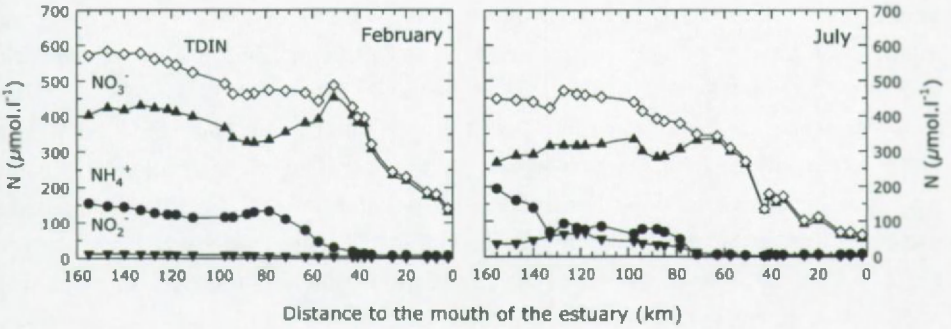

Figure 1.4: Spatial distribution of mean total inorganic nitrogen (TDIN), NO_3^-, NH_4^+ and NO_2^- during February and July in the Scheldt estuary during the period of study (1999-2003).

Table 1.2: N (organic + inorganic) fluxes as calculated from mass balances for the period 1973-1999

	N import (10^3 t.y^{-1})	N export (10^3 t.y^{-1})	N removal (10^3 t.y^{-1})	Period
Billen et al., (1985)	61	27	34	1973-1983
Soetaert and Herman (1995c)	71	56	15	1980-1986
Brion (ECSA, 2002)	31	25	16	1990-1999

Most of the N permanently removed from the water column can be attributed to denitrification converting nitrate to N_2 or N_2O which escapes to the atmosphere. It occurs, however, only in sections of estuaries that exhibit O_2 depletion and in sediments (Wollast, 1982; Billen et al., 1985; Soetaert and Herman, 1995c). Total denitrification modelled by Soetaert and Herman (1995c) and Brion (ECSA, 2002) was lower than reported by Billen et al. (1985) due to the fact that the oxygen deficient zone had moved upstream by approximately 10 km in the eighties compared to the seventies. This resulted in increased nitrogen discharge to the sea since only 20-21% was removed permanently (Soetaert and Herman, 1995c; Brion, ECSA 2002), compared to 40-50% in the 70-ies and early 80-ies (Billen et al., 1985). This was a situation predicted by Billen et al. (1985) when oxygen conditions were to be restored by wastewater treatment without reducing the nutrient load. Recently, another process

removing N permanently from the water has been described (Van De Graaf et al., 1995). This process, the anaerobic oxidation of ammonium (anammox) with nitrite, has not been observed in the Scheldt estuary so far (Middelburg, pers. comm.). On the other hand, nitrification can also release N to the atmosphere due the production of the intermediate N_2O (Wollast, 1982), which happens in O_2 limited conditions (de Bie et al., 2002b). The amount of N_2O produced was $0.28.10^3$ $t.y^{-1}$ with nitrification as the main source of N_2O in the Scheldt estuary (de Wilde and de Bie, 2000).

However, comparing only inorganic nitrogen input and output, the estuary is a large net nutrient exporter which is due to the fact that mineralization of organic matter exceeds production in the estuary (Soetaert and Herman, 1995b). Thus, despite the denitrification process that removes part of the nitrogen, the amount of dissolved nitrogen that is flushed to the sea is higher than the amount that enters from the river and from waste inputs (Soetaert and Herman, 1995b).

1.3.3. N speciation

The speciation and concentration of the various inorganic N compounds in the estuary is determined by the relative rates of the various pelagic processes within the water column as well as by the N fluxes passing through the estuarine boundaries (Regnier and Steefel, 1999). The three main processes described so far that modify the nitrogen species in the Scheldt are nitrification, denitrification and biological uptake (Wollast, 1982), nitrification being the most important process (Regnier et al., 1997).

1.3.3.1. Denitrification

Soetaert and Herman (1995c) showed that denitrification is important in the anaerobic freshwater part of the estuary. In the mixing zone, the higher O_2 concentrations preclude or inhibit the denitrification process. However, denitrification in the water column continues till the sea is reached, be it at very low levels (Soetaert and Herman, 1995c; Vanderborght et al., 2002). Soetaert and Herman (1995c) suggested that denitrification in the water column happens in flocs and aggregates in which strong gradients of oxygen concentration persist. The modeled data also showed that the largest amount of N is lost by pelagic rather than benthic denitrification. The latter was only important in the zone with large tidal flats (km 50) (Soetaert and Herman, 1995c).

1.3.3.2. Nitrification

Nitrification is the process having the largest effect on the N speciation (Soetaert and Herman, 1995c; Regnier and Steefel, 1999). Despite the high input of ammonium from untreated wastewater, almost all DIN that enters the sea is in the form of NO_3^- because of the efficiency of the nitrification process in the estuary (Regnier and Steefel, 1999). Soetaert and Herman (1995c), de Wilde and de Bie (2000), de Bie et al. (2002a) and Vanderborght et al. (2002) report highest nitrification rates in the freshwater-oligohaline estuarine part. The peak activity reported by de Bie et al. (2002a) is lower and located more upstream in the estuary than values reported by others due to the improved water quality in the Scheldt (de Bie et al., 2002a).

The nitrification rate depends on the temperature; it is low during winter and reaches a maximum during June (de Bie et al., 2002a). The role of benthic nitrification for the conversion of NH_4^+ is probably limited (de Wilde and de Bie, 2000).

1.3.3.3. Biological uptake and mineralization

Nitrogen assimilation is affected both by algal and bacterial uptake (Middelburg and Nieuwenhuize, 2000) of which nitrifying bacteria are the most important consumers (Vanderborght et al., 2002). Uptake rates of NH_4^+ are maximal in the oligohaline zone (<5 psu). Ammonium uptake rates decrease downstream as a result of decreasing ammonium concentrations. Maximum nitrate uptake rates occur in the middle part (between 5 and 10 psu) as nitrate uptake becomes only important at NH_4^+ concentrations < 2 $\mu mol.l^{-1}$, reflecting the fact that NH_4^+ is preferentially taken up above NO_3^- (Middelburg and Nieuwenhuize, 2000). There is a net consumption of NH_4^+ along the estuary which is due to the fact that aerobic mineralization and other ammonium generating processes are not able to meet the losses due to nitrification (Soetaert and Herman, 1995c). Particularly, nutrient removal due to phytoplankton uptake is considered insignificant in the overall estuarine cycle of the Scheldt (Soetaert and Herman, 1995c, Regnier and Steefel, 1999).

The short NH_4^+ and particulate nitrogen turnover times, compared to the water residence time, show that NH_4^+ is efficiently recycled within the estuary and that particulate matter is extensively modified. Production and consumption processes are thus closely coupled (Middelburg and Nieuwenhuize, 2000).

1.3.4. Primary production

1.3.4.1. Spatial distribution patterns

The presence and growth of phytoplankton generally depends on the temperature of the water, the availability of ambient nutrients, light intensity and mortality due to grazing and physiological stress (e.g. low light conditions or changing salinity). Because of the high nutrient content in the Scheldt water, the primary production by phytoplankton is never nutrient limited. On the other hand, the high turbidity causes severe light limitation for phytoplankton growth (Van Spaendonk et al., 1993; Kromkamp et al., 1995) so that it is limited to on average 2% of maximal production (Soetaert et al., 1994). However, phytoplankton in the Scheldt is adapted to low light conditions, leading to substantial primary production (Van Spaendonk et al., 1993). Lemaire et al. (2002) even observed maximum algal biomass in the zone between 0 and 5 psu, which corresponds to the maximum turbidity zone. Here, the highest gross production values are measured as a result of this high standing stock of algal biomass, while biomass-specific growth is relatively small (Soetaert et al., 1994). Muylaert et al. (2000a) investigated the freshwater stretch up to km 155 (compared to 100 km by Soetaert et al., 1994 and Lemaire et al., 2002). They found highest Chl-a levels extend to the lower freshwater zone (Fig. 1.5). The increased phytoplankton biomass observed in the freshwater-oligohaline zone results probably from a decrease in grazing pressure due to oxygen stress (<15% saturation) (Soetaert and Van Rijswijk, 1993; Muylaert and Sabbe, 1999). Also, Lemaire et al. (2002) concluded from the increased abundance of pheophytin relative to pheophorbide pigments in the maximum turbidity zone that bacterial degradation of phytoplankton plays a more important role in phytoplankton degradation than grazing. Downstream from the MTZ the presence of pheophytins and pheophorbides indicated that both heterotrophic bacterial degradation and grazing are important pathways for phytoplankton degradation in the estuary (Lemaire et al., 2002). Also Soetaert et al. (1994) concluded from modeled data that grazing is important in controlling the phytoplankton biomass in the marine and mesohaline stations.

Since the highest mortality of phytoplankton is observed in the zone between salinity 5 and 8 psu (the oligo-mesohaline transition), salinity stress, and not turbidity, seems to be a major factor inducing mortality (Muylaert and Sabbe, 1999). In this transition zone, a characteristic low abundance and biomass are observed (Soetaert et al., 1994; Muylaert and Sabbe, 1999; Muylaert et al., 2000a).

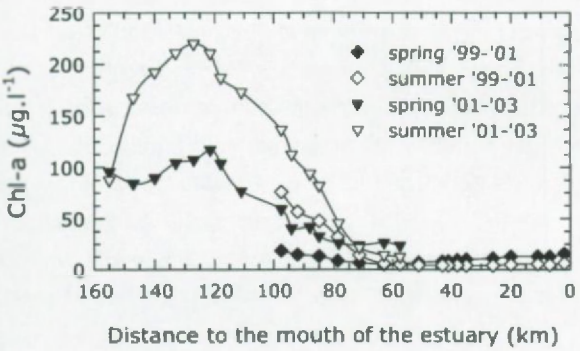

Figure 1.5: Spatial variation of mean Chl-a concentrations in the upper (triangle) and lower (diamond) half of the Scheldt estuary during spring (black) and summer (white).

1.3.4.2. Species distribution

In the Scheldt estuary, growth and decay rates of phytoplankton are related to environmental variables, while the spatial distribution in species composition is more related to the interaction of environmental variables with advective transport processes (Muylaert et al., 2000a).

In the estuary, diatoms are persistent throughout the year and dominate the phytoplankton assemblages both numerically and in biomass (Muylaert et al., 2000a; Lemaire et al., 2002). Cyanobacteria are not abundant in the Scheldt estuary (Lemaire et al., 2002), however, they can be an important group in the oligohaline (Muylaert et al., 2000a) and summer freshwater reaches (Muylaert et al., 1997). There are two zones in the estuary where a sharp shift in species composition and abundance is observed. A first shift occurs in the freshwater-oligohaline transition zone, while the second one occurs in the oligohaline-mesohaline transition zone (Muylaert et al., 2000a). The first shift is related to an increased mortality of allochthonous freshwater phytoplankton not adapted to the low light conditions. These species are, however, rapidly replaced by autochthonous populations adapted to low-light conditions (Soetaert et al., 1994; Muylaert et al., 2000a) and no decrease in abundance of biomass is observed (Muylaert et al., 2000a). The second shift is related to an increased mortality of species not resistant to changes in salinity conditions and results in a considerable decrease in species abundance and biomass (Soetaert et al., 1994; Muylaert et al., 2000a).

In the freshwater reaches of the Scheldt, the phytoplankton community of the upper and lower freshwater part differs in origin. As the short residence time severely restricts primary production in the upper freshwater part (km 155 - km 140), by far

the largest amount of phytoplankton is advected from the tributaries, while in the lower freshwater part (km 133 - km 111) an autochthonous phytoplankton community can develop when discharge is sufficiently low. However, when discharge increases after a period of high rainfall, the local community of the lower freshwater zone is also replaced by allochthonous riverine communities (Muylaert et al., 2000a; 2001). The local communities consist typically of diatoms of the genus *Cyclotella*, while riverine communities import mainly the green algae *Scenedesmus spp.* to the estuary (Muylaert et al., 2001). In the freshwater zone, only large diatoms are found, which is probably the result of grazing pressure by rotifers on small species (Muylaert et al., 2000a).

In the oligohaline stations, both typical freshwater and brackish water species are present (Muylaert et al., 2000a). Here, the diatom *Cyclotella sp.* dominates the phytoplankton community, but green algae, cyanobacteria and the flagellate *Euglena proxima* are also important (Muylaert and Sabbe, 1999).

The zone between a salinity of 5 and 8 psu (the oligohaline-mesohaline transition zone) is characterized by impoverished phytoplankton communities consisting of both freshwater and brackish water species (Soetaert et al., 1994; Muylaert and Sabbe, 1999).

In the most downstream mesohaline zone, the most abundant species both numerical and in biomass, are large marine and brackish water diatoms such as *Rhaphoneisamphiceros*, *Skeletonema costatum* and *Thalassiosira sp.* (Muylaert and Sabbe, 1999).

1.3.4.3. Seasonal variation

During autumn and winter and early spring, the lower temperature and incident light, the higher turbidity and increased river discharge inhibit the primary production almost entirely and respiration exceeds gross production (Soetaert et al., 1994; Muylaert et al., 1997). Only in summer net phytoplankton growth is possible except in the MTZ (Kromkamp et al., 1995), where the phytoplankton biomass is decaying all year round (Soetaert et al., 1994). When conditions are suitable for net phytoplankton growth, the phytoplankton blooms are local due to the relatively short turn-over time of phytoplankton in comparison to residence time (Van Spaendonk et al., 1993).

In the upper freshwater part, a small spring bloom is observed (Muylaert et al., 2000a). In the lower freshwater and oligohaline estuary, a phytoplankton bloom is observed during the summer months July, August and September (Van Spaendonk et al., 1993; Muylaert et al., 2000a); (Fig. 1.6). The spring bloom of the upper freshwater part is mainly induced by phytoplankton advected from the tributaries, while the

summer bloom in the lower freshwater part is predominantly produced in situ, the import from the tributaries being less important, but still present (Muylaert et al., 2000a). Also the mesohaline to marine estuary has a spring and summer bloom period (Van Spaendonk et al., 1993, Kromkamp et al., 1995). In the mesohaline zone, the spring bloom consists of characteristic species of clear coastal and estuarine water and the summer bloom consists of typical mesohaline species (Muylaert et al., 2000a).

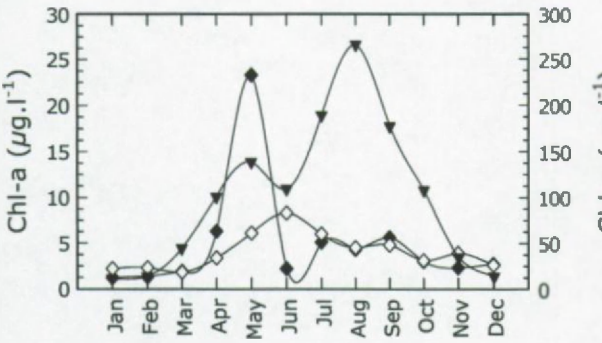

Figure 1.6: Seasonal variation of mean Chl-a concentrations at a characteristic freshwater (triangle), mesohaline (white diamond) and marine station (black diamond) of the Scheldt estuary for the period 1999-2001 (mesohaline and marine) and 2001-2003 (freshwater). Note that Chl-a concentrations in the freshwater section are an order of magnitude higher (right axis) than at the other stations (left axis).

1.3.5. Bacterial production

On an annual scale, no strong coupling exists between bacterial and primary production (Goosen et al., 1997) and bacterial metabolism is mainly fuelled by allochthonous carbon sources (Soetaert and Herman, 1995b). The bacterial production is mainly regulated by temperature since allochtonous POC and DOC substrates are present in non-limiting amounts. Nevertheless a strong positive correlation exists between bacterial production and DOC and POC concentration (Goosen et al., 1995; 1997). Billen et al. (1980) reported that bacterial density depended only on substrate production rate, while Regnier et al. (1997) specified that the rate of organic mater degradation is independent of the substrate concentration for high organic loads (>200 μmol.l^{-1} organic matter).

However, bacterial productivity and primary production may be temporarily and locally coupled. For instance, bacterial productivity is coupled to phytoplankton blooms in the lower estuary (averaged salinity concentration above 16-18 psu) due to the uptake of labile algal exudates by bacteria (Goosen et al., 1997) and in the freshwater-oligohaline transition zone, decaying phytoplankton populations produce organic matter that is easily degraded by bacteria (Vanderborght et al., 2002).

Introduction to the use of stable isotopes in ecological studies

Chapter 2

2.1. Introduction

During the last decades, there has been an increasing interest in the use of the natural distribution of stable isotopes in the environment as a means to follow elemental cycling in ecosystems. Stable isotopes are used as indicators of biogeochemical processes and as a tool to detect the origin of samples in mixtures (Peterson and Fry, 1987). The usefulness of stable isotopes to obtain process and source information essentially results from the unequal partitioning of heavy and light isotopes (fractionation) between source and product during chemical, physical and biological processes (Farquhar et al., 1989; O'Leary et al., 1992; Fry, 2003). The resulting variation in stable isotope composition of organic matter is then a tool to identify the origin of samples in mixtures (Peterson and Fry, 1987). This makes stable isotopes particularly useful for the study of food webs.

Generally, the stable isotopes of both C and N are used to study trophic interactions in ecosystems, since the possibility that the organic matter sources have different isotopic compositions increases with the use of a combination of stable isotopes of different elements (Rounick and Winterbourn, 1986; Owens, 1987; Peterson and Fry, 1987). Essentially, C and N isotopes are used to track C and N flow from the base of the food webs to the highest trophic levels providing as such information about the diet preferences of organisms. However, this requires a thorough understanding of the stable isotope composition of the organisms at the base of the food web and of the change in C and N stable isotope compositions of organic matter when it is transmitted to higher trophic levels. Here, we present an introduction to stable isotope terminology and applications followed by an overview of the factors setting, controlling and affecting the C and N stable isotopic composition of primary producers.

2.2. Natural abundance of stable C and N isotopes: definitions

In nature, there are two naturally occurring stable isotopes of carbon and nitrogen. For carbon, about 98.9% of the carbon is ^{12}C, while about 1.1% is ^{13}C (O'Leary, 1981). For nitrogen, the % abundance of ^{14}N and ^{15}N is 99.64% and 0.36%, respectively (Faure, 1986). Absolute abundances of stable isotopes cannot be measured with very great precision, but the small differences in the heavy to light ratio between two compounds can be accurately measured using a mass spectrometer. The % abundance of C and N isotopes, being $^{13}C/(^{13}C + ^{12}C)$ and $^{15}N/(^{15}N + ^{14}N)$, respectively, is commonly simplified to $^{13}C/^{12}C$ and $^{15}N/^{14}N$ since absolute abundances

of ^{13}C and ^{15}N are very small compared to the ones of ^{12}C and ^{14}N (Mariotti et al., 1981).

The stable isotopic composition of a sample is measured relative to a common standard. The international standard for $\delta^{13}C$ is PDB (PeeDee Belemnite) with a $^{13}C/^{12}C$ ratio of 0.00112372 while the one for N_2 is atmospheric air with a $^{15}N/^{14}N$ value of 0.0036765 (Fry, 2003).

The relative isotopic composition (δ) of a sample is expressed as:

$$\delta(‰) = \left(\frac{R_{sample}}{R_{standard}} - 1 \right) \times 1000 \qquad \text{Eq. 1}$$

$$R = {}^{13}C/_{12}C \quad \text{or} \quad R = {}^{15}N/_{14}N \qquad \text{Eq. 2}$$

The isotopic composition of the standard should not be very different from the measured samples, in order to minimize the systematic error, related to the use of the simplified R-expression, which increases with isotopic distance between standard and sample (Mariotti et al., 1981; Fry, 2003).

Samples depleted in ^{13}C or ^{15}N, i.e. enriched in ^{12}C or ^{14}N, compared to the standard assume negative values while samples enriched in ^{13}C or ^{15}N as compared to the standard assume positive values.

2.3. The use of stable isotopes in process studies

The distribution of stable isotopes in the natural environment is frequently used as an indicator of processes (Peterson and Fry, 1987). The way the stable isotopic composition of natural material is altered by chemical, physical and biological processes has been studied thoroughly so that observed isotope distributions can be interpreted in function of the underlying reaction conditions (Rounick and Winterbourn, 1986; Peterson and Fry, 1987). The process resulting in the re-distribution of isotopes between source and product is called isotope effect or fractionation. Fractionation occurs due to the mass differences between isotopes which makes the formation and destruction of bounds between heavy atoms more difficult than for light ones or which makes the heavy isotope to move slower than the light one in e.g. diffusion reactions (Farquhar et al., 1989).

2.3.1. Fractionation: terminology

The isotope effect, denoted by α, is defined as (Farquhar et al., 1989):

$$\alpha = \frac{R_s}{R_p} \qquad \text{Eq. 3}$$

where R_s and R_p are the $^{13}C/^{12}C$ or $^{15}N/^{14}N$ molar ratios of the source and product, respectively. Isotope effects are also expressed as the ratio of rate constants k_1 and k_2, for the light and heavy isotope, respectively:

$$\alpha = \frac{k_1}{k_2} \qquad \text{Eq. 4}$$

The extent of discrimination (ε) against an isotope is the deviation of α from unity (O'Leary et al., 1992, Hayes, 1993; Fry, 2003):

$$\varepsilon = 1000 \times (\alpha - 1) \qquad \text{Eq. 5}$$

Substituting eq. 1 and eq. 3 in eq. 5 gives

$$\varepsilon = 1000 \times \left(\frac{R_s}{R_p} - 1 \right) = \frac{\delta X_s - \delta X_p}{1 + \delta X_p / 1000} \qquad \text{Eq. 6}$$

where δX_s and δX_p represent the $\delta^{13}C$ or $\delta^{15}N$ signature of the source and product, respectively. The term $\delta X_p/1000$ in the denominator is usually small and can thus be ignored, so that:

$$\varepsilon \approx \delta X_s - \delta X_p \qquad \text{Eq. 7}$$

This equation holds for samples with δ–values differing by <20‰ and that are not too different from zero otherwise the use of eq. 6 is recommended (Mariotti et al., 1981; Hayes, 1993; Fry, 2003).

2.3.2. Thermodynamic and kinetic isotope fractionation

Generally, there are two types of isotope effects that lead to fractionation: kinetic and thermodynamic isotope effects. Kinetic fractionation occurs when different isotopes species are transferred at different rates. Thermodynamic fractionation is the balance of two kinetic effects at equilibrium (O'Leary, 1981; Farquhar et al., 1989; O'Leary et al., 1992). Whether the conversion of material from one state to the other

will result in thermodynamic as well in kinetic fractionation depends on the rate of conversion. When the rate of transformation of two states is rapid compared to the rates of steps preceding and following it, the transformation is in equilibrium and a thermodynamic fractionation is expressed. If, however, the transformation rate is slow compared to the other reactions a kinetic fractionation will be expressed (O'Leary, 1981).

A general rule for the partitioning of the heavy and light isotope between source and product is that due to thermodynamic fractionation the heavier isotope will concentrate in the more constraint environment (i.e. where the bonding of the atoms is more extensive); (O'Leary et al., 1992). Kinetic fractionation is a result of the heavier atom reacting more slowly than the light one, whereby the fractionations in physical processes are generally smaller than those in chemical processes. When chemical processes are catalyzed by enzymes, the resulting isotope fractionation will be smaller than when the chemical processes would occur without enzymes.

2.3.3. Fractionation in open and closed systems

The effect of isotope fractionation on the isotopic composition of the substrate and product differs between open and closed systems. In open systems (i.e. internal and external pools are connected) the pool of substrate is unlimited so that the isotopic content of the substrate can be assumed to remain constant since the effect of fractionation on the substrate isotopic composition will be negligible. In closed (i.e. isolated pool) systems, the pool of substrate is limited and the isotopic content of both substrate and product will change as the reaction proceeds. Here, the curvature of the changes in isotopic composition over time of the substrate and product will also depend on the reversibility of the reactions (see below). In all cases, the discrimination ε for a certain process is assumed to be constant, given that the prevailing conditions are stable (Mariotti et al., 1981).

2.3.3.1. Closed systems

In closed systems, the isotopic composition of substrates will be affected by processes discriminating against heavy or light isotopes. As a result, the isotopic composition of the instantaneous product, which reflects the isotopic composition of the substrate but with a constant offset ε, will also change over time. The accumulated product, however, will proceed to an isotopic composition similar to the original substrate when all substrate is being converted to product (Zeebe et al., 1999).

In closed systems, where the reaction causing fractionation is irreversible, the isotope ratio of the substrate is given by

$$\frac{R_s}{R_{s,0}} = f^{(\alpha-1)} \qquad \text{Eq. 8}$$

where R_s and $R_{s,0}$ are the isotope ratios of the substrate at time t and $t = 0$, respectively. f is the remaining fraction of the substrate, whereas α refers to the fractionation characteristic for the process (Mariotti et al., 1981; Zeebe et al., 1999). This equation is referred to as the Rayleigh equation. From this equation, the absolute and relative isotopic composition of the substrate, the instantaneous and accumulated product can be calculated. The inter-conversion between absolute and relative values results from substituting equations 1 and 5 into equation 8 (Mariotti et al., 1981); (Table 2.1).

Table 2.1: Absolute and relative isotope ratios of substrate, instantaneous and accumulated product in a closed system where a process causing fractionation is active. Equations are compiled from Mariotti et al. (1981) and Zeebe et al. (1999).

Absolute abundance	
Substrate	$R_s = R_{s,0} \times f^{(\alpha-1)}$
Instantaneous product	$R_{p,i} = R_{p,0} \times \alpha f^{(\alpha-1)}$
Accumulated product	$R_p = R_{p,0} \times \frac{f^\alpha - 1}{f - 1}$
δ-value	
Substrate	$\delta_s = \delta_{s,0} - \varepsilon \times \ln f$
Instantaneous product	$\delta_{p,i} = \delta_s - \varepsilon$
Accumulated product	$\delta_p = \varepsilon \times \frac{f \times \ln f}{1 - f} + \delta_{s,0}$

In a closed system where substantial back-reaction occurs, the isotopic composition of the substrate, instantaneous and accumulated product will show linear

changes with increasing fractionation instead of Rayleigh type fractionation (Macko et al., 1986). In that case, the isotopic composition of the product and the substrate can be calculated using simplified equations (Table 2.2); (Macko et al., 1986).

Table 2.2: δ-values of substrate and product in a closed system where a process characterized by considerable back-reaction discriminates between isotopes.

Closed system: reversible reaction	δ-value
Substrate	$\delta_s = \delta_{s,o} + (1-f) \times \varepsilon$
Instantaneous product	$\delta_p = \delta_{s,o} - f \times \varepsilon$

The effect of fractionation on the isotopic composition of substrate and product during irreversible and reversible reactions in closed systems is illustrated in Fig. 2.1.

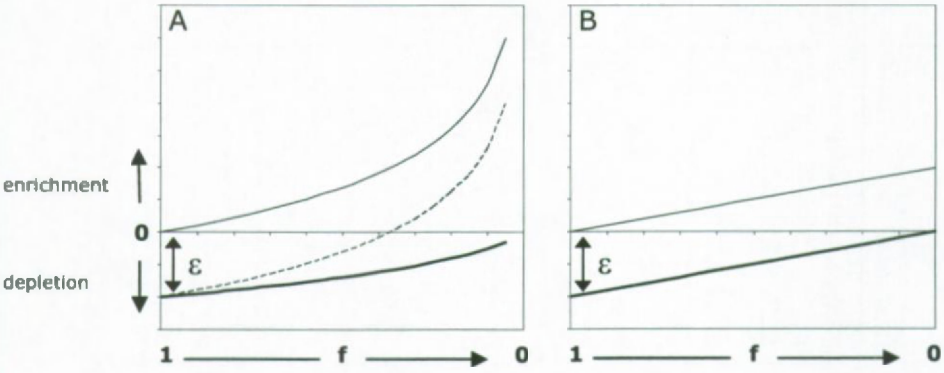

Figure 2.1: Change in isotopic composition of substrate and product with decreasing fraction *f* of the substrate remaining in the pool for a situation where $\varepsilon > 0$ and $\delta_{s,0}$ = 0‰. The substrate (solid) and accumulated (solid, bold) and instantaneous (dashed) products follow a Rayleigh fractionation (A) in case reactions are irreversible. In case considerable back-reaction occurs (B), substrate and product increase linearly with decreasing substrate fraction remaining. Redrawn from Owens et al. (1985) and Macko et al. (1986).

2.3.3.2. Open systems

In open systems, a substrate enters the system after which some fraction is converted to product (Fry, 2003). If the substrate can be considered as an infinite reservoir compared to the quantity of the product, R_s or δ_s will not change and *f* is

always close to 1. Then, the equations from Table 2.1 can be simplified (Table 2.3). Note that both product and substrate isotopic compositions are stable over time.

Table 2.3: Isotope composition of substrate and product in open systems.

Open system	Absolute isotope ratio	δ-value
Substrate	$R_s = R_{s,0}$	$\delta_s = \delta_{s,0}$
Accumulated product	$R_p = R_{p,0}$	$\delta_p = \delta_s - \varepsilon$

2.3.4. Fractionation in steady-state flow systems

If we consider a steady-state flow through a system, the isotopic composition of the substrate pool (source) equals the one of the product pool (output) so that we can write (Fry, 2003):

$$\delta_{input} = \delta_{output}$$

$$\delta_{source} - \varepsilon_1 = \delta_{pool} - \varepsilon_2$$

where δ_{source} and δ_{pool} are the δ-values for the source and the internal pool, respectively, and ε_1 and ε_2 the discrimination values during uptake and loss, respectively.

The isotopic composition of the source and internal pool will change linearly with decreasing fraction remaining if the substrate pool is limited (Table 2.4); (Fry, 2003).

Table 2.4: Change in isotopic composition of source and pool in case the source is limited and fractionation occurs both during uptake and release processes.

Flow system: limited resource	δ-value
Substrate	$\delta_{source} = f \times (\delta_{s,0} - \varepsilon_1) + \varepsilon_1$
Pool	$\delta_{pool} = \delta_s - \varepsilon_1 + \varepsilon_2$

2.4. The use of stable isotopes to reveal source information

The use of stable isotopes as source indicators is subject to following conditions: (1) the isotopic composition of the sources must be known and sufficiently distinct from each other, (2) all potential sources have to be included in the search for constituting pools and (3) fractionation eventually occurring during transfer from one pool to the other is quantified (Fry and Sherr, 1984; Owens, 1987; Vander Zanden and Rasmussen, 2001).

2.4.1. Mixing of two sources

The isotopic composition of a mixture of two components is the weighted average of the isotope ratios of the two constituents ('end-members'). The isotopic composition of the mixture, δX_{mix}, can be described by the following equation (Gannes et al., 1997):

$$\delta X_{mix} = f \times \delta X_1 + (1 - f) \times \delta X_2 \qquad \text{Eq. 9}$$

where *f* equals the fraction of source 1 from the mixture and δX_1 and δX_2 are the isotope signatures of the two sources. The δX_{mix} varies linearly between δX_1 and δX_2 when one source becomes gradually replaced by the other (Fig. 2.2).

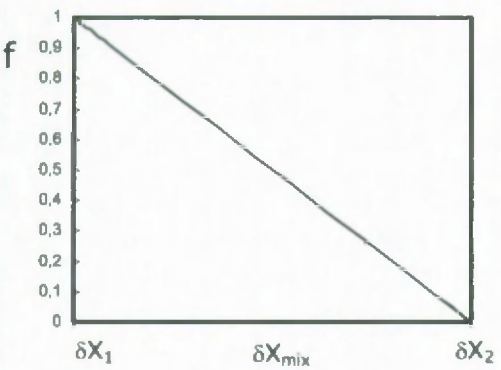

Figure 2.2: Variation in the isotopic composition of a mixture due to changing fractional contribution of source 1 and 2 to the mixture. Redrawn from Fry (2003).

In case the amount of source 1 in the mixture is fixed while the amount of source 2 can change, the relationship between *f* and δX_{mix} will turn into an asymptotic one. Considered that M_1 represents the mass of the fixed source, the mass of the second source can overwhelm the first, so that M_1/M_{mix} becomes very small. In that case, the mixing curve will show an asymptotic mixing relationship (Fry, 2003); (Fig. 2.3).

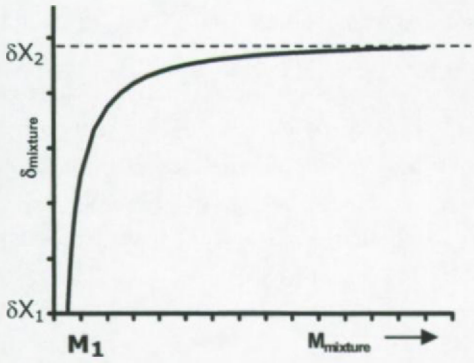

Figure 2.3: Change in δX_{mix} as a result of increasing weight of source 2 to the total weight of the mixture in case the input of source 1 is fixed. Redrawn from Fry (2003).

Sometimes, additional fractionation occurs after mixing. In that case, this fractionation value must first be subtracted from the mixing value before mixing sources can be determined (Fig. 2.4B). If a third source, which exhibits a value intermediate to source 1 and 2, is present, no unambiguous interpretation of contributing sources can be made (Fig. 2.4C).

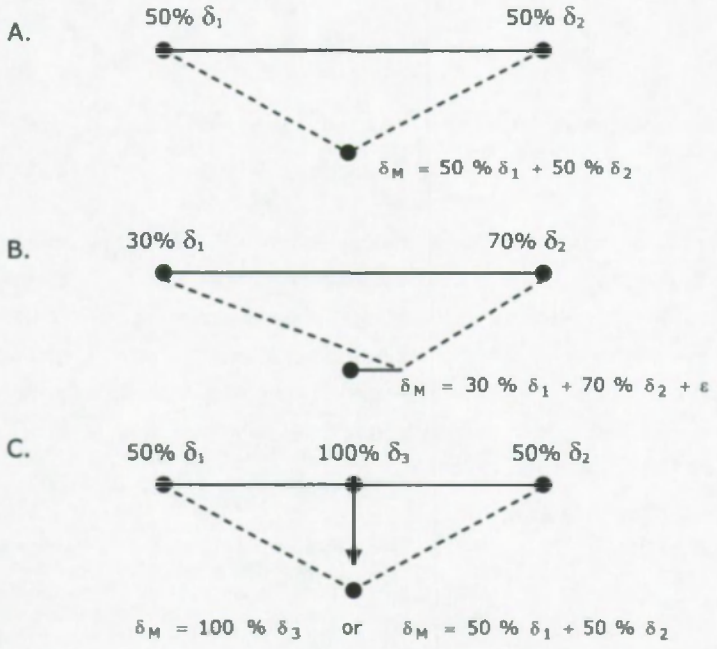

Figure 2.4: Interpretation of isotope mixing models. In all three cases the same isotopic composition is observed, but the contribution of the sources is different. In case A, the mixture is the average of two sources each contributing for 50% to the mixture. In case B, the isotopic composition of the mixture has shifted with a value equal to the fractionation occurring after mixing. Finally, in case C, no unambiguous conclusion can be drawn from the δ–value of the mixture if a third source is present with a value equal to the average of source 1 and 2. Modified from Fry and Sherr (1984).

2.4.2. Use of multiple stable isotopes in source studies

In case the stable isotope signature of the mixture is a combination of only two sources, its isotopic signature is positioned somewhere on the line connecting both sources. If, however, additional sources contribute to the final δ-value of the mixture, the ($\delta^{15}N$, $\delta^{13}C$) co-ordinate of the mixture is situated within the triangular space enclosed by lines connecting the ($\delta^{15}N$, $\delta^{13}C$)-coordinates of the sources. An illustration for 2 and 3 sources is given in Figure 2.5.

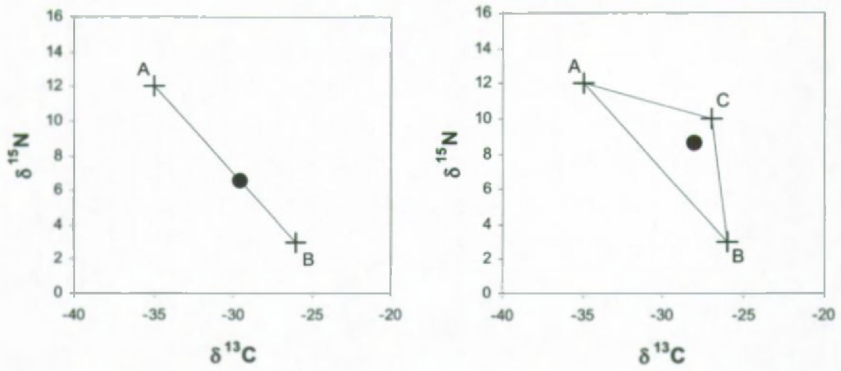

Figure 2.5: Graphic presentation of the relationship between the isotopic composition of a mixture and its contributing sources A, B and C. Left: The sample (black dot) is a mixture of only two sources A and B. Right: Situation where a third source C contributes to the mixture.

The above mentioned mixing model assumes that the proportional contribution of a source to a mixture is the same for both elements C and N. Since the contribution of elements to the mixture is proportional to their concentration in the source, this assumption will not hold for sources displaying rather distinct elemental concentrations. In that case, a concentration-weighted linear mixing model (Fig. 2.6) needs to be applied to determine the fractional contribution of a particular source to the mixture (Philips and Koch, 2002).

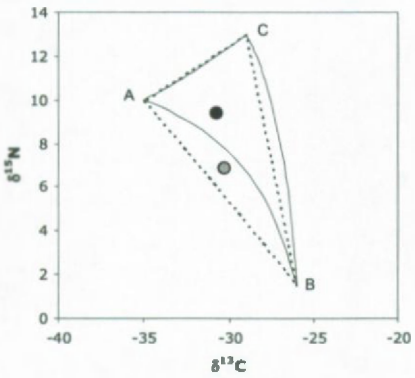

Figure 2.6: Graphic representation of the concentration-weighted linear mixing model (solid line) for a situation where the 3 sources have distinct C/N ratios. The isotope signature of the first sample (black dot) is a combination of the three sources A, B and C. The isotopic composition of the second sample (grey dot) could erroneously be interpreted as being a mixture of source A, B and C if no correction is made for the proportional distribution of elements in the sources, since it is positioned in the triangle connecting the three sources (dashed lines).

2.5. $\delta^{13}C$ and $\delta^{15}N$ in food web research

The study of trophic relations between organisms by means of C and N stable isotopes can essentially be seen as the tracking of C and N flow between trophic levels. Organic matter transferred between trophic levels affects the $\delta^{13}C$ and $\delta^{15}N$ compositions of the consumer in a predictive way so that its isotopic signature can be related to its food source(s). If consumers have multiple food sources, the proportional contribution of the different components can be calculated by means of mixing equations. Similarly, the isotopic signature of primary producers thriving on multiple food substrates will reflect the different food substrates of which the proportional contribution can be determined via mixing equations. As mentioned before, the isotopic compositions of the prey and feeding substrates have to be known and sufficiently distinct from each other, fractionation during the transfer of C and N isotopes needs to be quantified and all potential prey and food substrates have to be considered before mixing equations can be applied (Fry and Sherr, 1984; Owens, 1987; Vander Zanden and Rasmussen, 2001).

In estuarine aquatic systems, the organisms forming the base of the food web are often closely intermingled with the other components of the suspended matter pool. Suspended matter pools generally contain organic matter from both terrestrial as aquatic origin and organisms can be alive or in different stages of decomposition ranging from fresh till fully refractory detritus. The $\delta^{13}C$ and $\delta^{15}N$ signature of terrestrial and aquatic components differ due to the mechanisms through which C and N are incorporated into plant or algal tissue and due to additional changes in the isotopic composition occurring during degradation processes.

In the following we present an overview of the mechanisms setting the $\delta^{13}C$ and $\delta^{15}N$ of organisms at the base of the food web by reviewing the underlying mechanisms for the observed differences in $\delta^{13}C$ and $\delta^{15}N$ of the different organic matter sources in the suspended matter pools. Then, an overview is given of the fractionation processes occurring during degrading processes and during the transfer of C and N containing compounds between two trophic levels.

2.5.1. Factors affecting $\delta^{13}C$ of photosynthetic organisms

There are three main factors that affect the $\delta^{13}C$ of photosynthetic organisms, being the $\delta^{13}C$ of the external carbon pool ($CO_{2(ext)}$), the fractionation during C uptake and the $\delta^{13}C$ of respired CO_2. In the following we discuss how these three factors affect the $\delta^{13}C$ composition of primary producers and how environmental conditions influence

the magnitude of the effects. An overview of factors setting the final $\delta^{13}C$ value of primary producers is given in Figure 2.7.

$\delta^{13}C$ of primary producers

- $\delta^{13}C$ of the ambient CO_2 pool
- fractionation during C uptake
  - CO_2 assimilation to supply ratio
    - CO_2 supply ~ cell membrane leakiness
      ~ CO_2 flux toward organism
      - ambient CO_2 concentration
      - water flow
      - CO_2 concentrating mechanisms
    - C assimilation ~ growth rate
  - metabolic pathway
    - C_3 plants
    - C_4 plants
    - CAM plants
    - Phytoplankton
- fractionation during respiration

Figure 2.7: Schematic overview of factors affecting the $\delta^{13}C$ composition of primary producers

2.5.1.1. $\delta^{13}C$ of ambient C-sources (CO_2 versus HCO_3^-)

A first factor setting the $\delta^{13}C$ of primary producers is the $\delta^{13}C$ signature of the source carbon. Primary producers exposed to air use atmospheric CO_2 as a carbon source. In aquatic environments, carbon is mainly present in the form of HCO_3^- but dissolved molecular CO_2 ($CO_{2(aq)}$) remains the preferred inorganic C substrate (Degens et al., 1968, Maberly and Spence, 1983; Keeley and Sandquist, 1992). However, HCO_3^- uptake by phytoplankton has been reported for situations where a CO_2 concentrating mechanism is activated to complete cellular C demand (see below).

The variability of $\delta^{13}C$ of primary producers in aquatic environments is higher than for species using atmospheric CO_2 (Osmond et al., 1981; Descolas-Gros and Fontugne, 1990) a feature that can be linked to the $\delta^{13}C$ of the C-source. Indeed, $\delta^{13}C$ of atmospheric CO_2 is usually −7.9‰ (Farquhar et al., 1989) while $\delta^{13}C$ values of CO_2 dissolved in water range between +1‰ for HCO_3^- derived from limestone, over −7‰ for a situation where dissolved CO_2 (= $CO_{2(aq)}$ + HCO_3^-) is in equilibrium with $CO_{2(atm)}$,

to -27‰ when most of the dissolved CO_2 is respired CO_2 from C_3 plants (Keeley and Sandquist, 1992; Osmond et al., 1981). Moreover, the $\delta^{13}C$ signature of $CO_{2(aq)}$ may temporarily shift to higher values as a result of physico-chemical or biological processes draining the $CO_{2(aq)}$ pool so that more $^{13}CO_2$ enters the $CO_{2(aq)}$ pool (Degens et al., 1968; Descolas-Gros and Fontugne, 1990; Keeley and Sandquist, 1992; Maberly et al., 1992). Another factor contributing to the higher variability of $\delta^{13}C$ in aquatic environments is the fact that the equilibrium isotope fractionation value for CO_2 dissolved in water decreases with increasing temperatures (between 7-11‰ in natural environments); (O'Leary, 1981; Keeley and Sandquist, 1992; Rau et al., 1997). The $\delta^{13}C$ composition of aquatic primary producers will thus increase with increasing water temperature.

Generally, species restricted to CO_2 as the only C-source will have more negative $\delta^{13}C$ values than species using HCO_3^- as an additional C source (Osmond et al., 1981; Maberly and Spence, 1983; Turpin et al., 1991; Maberly et al., 1992; Burkhardt et al., 1999a), since $\delta^{13}C$ values of HCO_3^- are enriched in ^{13}C compared to $CO_{2(aq)}$ due to the preferential retention of ^{13}C in the water phase (O'Leary, 1981; Keeley and Sandquist, 1992).

2.5.1.2. Fractionation during C uptake

The second important factor affecting the $\delta^{13}C$ of primary producers is the magnitude of the overall fractionation associated with the different steps involved in the uptake and assimilation of CO_2. The magnitude of this apparent fractionation is the resultant of fractionation associated with the processing transporting CO_2 to the site of uptake and with the enzymatic assimilation of CO_2 (O'Leary, 1981). Since the latter is largely independent of CO_2 or O_2 concentrations, pH and temperature for a specific enzyme (Roeske and O'Leary, 1984; Berry, 1989), variations in the isotopic composition of plants are related to differences in the δ-value of the internal CO_2-pool. The internal $\delta^{13}C$ pool may vary due to variations in the assimilation to supply ratio and the metabolic pathway used to incorporate CO_2. The contribution of these factors to C fractionation is discussed below.

<u>Factors affecting the assimilation to supply ratio</u>

The extent to which the internal C pool will be enriched in ^{13}C as a result of C consuming processes depends on the rate to which $^{13}CO_2$ can be removed and substituted by $^{12}CO_2$ from the ambient pool. The supply of $^{12}CO_2$ to the internal pool depends on the CO_2 flux toward the cell and the cell membrane permeability (or

leakiness) which regulates flux across the cell wall (Rau et al., 1996; Riebesell et al., 2000). The contribution of CO_2 flux toward the cell to the overall fractionation during CO_2 uptake is especially important in aquatic environments and depends on the ambient CO_2 concentration, the water flow and the presence of a CO_2 concentrating mechanism.

a) CO_2 supply rate

i. Leakiness

The leakiness of a cell membrane is defined as the magnitude of the efflux to influx ratio (Sharkey and Berry, 1985) and depends on the permeability of the cell membrane in case of phytoplankton (Sharkey and Berry, 1985) and on the stomatal resistance in case of plants (O'Leary, 1981; Farquhar et al., 1989). An increase in the diffusive resistance of CO_2 in C_3 plants and phytoplankton results in increasing $\delta^{13}C$ values, while for C_4 plants $\delta^{13}C$ values decrease with increasing resistance. For C_3 plants and phytoplankton, this can be explained by the fact that a decreasing permeability for CO_2 (1) decreases the extent of fractionation against ^{13}C due to the accumulation of $^{13}CO_2$ in the cell (O'Leary, 1981; Farquhar et al., 1989) and (2) decreases the internal CO_2 concentrations or partial pressure since CO_2 removed by the assimilation process cannot be replenished at time (Maberly et al., 1992; Rau et al., 1996). For C_4 plants, which use HCO_3^- as a C-substrate, increasing stomatal resistance results in increasing fractionation against ^{13}C since the drain of HCO_3^- causes a shift toward more ^{12}C-rich HCO_3^- in the HCO_3^- pool (O'Leary, 1981).

The magnitude of the influx to efflux ratio is also affected by the rate of carbon assimilation (O'Leary, 1981; Riebesell et al., 2000). At low assimilation rates, the rate of influx is lower than the rate of efflux and a large discrimination against ^{13}C will be observed (O'Leary, 1981) but at high assimilation rates, the rate of efflux will be lower than the rate of influx and internal isotope enrichment will occur (O'Leary, 1981; Berry, 1989; Riebesell et al., 2000).

ii. CO_2 flux

- *ambient CO_2 concentrations*

In air, a constant supply of ^{12}C is assured during the CO_2 fixation in plants since the $CO_{2(ext)}$ pool is sufficiently large so that no change in its concentration or isotopic

composition occurs as a result of photosynthetic activity (O'Leary, 1981). In the aquatic environment, $CO_{2(aq)}$ concentrations may be low as a result of increasing temperature (Degens et al., 1968; Descolas-Gros and Fontugne, 1990; Rau et al., 1996) and pH (Degens et al., 1968). Additionally, also photosynthesis can rapidly reduce the total C concentration in the water, thereby raising the pH of the water and shifting the positions of the carbonate equilibria so that free dissolved CO_2 is virtually zero (Maberly and Spence, 1983; Hinga et al., 1994). Lowered ambient CO_2 concentrations result in a decrease of the CO_2 flux toward the cell (Burkhardt et al., 1999a) and increase the percentage of cellular CO_2 leaking back to the environment (Burkhardt et al., 1999a). As a result, the possibility to discriminate against ^{13}C decreases which results in increasing $\delta^{13}C$ values of primary producers (Rau et al., 1996; Rau et al., 1997; Burkhardt et al., 1999a; Burkhardt et al., 1999b; Riebesell et al., 2000).

- *water flow*

The diffusive resistance to CO_2 is 10,000 times larger in water than in air which limits the CO_2 flow to the cell so that almost all $CO_{2(aq)}$ available is consumed and overall C fractionation expressed is minimized (Osmond et al., 1981; Maberly and Spence, 1983; Keeley and Sandquist, 1992). However, increasing temperatures may increase the diffusivity of CO_2 in water (Hinga et al., 1994; Rau et al., 1996). The mixing of the carbon pool in the boundary layer of a photosynthesizing cell with that of bulk solution is much smaller in water compared to air due the greater viscosity of water. This permits the development of relatively unstirred boundary layers around objects in water (Maberly and Spence, 1983; Descolas-Gros and Fontugne, 1990) of which the thickness is strongly increased by reduced water current velocity (Osmond et al., 1981; Keeley and Sandquist, 1992).

- *CO_2 concentrating mechanisms*

In some phytoplankton species a CO_2 concentrating mechanism is induced at low CO_2 concentrations (Sharkey and Berry, 1985; Berry, 1989) or under high growth conditions (Laws et al., 1997). Here, CO_2 and/or HCO_3^- are actively transported across the cell membrane. The mechanism of this active transport is not yet fully understood and the magnitude of inferred isotope fractionation differs between the mechanisms proposed.

A first possible mechanism is that an external enzyme, carbonic anhydrase, converts HCO_3^- to CO_2 at the cell surface after which it is transported into the cell either by active transport or by diffusion (Laws et al., 1997). In this case no net fractionation should be observed since carbonic anhydrase discriminates against ^{13}C so

that CO_2 enzymatically converted from HCO_3^- has similar $\delta^{13}C$ values as $CO_{2(aq)}$ (Riebesell and Wolf-Gladrow, 1995).

Another possible mechanism is that HCO_3^- is converted to CO_2 by carbonic anhydrase in the cell, so that the $\delta^{13}C$ of intracellular CO_2 equals that of HCO_3^- which is relatively enriched compared to $CO_{2(aq)}$ (Sharkey and Berry, 1985). Thus, the presence of a CO_2 concentrating mechanism makes the effects of CO_2 concentrations on ε less prominent (Burkhardt et al., 1999a).

b) Carbon assimilation rate

The rate to which carbon is assimilated depends on the carbon demand. High carbon demands compared to C supply will decrease the intracellular $CO_{2(aq)}$ available and thus the degree to which the cell may preferentially fix $^{12}CO_2$ (Descolas-Gros and Fontugne, 1990; Hinga et al., 1994; Rau et al., 1996; Rau et al., 1997; Burkhardt et al., 1999a; 1999b) which results in an increase in the $\delta^{13}C$ of primary producers. The carbon demand is positively correlated to growth rate (or metabolic activity) (Rau et al., 1996) and the magnitude of isotope fractionation will be related to factors controlling growth rate (Rau et al., 1996; Rau et al., 1997; Burkhardt et al., 1999a; 1999b; Riebesell et al., 2000). Several factors such as increasing temperature, $CO_{2(aq)}$, nutrients and light intensity (MacLeod and Barton, 1998) can increase growth rate and thus decrease fractionation values. Larger species have higher C demands and will show lower discrimination values (Rau et al., 1996; Rau et al., 1997; Burkhardt et al., 1999a; 1999b). Also day length and salinity have been reported to affect isotope discrimination but the direction and the magnitude of the effect is largely species-dependent (Leboulanger et al., 1995; Burkhardt et al., 1999a; 1999b).

Metabolic pathways of C assimilation

The metabolic pathway of CO_2 assimilation is a second important factor that influences the extent of C fractionation during CO_2 uptake. The carbon fixation in primary producers is mediated through the C_3, C_4 or CAM metabolic pathway, each characterized by a specific fractionation factor. The difference in the magnitude of C fractionation during these fixation pathways results from different enzymes catalyzing the CO_2 fixation and the amount of steps involved in it and from the preferential uptake of CO_2 or HCO_3^- of which the $\delta^{13}C$ is determined by their relative concentration in the cell (see above).

a) C_3 plants

In C_3 plants ribulose-1,5-biphosphate carboxylase-oxygenase (Rubisco) is responsible for the carboxylation of ribulose-1,5-biphosphate (RuBP) (O'Leary, 1981). The fractionation associated with CO_2 assimilation by Rubisco is 29‰ (Roeske and O'Leary, 1984), but the overall observed fractionation during C assimilation can decrease depending on the extent of stomatal resistance against diffusion (O'Leary, 1981). In general, plants following the C_3 pathway will have $\delta^{13}C$ values ranging between -22 and -33‰ (Bender, 1971).

b) C_4 plants

C_4 plants use phosphoenolpyruvate carboxylase (PEPC) to convert phosphoenolpyruvate (PEP) into a C_4 acid, which is transported from the outer layer of photosynthetic cells (mesophyll cells) to the inner layer (bundle sheath cells) where it is decarboxylated. The released CO_2 is subsequently fixed by Rubisco and is further processed in the Calvin cycle. Since the substrate for PEPC is HCO_3^- rather than CO_2 (Rubisco), an additional fractionation step is present in C_4 plants compared to C_3 plants (O'Leary, 1981). The fractionation related to the incorporation of HCO_3^- into C_4 acids by PEP carboxylase is relatively small (2 to 2.5‰; O'Leary, 1981). Since some CO_2 released during the decarboxylation of PEP escapes, RuBP carboxylase contributes slightly to fractionation but is much smaller than in C_3 plants (O'Leary, 1981). As a result, plants that follow the C_4 metabolic pathway have relatively enriched $\delta^{13}C$ values ranging between -10 and -20‰ (Bender, 1971; O'Leary, 1981).

c) CAM plants

Crassulacean acid metabolism (CAM) plants fix CO_2 through the C_4 pathway at night in the form of malate. They switch to C_3 metabolism during the light period where CO_2 is released by decarboxylating malate and subsequently refixed through the C_3 pathway (O'Leary, 1981). CAM plants are able to switch their major flow of CO_2 via the PEP or RuBP carboxylase in response to environmental changes (Wong and Sackett, 1978). Variation in $\delta^{13}C$ in CAM plants then reflects the partitioning of these carboxylation pathways (O'Leary, 1981; Berry, 1989). The isotopic composition of CAM plants will show values intermediate to C_3 and C_4 plants depending on the relative importance of the C_3 versus C_4 metabolism (Bender, 1971; Maberly et al., 1992).

d) phytoplankton

Carbon fixation in phytoplankton cells follows the C_3 metabolism (Sharkey and Berry, 1985; Desgolas-Gros and Fontugne, 1990) and is catalyzed by Rubisco on which β-carboxylation is superimposed (Descolas-Gros and Fontugne, 1990). Recently, Reinfelder et al. (2000) reported the presence of a C_4 metabolic pathway in diatoms as a means of CO_2 storage in the cells. Such storage system could be activated in communities exhibiting light stress where the stored CO_2 could be released and fixed by Rubisco when light is available. Activation of the C_4 metabolic pathways will then lead to increased $\delta^{13}C$ signatures since PEP uses HCO_3^- instead of CO_2 as a C-source (Riebesell, 2000).

Also nutrient conditions can change the relative importance of CO_2 and HCO_3^- demand (Turpin et al., 1991; Riebesell et al., 2000). Indeed, the production of the whole range of amino acids requires three distinct C fixation reactions for the supply of carbon skeletons, being the CO_2 fixation by Rubisco, the HCO_3^- fixation by PEPC and the HCO_3^- fixation by carbamoyl phosphate synthetase (CPS). In NH_4^+ replete conditions and in case metabolizable exogenous resources are lacking, assimilation of NH_4^+ depends on recent products of CO_2 fixation by Rubisco. In nutrient deplete conditions, increased endogenous carbohydrate reserves supply the carbon skeletons for amino acid synthesis (Turpin et al., 1991). As such, NH_4^+ assimilation not longer depends on photosynthetic CO_2 fixation and β-carboxylation pathways increase in importance. The decreasing dependence of amino acid C derived from Rubisco metabolism with decreasing nutrient concentrations thus results in an increase in the $\delta^{13}C$ composition of phytoplankton (Turpin et al., 1991; Fouilland et al., 2002).

2.5.1.3. Fractionation during respiration

The fractionation during respiration is the third main factor affecting the $\delta^{13}C$ of primary producers. Photorespiration can both increase or decrease $\delta^{13}C$ of primary producers since both $^{13}CO_2$ as $^{12}CO_2$ is observed to be preferentially released during respiration (O'Leary, 1981). Indeed, Ivlev et al. (1996) and Igamberdiev et al. (2001) measured considerable and species dependent in vitro isotope fractionation by the glycine decarboxylase complex during respiration with values ranging between -8 and +16‰.

2.5.1.4. Factors influencing $\delta^{13}C$ of phytoplankton in the Scheldt estuary

In the Scheldt estuary, variation in the $\delta^{13}C$ signature of DIC is the most important factor accounting for the variation in the $\delta^{13}C$ composition of phytoplankton (Boschker et al., 2005). $\delta^{13}C_{DIC}$ signatures are low during winter due to a continuous input of respiratory light CO_2 and increase during the growth season due to preferential removal of $^{12}CO_2$ during algal uptake. Moreover, $\delta^{13}C_{DIC}$ values increase gradually in downstream direction due to the mixing with seawater which has enriched $\delta^{13}C_{DIC}$ values compared to freshwater (Hellings et al., 1999; 2001).

Residual variation in $\delta^{13}C$ of phytoplankton results from a combination of variations in growth rate, cell size, species composition and ambient CO_2 concentration. In general, overall fractionation during CO_2 uptake is smaller in the marine reaches compared to the oligohaline reaches (Boschker et al., 2005). The downstream decrease in fractionation results from an increase in phytoplankton growth rate, since growth rates in the oligohaline reaches are suppressed by light limitation, and from the downstream decrease in $CO_{2(aq)}$ concentrations (Boschker et al., 2005). Moreover, the phytoplankton community in the oligohaline reaches consists of small green algae and diatoms (Muylaert and Sabbe, 1999) while the relative contribution and the size of diatoms increases in downstream direction (Muylaert and Sabbe, 1999; Boschker et al., 2005). Since the silica containing cell wall of the diatoms might hamper the CO_2 flux through the cell wall, the enrichment of the internal C-pool may be larger for diatoms than for non-diatom species, which would result in a decrease in the overall fractionation in diatoms. In addition, fractionation is reported to decrease with increasing cell size (Rau et al., 1996; 1997; Burkhardt et al., 1999a; 1999b), so that an overall increase in the size of phytoplankton species will further decrease the overall fractionation. In the freshwater reaches, both large diatom and small non-diatom species dominate the phytoplankton community (Muylaert, 1999). Variation in $\delta^{13}C$ of phytoplankton might thus result from varying contributions of both phytoplankton groups to the phytoplankton community; when large diatoms dominate, the overall $\delta^{13}C$ signature of phytoplankton may be higher than when small, non-diatom species dominate. In the high turbidity reaches of the estuary, light limitation might decrease the overall fractionation during CO_2 uptake in diatoms exhibiting light stress via the activation of the C_4 metabolic pathway (Riebesell, 2000).

2.5.2. N fractionation in primary producers

Generally, knowledge about the fractionation during assimilation of N for the different N species is scarce compared to knowledge about fractionation associated with carbon assimilation. Moreover, many studies measured the assimilatory fractionation of N for cultured species, but culture fractionation values often differ substantially from the ones in the natural environment (Fogel and Cifuentes, 1993), especially for NH_4^+ uptake (Waser et al., 1998). Part of this discrepancy between fractionation values found in cultures and in the natural environment can be related to the fact that culture conditions rarely resemble these in the environment (Fogel and Cifuentes, 1993).

The $\delta^{15}N$ signature of primary producers is mainly set by the $\delta^{15}N$ signature of the N sources, the fractionation during N-uptake (Hoch et al., 1994) and fractionation during N-excretion (Yoneyama et al., 2001). Below, we present an overview of factors influencing N isotopic signatures in primary producers.

2.5.2.1. $\delta^{15}N$ of N sources

The three main N sources for primary producers are atmospheric N_2, NO_3^- and NH_4^+ (Yoneyama et al., 1993; 2001; Werner and Schmidt, 2002). The $\delta^{15}N$ composition of N_2 is 0‰ since it represents the standard for $\delta^{15}N$ (Mariotti, 1983) while the $\delta^{15}N$ composition of NO_3^- and NH_4^+ is highly variable and is set by biogeochemical processes such as denitrification, nitrification and biological uptake (Cifuentes et al., 1988).

During denitrification, anaerobic bacteria oxidize organic matter whereby NO_3^- serves as the electron acceptor while N_2-gas is produced (Cline and Kaplan, 1975). The denitrification process discriminates against ^{15}N so that N_2 produced is depleted in ^{15}N. Isotope fractionation values measured for denitrification vary considerably and appear to be affected by environmental conditions. Generally, the magnitude of isotope fractionation decreases with decreasing NO_3^- availability, increasing light levels or growth rate of denitrifying bacteria and by increasing availability of C-sources relative to the N-source (Wada, 1980). Isotope fractionations reported are 30-40‰ (Cline and Kaplan, 1975) and 28‰ (Yoshida et al., 1989) for in situ ocean denitrification, 29.4 ± 2.4‰ at 20°C decreasing to 24.6 ± 0.9‰ at 30°C (Mariotti et al., 1981), 13.9‰ (Smith et al., 1991) and 22.5 ± 0.6‰ (Dhondt et al., 2003) for soil denitrification and 2 to 12‰ for a culture of denitrifying bacteria (Wada, 1980).

The isotope fractionation value reported for a culture of nitrifying bacteria was 35‰ and did not change at varying NH_4^+ concentrations (Mariotti et al., 1981). The

range of fractionation values reported by Horrigan et al. (1990) for a coastal bay system (12.7 - 16.0‰) was yet much lower.

N uptake processes discriminate against ^{15}N (see below), so that the residual pool of N will increase with increasing biological uptake (Cifuentes et al., 1988).

2.5.2.2. Fractionation during uptake

Uptake of NH_4^+

a) Expression of fractionation during NH_4^+ uptake

The extent of isotope fractionation expressed during uptake of NH_4^+ varies considerable between studies and both negative and positive fractionation values have been reported (Table 2.5).

Table 2.5: Isotope fractionation associated with NH_4^+ uptake

ε	System	Reference
-9.7 to -5.3‰	Batch culture	Wada and Hattori, 1978
3.2 to 7‰	Batch culture	Wada, 1980
5 to 15‰	Natural system	Velinsky et al., 1991
20 to 30‰	Natural system	Velinsky et al., 1991
3.6 to 12.6‰	Plants	Yoneyama et al., 1991
10‰	Batch culture	Hoch et al., 1994
7.8 to 27.2‰	Batch culture	Pennock et al., 1996
20‰	Batch culture	Waser et al., 1998

b) NH_4^+ uptake pathways

The magnitude of isotopic fractionation during NH_4^+ uptake depends on the mechanism of NH_4^+ uptake through the cell membrane. There are two pathways for NH_4^+ uptake of which the induction depends on the ambient NH_4^+ concentration. The first pathway is responsible for the uptake of NH_4^+ at concentrations >1000 $\mu mol.l^{-1}$ and consists of membrane diffusion (passive) of NH_3 and its subsequent assimilation catalyzed by glutamate dehydrogenase (GDH). The second pathway consists of active NH_4^+ transport followed by glutamine synthetase (GS) catalyzed assimilation and is

responsible for the major part of NH_4^+ uptake at concentration levels below 100 μmol.l^{-1}. At ambient NH_4^+ concentrations between 100 and 1000 μmol.l^{-1}, both pathways contribute to uptake (Hoch et al., 1992).

c) Fractionation associated with the different steps during NH_4^+ uptake

The different processes contributing to NH_4^+ or NH_3 uptake each have their specific fractionation values. The fractionation due to deprotonation of NH_4^+ into NH_3 and diffusion of NH_3 is 19.2‰ (pH 7) and 20‰, respectively. Fractionation due to active NH_4^+ transport is not known (Hoch et al., 1992). The enzymatic fractionation of GS and GDH is strongly dependent on pH. Fractionation for GS changes from -10.8‰ to -2.8‰ between pH 7.1 and 8.6 (Hoch et al., 1992), while the one for GDH changes from -2‰ to -19.2‰ between pH 5.8 and 9.2. The negative fractionation of the enzymes is a result of the reversible character of their activity so that ^{15}N gets concentrated in the molecule with the strongest bound (glutamate); (Fogel and Cifuentes, 1993).

d) Factors affecting fractionation during NH_4^+ uptake

Finally, it is the fractionation associated with the rate limiting reaction during NH_4^+ uptake that will ultimately be expressed (Hoch et al., 1992). The nature of the rate limiting reaction is determined by the ratio of the NH_4^+ demand to the ambient NH_4^+ concentration (Hoch et al., 1994). Moreover, if the N-demand is high compared to the ambient NH_4^+ concentration, for instance for high growth rates (Wada, 1980; Yoneyama et al., 2001), the opportunity of $^{15}NH_4^+$ efflux will decrease and the fractionation expressed will decrease (Yoneyama et al., 2001).

At high NH_4^+ concentration (>1000 μmol.l^{-1}), GDH is the rate limiting step since diffusion will be rapid compared to NH_4^+ demand so that isotopic equilibrium for diffusion is attained and diffusion does not contribute to fractionation. The lower the ambient NH_4^+ concentration, the lower the flux toward the cell and the more the diffusion will contribute to fractionation and the higher ε. When diffusion does not satisfy cellular N demand, the active NH_4^+ transport systems is activated and NH_4^+ uptake by GS become the dominant enzymatic NH_4^+ uptake mechanism. Between 1000 and 100 μmol.l^{-1}, when both uptake pathways are active, the expression of fractionation reaches a maximal value of 27‰ (Hoch et al., 1992; Pennock et al., 1996). At concentrations below 100 μmol.l^{-1}, fractionation decreases again and the fractionation associated with both active transport and assimilation by GS will contribute to the overall fractionation expressed. The importance of the active NH_4^+

transport increases with decreasing ambient NH_4^+ concentration. Under very low NH_4^+ conditions, part of the ^{15}N depleted NH_3 that diffuses out of the cell into the boundary layer is protonated and re-assimilated, which result in an additional decrease in the fractionation expressed during NH_4^+ assimilation. As a result, fractionation during NH_4^+ uptake can reach values as low as 4‰ for NH_4^+ concentrations of 20 μmol.l^{-1} (Hoch et al., 1992). A similar phenomenon has been reported for plants, where ^{15}N-depleted NH_4^+ released during photorespiration is re-assimilated (Yoneyama et al., 1993).

Uptake of NO_3^-

Fractionation associated with NO_3^- is smaller than for NH_4^+. This is probably due to the smaller size of NH_4^+ molecules that provide a greater opportunity for discrimination than the large NO_3^- molecules (Yoneyama et al., 1993). Overall fractionation values calculated for NO_3^- uptake vary between studies (Table 2.6).

Table 2.6: Isotope fractionation (ε) associated with nitrate assimilation

ε	System	Reference
3 to 4‰	Natural system	Cline and Kaplan, 1975
0.7 to 23‰	Batch culture	Wada and Hattori, 1978
5‰	Natural system	Wada, 1980
0.4 to 14.8‰	Batch culture	Wada, 1980
7‰	Natural system	Horrigan et al., 1990
2.5‰	Natural system	Altabet and Francois, 1994
7 to 10‰	Natural system	Altabet and Francois, 1994
0.9 to 12.1‰	Continuous culture	Montoya and McCarthy, 1995
9.0‰	Batch culture	Pennock et al., 1996
5.2‰	Batch culture	Waser et al., 1998
-3.2 to 5.1‰	Plants	Yoneyama et al., 2001
4 to 5‰	Natural system	Karsh et al., 2003
7 to 10‰	Natural system	Karsh et al., 2003
5 to 7‰	Natural system	Lourey et al., 2003
2.2 to 6.2‰	Batch culture	Needoba et al., 2003

a) Nitrate assimilation pathway

Uptake of NO_3^- through the cell membrane in plants and micro-organisms is catalyzed by a special carrier system (Werner and Schmidt, 2002). In the cell, NO_3^- is transformed to NH_4^+ by the nitrate and nitrite reductase reaction after which NH_4^+ is incorporated into organic compounds (e.g. amino acids) (Wada and Hattori, 1978; Wada, 1980; Yoneyama et al., 1993).

b) Fractionation associated with the different steps during NO_3^- uptake

Nitrate reductase discriminates against ^{15}N (a maximum of 23‰ was calculated) while fractionation in the nitrite reductase reaction is negligible (Wada and Hattori, 1978). The isotope effect associated with NO_3^- uptake through the cell membrane is probably small (Wada and Hattori, 1978; Yoneyama et al., 2001). As a result, the produced NH_4^+ and consequently also amino acids are depleted in ^{15}N while ^{15}N-rich NO_3^- is accumulated and/or transported out of the cell (Yoneyama and Tanaka, 1999; Werner and Schmidt, 2002).

c) Factors affecting isotope fractionation during NO_3^- uptake

When NO_3^- uptake through the plasmalemma is the rate limiting step, NO_3^- reduction reactions will not contribute to isotope discrimination because they are unidirectional with total consumption of the substrate (Montoya and McCarty, 1995; Schmidt, 1999). The high isotope fractionation associated with nitrate reduction will only contribute to the overall fractionation if there is leakage of NO_3^- out of the cell (Needoba et al., 2003). On the other hand, if active transport of NO_3^- is sufficient to maintain high intracellular NO_3^- concentrations, nitrate reductase will be the major contributor to isotope fractionation and ε will be independent of the ambient NO_3^- concentration (Pennock et al., 1996). If NO_3^- uptake through the plasmalemma contributes largely to isotope fractionation, diffusion toward the cell surface may make a significant additive contribution to isotope fractionation so that cell motility of micro-organisms may reduce the isotope fractionation (Montoya and McCarthy, 1995; Needoba et al., 2003).

Fractionation during NO_3^- assimilation is reported to be inversely correlated to growth rate (Wada and Hattori, 1978; Wada, 1980; Montoya and McCarthy, 1995) although Needoba et al. (2003) did not find any relationship with growth rate. Factors affecting growth rate such as light (Wada and Hattori, 1978; Wada, 1980; Needoba et al., 2003) and iron (Karsh et al., 2003) limitation would increase the isotope

fractionation expressed and thus decrease the $\delta^{15}N$ composition of primary producers. The effect of light limitation on the fractionation expressed during NO_3^- uptake results from the fact that NO_3^- is an active process requiring light energy (Montoya and McCarthy, 1995; Needoba et al., 2003). The effect of iron limitation can be explained by the fact that nitrate reduction is catalyzed by two iron-containing enzymes (Karsh et al., 2003). However, there are large inter- and intraspecific variations in isotope fractionation with changes in growth rate (Montoya and McCarthy, 1995; Needoba et al. 2003). Nutrient limited growth rate would not affect fractionation (Montoya and McCarthy, 1995). When growth rate is not nutrient limited, increasing NO_3^- concentrations have been reported to result in increasing fractionation values (Wada and Hattori, 1978; Yoneyama et al., 2001).

Uptake of NO_2^-, urea and N_2 fixation

Isotope fractionation values reported for the incorporation of NO_2^- are 0.9‰ (Waser et al., 1998) and 0.7‰ (Wada and Hattori, 1978). For the incorporation of urea, an isotope fractionation of 0.8‰ has been reported (Waser et al., 1998). For N_2, the enzyme nitrogenase catalyses the assimilation of N_2 (Fogel and Cifuentes, 1993). There is only a small fractionation involved in N_2 fixation which is probably due to a lack of backward reaction in certain steps of N_2 fixation (Wada, 1980).

2.5.2.3. Effect of N release on the $\delta^{15}N$ of primary producers

The release of N-compounds by plants and micro-organisms can result in a significant enrichment of the residual organic matter (Yoneyama et al., 2001). For instance, the release of ^{14}N-rich NH_4^+ may cause ^{15}N enrichment in the remaining ureides of plants (Yoneyama and Tanaka, 1999). Isotope fractionation associated with the release of NH_4^+ by bacteria or protists has not been directly measured, but the released NH_4^+ is probably depleted in ^{15}N by 3‰ (Hoch et al., 1994). Also the release of DON with low ^{15}N content through excretion or cell lysis may increase the $\delta^{15}N$ of the residual organic matter, which may be more important for slow growing phytoplankton (Montoya and McCarthy, 1995).

2.5.3. Fractionation during C and N metabolism

Once CO_2 and NH_4^+ are assimilated, additional fractionation may occur during the metabolism of organic compounds when reactions implying kinetic isotope effects

occur at metabolic branching points (O'Leary, 1981; Schmidt, 1999). The resulting metabolites then have isotopic compositions that differ from the ones of the overall cell (O'Leary, 1981) whereby the final isotopic signatures of the metabolic groups are determined by the pathway through which they are synthesized (Werner and Schmidt, 2002) and the relative yield of the end-products. Here, the end-product with the highest yield will be depleted relative to the original source while the one with the lowest yield will be enriched compared to the original source (Schmidt, 1999). The δ-value of the overall cell will, however, remain equal to the original isotopic signature of the CO_2 and NH_4^+ assimilated (O'Leary, 1981; Hayes, 1993).

Generally, lipids are highly depleted in ^{13}C compared to other organic compounds, while the carboxyl group of amino-acids roughly equals the original $\delta^{13}C$ (Abelson and Hoering, 1961). Also lignin is depleted in ^{13}C compared to bulk material, while proteins and carbohydrates (e.g. cellulose) are generally enriched in ^{13}C compared to total plants tissue (Fernandez et al., 2003).

Proteins are generally enriched in ^{15}N, while chlorophyll, lipids, amino sugars and alkaloids are generally depleted in ^{15}N. All N containing organic compounds are synthesized ultimately from glutamine. Fractionation during amino-acids metabolism depends on the enzyme catalyzing the transfer of the NH_2-group from glutamine (Macko et al., 1986; Werner and Schmidt, 2002). Moreover, fractionation involved in transamination reactions differs according to the direction of the reaction (Macko et al., 1986).

2.5.4. Fractionation during decay processes

Decomposition is a complex process involving dissolution of soluble substances from cells, autolysis, deamination, ammonification, coagulation of dissolved substances and bacterial growth (Wada, 1980). Potential mechanisms leading to changes in the isotopic signal of degrading organic matter involve preferential loss of isotopically distinct fractions, kinetic isotopic fractionation during release processes (Lehmann et al., 2002) and the addition of organic matter with different δ-values from bacterial growth (Caraco et al., 1998; Lehmann et al., 2002). The fractionation reported for mineralization of particulate organic nitrogen is 3-6‰ (Montoya et al., 1992).

The difference in isotopic signatures of metabolic groups can be important in case of preferential decomposition of molecules (Hayes, 1993). If one specific protein is degraded relative to another, then overall isotopic composition of the bulk material can shift in response to preferential decay or preservation of particular molecules (Harvey et al., 1995; Fogel and Tuross, 1999). For instance, proteins and carbohydrates are utilized more rapidly than lipids during degradation (Harvey et al., 1995). Also

hydrolysis of peptides can also markedly increase the $\delta^{15}N$ and $\delta^{13}C$ composition of the remaining organic matter (Bada et al., 1989). Isotope fractionations during hydrolysis of peptides of 2.5 to 4‰ (Silfer et al., 1992) and 10‰ (Bada et al., 1989) have been reported.

2.5.5. C and N fractionation during transfer to higher trophic levels

Fractionation has been reported to occur both during the assimilation of C and N compounds. The increase in $\delta^{13}C$ and $\delta^{15}N$ relative to the food source and per trophic level averages 0.8 ± 1.1‰ (DeNiro and Epstein, 1978; Fry and Sherr, 1984; Vander Zanden and Rasmussen, 2001) and 3.4 ± 1.1‰ (Minagawa and Wada, 1984; Vander Zanden and Rasmussen, 2001), respectively. The relative constancy of these values for different habitats and for organisms with distinct metabolism makes that $\delta^{13}C$ and $\delta^{15}N$ can be used both for food source as trophic level indicators (Fry and Sherr, 1984, Minagawa and Wada, 1984). As a result, combining $\delta^{13}C$ and $\delta^{15}N$ measurements offers the opportunity to clearly distinguish between consumer and producer groups and their respective food sources.

The enrichment in ^{13}C with trophic level results from the release of respiratory CO_2 depleted in ^{13}C (DeNiro and Epstein, 1978; Rau et al., 1983). However, large deviations from the 0.8‰ enrichment are reported in cases where animals have high body-lipid content (Focken and Becker, 1998), which is known to be highly depleted in ^{13}C (Abelson and Hoering, 1961).

The overall enrichment in $\delta^{15}N$ in organisms results from the higher fractionation associated with the release of N-compounds during metabolism compared to the one associated with N-assimilation. Amino acids taken up from the food have been deaminated during assimilation, a process discriminating against ^{15}N, so that the amino acids taken up are lighter than the bulk food (Macko et al., 1986; 1987). Then, additional fractionation occurs during the catabolism of body-proteins for the excretion of NH_4^+. The net result is that organisms get enriched compared to their food source (Ponsard and Averburch, 1999). However, it must be noted that enrichments higher than 3.4‰ can occur when organisms experience stress situations like fasting or nutrient deficiency. In that case, nitrogenous compounds used for protein synthesis are derived from catabolism of available proteins already enriched in ^{15}N compared to the food source which result in additional enrichment (Hobson and Clark, 1992; Hobson et al., 1993).

Material and Methods

Chapter 3

3.1. Field sampling

Field samplings performed in the studies described in the following chapters fall into three categories. First, between May 1999 and April 2001 a monthly sampling campaign was conducted in the freshwater to mesohaline section of the estuary to cover both spatial and temporal variation of the parameters under study. Second, between February 2001 and July 2001 some additional sampling was done to extend the study area to the polyhaline to marine part of the estuary. Samplings for these campaigns were done on board of the vessels MS Veremans, Scaldis II or Luctor. Environmental data such as O_2, pH, salinity, conductivity, temperature and ammonium, nitrate, nitrite, and chlorophyll *a* concentrations were monitored on board in the frame of the OMES project and provided by S. Van Damme and T. Maris (University of Antwerp) or J. Middelburg (Centre for Estuarine and Marine Ecology, The Netherlands). Third, between October 2001 and April 2003 an in situ experiment was carried out at a freshwater station to study the seasonal patterns of some specific parameters into more detail. Here, sampling and monitoring of physico-chemical parameters was conducted from a floating pontoon attached to the river bank.

3.1.1. Suspended particulate organic matter

Suspended particulate organic matter (SPOM) for $\delta^{13}C$, $\delta^{15}N$, C/N analyses and suspended particulate matter load (SPM) measurements was collected by sampling surface water with a clean polyethylene bucket or a niskin bottle. The water sample was thoroughly homogenized before a subsample was taken. Depending on suspended matter load, 80 to 300 ml of water was immediately filtered in triplicate through pre-weighted Whatman GF/C glassfiber filters (Ø = 47 mm, nominal pore size 1 μm). After filtration, samples were immediately frozen in liquid nitrogen or transported to the laboratory in a cooling box. In the laboratory, samples were thawed and dried at 50°C till constant weight. Concentrations of SPM were calculated based on the dry weight of the suspended material collected on the filter and the volume of water filtered. Particulate organic nitrogen and carbon (PON and POC) concentrations were calculated based on the amount of organic N and C trapped on the filter and the volume of water filtered.

3.1.2. Zooplankton

Zooplankton was sampled by towing a 300 μm net below the water surface for 10 to 15 minutes and kept in filtered (GF/C, nominal pore size 1 μm) Scheldt water for 2 hours to empty their gut contents. A period of 2 hours largely exceeds the time needed to clear the gut content of copepods since estimates of the gut clearance time based on the linear regressions provided by Dam and Peterson (1988) range between 90 and 20 min for temperature ranging between 0 and 20°C. The zooplankton sample was then strained over a small 300 μm net cut-out (Ø = ± 7 cm) and frozen in liquid nitrogen. In the laboratory, samples were stored at −80°C until analysis. Prior to analysis, zooplankton were thawed in distilled water. Copepods were hand-picked from the detritus-rich sample whereby calanoid and cyclopoid copepods were grouped together and dried at 50°C. An average of 300 to 800 copepods had to be pooled to ensure reliable C and N isotopic measurements.

3.1.3. Total alkalinity and $\delta^{13}C_{DIC}$

For the analysis of $\delta^{13}C_{DIC}$, a penicillin flask of 25 ml ($\delta^{13}C_{DIC}$) was filled with water collected in a clean polyethylene bottle while care was taken to avoid trapping air bubbles. Bottles were rinsed 3 times with Scheldt water before the actual sample was taken. 20 μl of a saturated $HgCl_2$ solution was added to stop all biologic activity after which the bottles were closed airtight and stored in a refrigerator until analysis.

3.1.4. Nutrients

Surface water samples for the analysis of NH_4^+, NO_3^- and NO_2^- were taken using a polyethylene bucket. Samples were filtered through GF/C Whatman filters (Ø = 47 cm, nominal pore size 1 μm), and stored in 50 ml polypropylene bottles at -20°C until analysis. NH_4^+ was analyzed using the indophenol blue method. NO_3^- and NO_2^- were analyzed with the cadmium reduction method using a Technicon auto-analyzer.

3.1.5. Chlorophyll-a

Suspended matter for determination of chlorophyll *a* concentrations was collected by sampling surface water with a clean polyethylene bucket. Depending on suspended matter load, 120 to 250 ml of water was filtered in triplicate on Whatman GF/C glassfiber filters (Ø = 47 mm, nominal pore size 1 μm). The filters were

immediately transferred to a cooling box for storage at -80°C at arrival in the home laboratory. Chlorophyll *a* concentrations were analyzed using the spectrophotometric method of Lorenzen (1967) and calculated using following equation:

$$\text{Chl a } (\mu g/l) = k \times F \times (A^{0}_{max} - A^{a}_{max}) \times \frac{v}{V}$$

Where k = 11, the absorption coefficient of Chl-a

F = 2.43, the factor to equate the reduction in absorbancy to initial concentration of Chl-a

$A^{0}_{max} = A_{max} - A_{750nm}$,

$A^{a}_{max} = A^{acid}_{max} - A^{acid}_{750nm}$

A_{max} = maximum absorbance of the sample at a wavelength λ between 663 and 669 nm

A_{750nm} = absorbance at 750 nm before acidification

A^{acid}_{max} = maximum absorbance at a wavelength λ between 663 and 669 nm after acidification of the sample with 1N HCl

A^{acid}_{750nm} = absorbance at 750 nm after acidification

v = volume of the extract (ml)

V = filtration volume (l)

3.1.6. O_2, pH and temperature

During the in situ experiments, dissolved oxygen concentration, pH and temperature were measured in situ using an O_2-meter (Thermo Orion 810A *plus*) and a pH-meter (Thermo Orion 230A *plus*).

3.2. Pre-treatment of samples for $\delta^{13}C$, $\delta^{15}N$ and C/N measurements

For $\delta^{13}C$ and C/N analyses of sediment or plant material, dry and homogenized samples were transferred into silver cups to which a drop of HCl 1M was added to remove all inorganic carbon. The samples were dried at 50°C for 24 hours before closing the cups. Filter samples for C/N_{SPOM} and $\delta^{13}C_{SPOM}$ were sub-sampled using a circle cutter of 14 mm and 10 mm diameter, respectively. Cut-outs were left in a HCl acid vapor environment for 2 hours to remove carbonates and subsequently dried at 50°C for 24 hours, before being packed in tin cups.

For the analysis of $\delta^{15}N$ of plants and sediment material and for $\delta^{13}C$ and $\delta^{15}N$ analyses of animal tissue, dry and homogenized material was transferred into Sn cups. Filter samples for $\delta^{15}N$ and PON contents were subsampled using a circle cutter (Ø = 14 mm) before being packed in Sn cups.

In case of zooplankton, the amount of samples obtained by handpicking was usually small so that both $\delta^{13}C$ and $\delta^{15}N$ measurements had to be performed on the same sample. Animal tissue did not require acid treatment since animal tissue does not contain inorganic carbon. Moreover, addition of acid can affect the $\delta^{15}N$ composition (Bunn et al., 1995).

3.3. Laboratory analyses

3.3.1. C/N ratio, PON and POC content

Measurements of C/N ratios and organic contents of nitrogen and carbon were conducted using a Carlo Erba NA 1500 elemental analyzer (Nieuwenhuize et al., 1994). This instrument converts all particulate C and N to a purified stream of CO_2 and N_2 gas through combustion.

Samples, packed in Sn or Ag cups, are introduced in a combustion column at 1010°C, containing chromium trioxide (Cr_2O_3) and silver-coated cobaltic oxide ($AgCo_3O_4$) as oxidation catalysts. Under excess of ultra-pure O_2, samples are flash combusted (temperature rises to 1700°C) to CO_2, NO_x, H_2O, sulphur and halogenated gaseous compounds. A constant flow of ultra pure helium flushes the gasses through a combustion and reduction column, a water trap and a chromatographic column. Halogenated gasses are retained by the silver coating on the cobaltous oxide in the combustion column. The reduction column contains Cu which retains all excess O_2 and reduces NO_x to N_2, forming CuO. The remaining CO_2, N_2 and H_2O gasses are swept over a magnesium perchlorate filter to remove the water vapor. CO_2 and N_2 are separated by the gas chromatographic column while a signal proportional to their concentration is generated by a thermal conductivity detector (TCD). The CO_2 and N_2 peaks on the gas chromatogram are subsequently integrated using the Eager200 software. The conversion of the sample peak area to POC and PON concentrations is obtained by a conversion factor *K*, which is determined based on the peak area of the reference material acetanilide (C_8H_9ON), its C and N composition (C: 71.09%, N: 10.36%) and the amount of reference material analyzed. In case filters were analyzed, PON and POC

concentrations are back-calculated using the ratio filter cut-out/whole filter and the filtered volume.

3.1.1. $\delta^{13}C$ and $\delta^{15}N$ measurements

$\delta^{15}N$ and $\delta^{13}C$ measurements were performed using both a manual and an automated procedure. The manual method consists of the off-line cryogenic purification of CO_2 and N_2 gasses produced by combustion in the NA1500 elemental analyzer and subsequent measurement on a Delta E isotope ratio mass spectrometer (IRMS). A complete description of the manual method can be found in Marguillier (1998), Hellings (2000) and Bouillon (2002). Automated $\delta^{13}C$ and $\delta^{15}N$ were performed using a Thermo Finnigan Delta^{PLUS}XL IRMS connected to an elemental analyzer (EA) (Flash series 1112) by a continuous flow interface (Finnigan Conflo III). Here, isotope ratios of samples and standards were calculated relative to a reference working gas (CO_2 or N_2) with a fixed δ-value being $\delta^{13}C$ = 29.2‰ for CO_2 and $\delta^{15}N$ = 0.0‰ for N_2. The δ-values of these gasses were chosen arbitrarily, but close to the real value. The isotopic composition of a sample, measured relative to the working reference gas, varies linearly with increasing deviation between the pressure of reference working gas and sample. Therefore, in order to accurately correct for this linear variation, reference material with accurately known isotopic composition was analyzed in replicate ($\geq$ 5) whereby the amplitudes of the N_2 and CO_2 peaks of the reference material spanned the range of sample amplitudes. Measured values of samples and reference material were first blank-corrected, taking into account isotopic values and relative masses of sample or reference and blank cup, after which a correction for deviations due to linear variation was performed. Finally, a last correction corrected for the deviation between the real value of a sample and the one that was measured relative to the arbitrarily chosen δ-value of the reference gas by using the known isotopic signature of the reference material.

For the measurements of $\delta^{15}N$, reference materials used were IAEA-N1: $\delta^{15}N$ = +0.43 ± 0.7‰ and IEAE-N_2: $\delta^{15}N$ = +20.41 ± 0.12‰. For $\delta^{13}C$ measurements IAEA-C6 (sucrose): $\delta^{13}C$ = -10.4 ± 0.1‰ was used as reference material.

The repeatability of repeated measurements of the reference material (n = 5 to 8) was <0.1‰ for $\delta^{13}C$ and $\delta^{15}N$ of plant material, sediments and animal tissue. For glassfiber filters, which are difficult to combust, precision decreased to <0.3‰ and <0.2‰ for $\delta^{15}N$ and $\delta^{13}C$ measurements, respectively.

3.1.2. $\delta^{13}C_{DIC}$

For the $\delta^{13}C_{DIC}$ measurements, two procedures were used. The first procedure is a manual method modified from Kroopnick (1974) and is described in detail in Hellings (2000) and Bouillon (2002). In the second procedure DIC measurements are automated by injecting CO_2 sample and standard gas directly in the elemental analyzer. Samples are prepared following a modified method of Miyajima et al. (1995): 5 ml of helium is injected in the penicillin bottle to create a head-space in the bottle while the same amount of water is simultaneously removed with a syringe. All DIC is converted to CO_2 by injecting 250 μl of pure ortho-phosphoric acid in the bottle. Bottles are shaken and kept on their side to prevent accidental CO_2 exchange with the air through the injection hole and kept overnight at room temperature to allow the conversion to CO_2 to complete. Prior to injection of CO_2 into the EA, a syringe is flushed with helium to prevent air CO_2 to be trapped in the syringe. Sample gas from the headspace, consisting of a mixture of He, CO_2 and H_2O, is subsequently injected in an injection tube located between the reduction column and the water trap of the EA. The carrier gas (He) flushing the EA sweeps the gasses over the magnesium perchlorate filter to remove the H_2O vapor while CO_2 is transferred to the IRMS. Injections of standard CO_2 gas, of which the exact $\delta^{13}C$ composition is measured relative to MAR 1 ($CaCO_3$ laboratory standard, calibrated against the certified carbonate standard NBS 19), are used to correct for deviations relating to the use of reference working gas with an arbitrarily chosen $\delta^{13}C$ composition. The repeatability of repeated measurements of reference material was <0.2‰.

Autotrophic versus heterotrophic food sources of calanoid and cyclopoid copepods in the freshwater to mesohaline reaches

Chapter 4

4.1 Introduction

Estuaries are aquatic systems typically carrying large amounts of organic matter from allochthonous and autochthonous origin. The presence of large amounts of organic matter leads to high bacterial production supporting heterotrophic food chains (Azam et al., 1983; Findlay et al., 1991). In aquatic systems showing a gradient of decreasing suspended matter load, the relative importance of heterotrophic feeding decreases favoring autotrophic grazing (Koski et al., 1999). The autotrophic food web is then characterized by a phytoplankton-copepod link, while in the microbial loop bacteria, ciliates and flagellates are the dominant food items (Azam et al., 1983; Koski et al., 1999).

The Scheldt estuary is characterized by high suspended matter loadings, with maxima up to a few 100 mg per liter in the maximum turbidity zone situated in the mixing zone of freshwater and seawater (Chen, 2003). The suspended matter load declines towards the mouth of the estuary (Chen, 2003), which suggests that there should be a gradual increase in the importance of the photo-autotrophic food chain in downstream direction. Indeed, Hummel et al. (1988) and Hamerlynck et al. (1993) reported on the existence of two distinct food chains in the Scheldt estuary: a detritus-based food chain in the mesohaline reaches, situated roughly between 40 to 60 km from the mouth of the estuary, and a photo-autotrophic food chain in the lower marine reaches (between km 20 and km 0). Reports on food webs are lacking for the zone between km 40 and 20 (Hamerlynck et al., 1993) and the oligohaline zone upstream from km 60 (Soetaert and Herman, 1994) since the copepod community was nearly or completely absent in these sections of the estuary. The absence of the copepod community in the oligohaline zone upstream of km 60 was merely due to the prevailing anoxic conditions (Soetaert and Herman, 1994). During the nineties, the O_2 concentrations in the Scheldt system improved due to enhanced wastewater treatment (Van Damme et al., *in press*). As a result, the copepod biomass increased drastically in the zone upstream of km 60 (Appeltans et al., 2003) and has increased by two orders of magnitude compared to the sixties (Tackx et al., *in press*). Nowadays both calanoid (*Eurytemora affinis* and *Acartia tonsa*) and cyclopoid copepod (mainly *Acanthocyclops* sp.) species reside in this section (Azemar, *unpubl. res.*). The calanoid *E. affinis* has even penetrated the freshwater reaches (Appeltans et al., 2003). In the mid-nineties, a heterotrophic food web has been described for the freshwater and oligohaline reaches in which cyclopoid copepods were assumed top-predators. However, their role as grazers of phytoplankton is not exactly known (Muylaert, 1999).

The high loads of detritus in the Scheldt estuary led Hummel et al. (1988) assume that the calanoid copepods *Eurytemora affinis* and *Acartia tonsa* fed mainly on

detritus. *Acartia* species are mainly omnivorous, although with an increasing preference for motile prey like ciliates and flagellates as turbulence increases (Rollwagen Bollens and Penry, 2003). Also *E. affinis* switches to a more carnivorous feeding mode when suspended matter concentrations increase (Gasparini and Castel, 1997). However, a more recent study of the food selection of *E. affinis* in the Scheldt estuary has shown that *E. affinis* can feed very selectively on phytoplankton, even in extreme turbid conditions (Tackx et al., 2003). Thus, the presence in the freshwater and oligohaline reaches of calanoid copepods would imply that there is an adequate pelagic food web operating there, with autotrophic and heterotrophic components.

Stable C and N isotopes offer an interesting tool to investigate heterotrophic and autotrophic feeding patterns since consumers reflect the isotopic composition of their prey within the range of a few units. Because of the constant fractionation between animals and their prey, comparisons between isotopic signatures of animal and prey reveal both diet and trophic level information (Chapter 2). However, the isotopic signatures of small organisms such as copepods and their prey may vary considerably since short-living organisms with high tissue-turnover rates have the potential to rapidly reflect variation in C and N isotopic signatures of their food substrates (Goering et al., 1990; Montoya et al., 1990; Leggett et al., 1999; Grey et al., 2001; Vizzini and Mazzola, 2003).

Earlier studies on the isotopic signature of SPOM in the Scheldt estuary already reported on the highly variable nature of the $\delta^{15}N_{SPOM}$ and $\delta^{13}C_{SPOM}$ signatures, induced by the presence of phytoplankton thriving on inorganic substrates with highly variable isotopic composition (Mariotti et al., 1984; Hellings et al., 1999). We may thus expect zooplankton isotopic signatures to show considerable spatio-temporal variation in the Scheldt estuary.

Our main objective is to investigate spatial and seasonal variation in the importance of heterotrophic and autotrophic food sources of calanoid and cyclopoid copepods. Therefore, we investigated the monthly variation of C and N isotopic signatures of copepods at different stations along the salinity gradient and related their isotopic signatures to the ones of SPOM to check if changes observed in isotopic signatures do originate from natural changes in the isotopic composition of the food sources or from changes in the autotrophic and heterotrophic sources at the base of the food web.

4.2 Material and Methods

Samples for the determination of $\delta^{13}C$, $\delta^{15}N$ of zooplankton and $\delta^{13}C$, $\delta^{15}N$ of C/N of SPOM were collected at 4 stations along the Scheldt estuary during longitudinal transects in the frame of the OMES project (Figure 4.1). Stations S1 (freshwater section) and S4 (mesohaline zone) were sampled monthly between May 1999 and March 2001 (S4) or April 2001 (S1); stations S2 and S3 (oligohaline zone) were sampled monthly between October 1999 and March 2001. Detailed descriptions of the sampling procedure for suspended matter and zooplankton and the analysis of $\delta^{13}C$, $\delta^{15}N$ and C/N are provided in Chapter 3.

Environmental parameters (ammonium, nitrate, nitrite, O_2, temperature, conductivity, suspended matter load, particulate organic carbon and nitrogen load and Chl a) were monitored during the same cruises used for SPOM sampling. Data of nutrients, O_2, temperature and conductivity and data of Chl-a, suspended matter load and particulate organic carbon (POC) and nitrogen (PON) load were kindly provided by S. Van Damme (University of Antwerp) and J. Middelburg (NIOO-CEME, Yerseke), respectively. Discharge data, measured at Schelle (km 90), were obtained from Taverniers (1999; 2000; 2001).

Correlations between $\delta^{13}C$ and $\delta^{15}N$ of SPOM, copepods and environmental parameters were investigated using Spearman Rank correlation statistics.

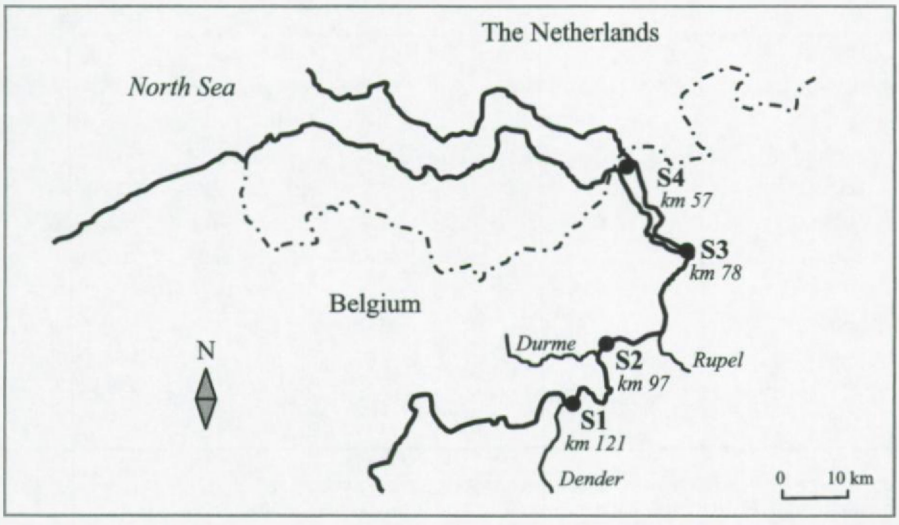

Figure 4.1: Map of the Scheldt estuary showing the sampling stations S1 to S4 and their respective distance to the mouth of the estuary.

4.3 Results

4.3.1 Environmental parameters

Ambient O_2 concentrations were highest during winter and decreased considerably during summer (Fig. 4.2; Table 4.1). Nutrient loads were high with NO_3^- as the dominant N-species. NH_4^+ concentrations were lowest and NO_2^- concentrations highest during summer, while NO_3^- concentrations showed a minimum during autumn. At station S4, O_2 conditions improved and NH_4^+ and NO_2^- concentrations lowered due to the mixing of Scheldt water with O_2-rich and nutrient poor seawater.

Phytoplankton blooms occurred in spring and early summer (downstream area) or in spring and mid-summer, early-autumn (upstream reaches) with maximum Chl-a concentrations up to 10 $\mu g.l^{-1}$ and 140 $\mu g.l^{-1}$ in the downstream and upstream area, respectively. Suspended matter load was high, ranging between 20 and 345 $mg.l^{-1}$ with highest values observed at S2. C/N ratios ranged between 5.1 and 13.7 and showed no specific seasonal pattern at any station. Overall POC and PON concentrations were highest at station S2. During the course of the sampling period, discharge varied between 53 and 315 $m^3.s^{-1}$, with highest values observed during winter.

Table 4.1: Range of values (min-max) of ambient parameters at stations S1 to S4 of the Scheldt estuary (1999-2001).

	S1	S2	S3	S4
Temperature (°C)[a]	6.1 - 23.6	6.4 - 23.5	5.8 - 22.4	6.3 - 22.3
Conductivity ($\mu S.cm^{-1}$)[a]	710 - 1156	694 - 1791	669 - 14390	2160 - 22100
O_2 ($mg.l^{-1}$)[a]	0.3 - 7.6	0.5 - 7.7	0.2 - 7.0	3.6 - 8.6
NH_4^+ ($\mu mol.l^{-1}$)[a]	<6 - 407.1	<6 - 335.7	<6 - 235.7	<6 - 114.3
NO_3^- ($\mu mol.l^{-1}$)[a]	100.0 - 464.3	200.0 - 471.4	228.6 - 392.9	221.4 - 414.3
NO_2^- ($\mu mol.l^{-1}$)[a]	8.6 - 90.7	8.6 - 45.7	<6 - 34.3	2.1 - 13.6
SPM load ($mg.l^{-1}$)[b]	---	20.0 - 344.5	16.8 - 129.1	16.0 - 177.6
Chl-a ($\mu g.l^{-1}$)[b]	---	3.2 - 139.6	1.1 - 69.1	1.0 - 9.5
POC ($mg.l^{-1}$)[b]	---	1.7 - 15.0	1.2 - 7.3	0.5 - 7.6
PON ($mg.l^{-1}$)[b]	---	0.1 - 1.6	0.1 - 0.7	0.1 - 0.7
C/N_{SPOM}	6.6 - 10.8	5.1 - 10.0	6.0 - 11.7	7.5 - 13.7
Discharge ($m^3.s^{-1}$)[c]	53 - 315			

--- : no data
[a]: data source: T. Maris, University of Antwerp, Belgium, pers. comm.
[b]: data source: J. Middelburg, NIOO-CEME, The Netherlands, pers. comm.
[c]: data source: Taverniers (1999; 2000; 2001)

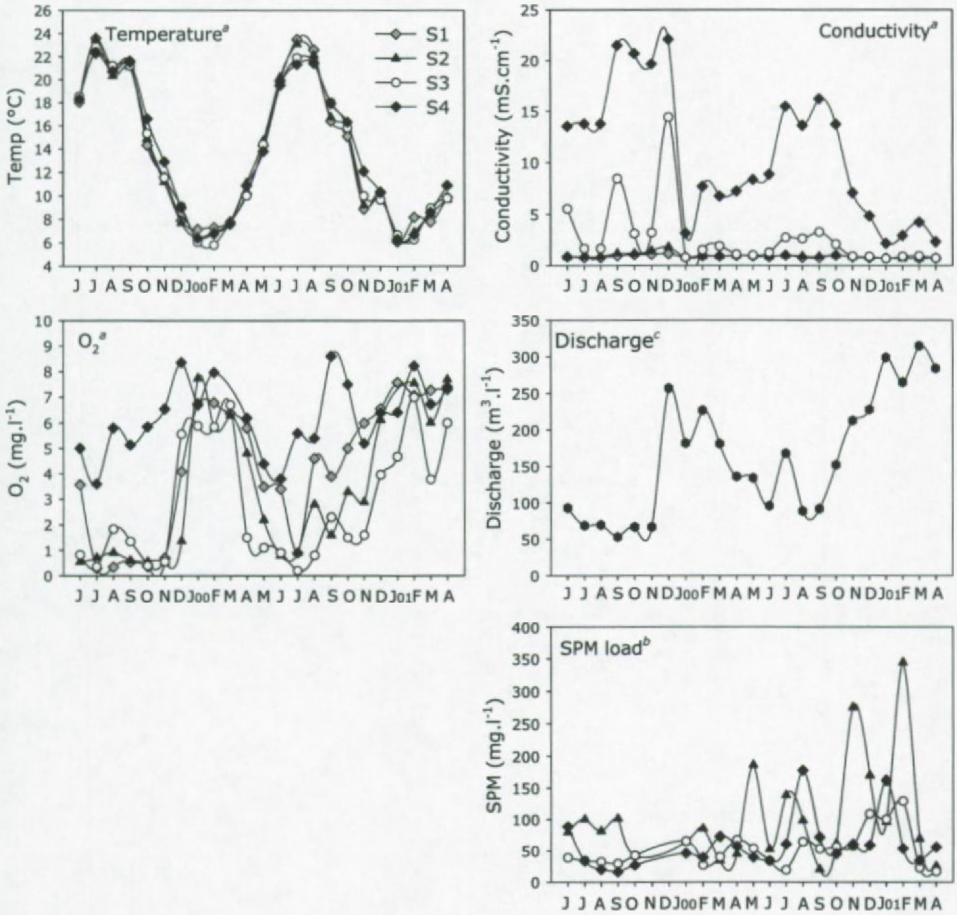

Figure 4.2: Monthly variation of environmental parameters at stations S1 (grey diamond), S2 (triangle), S3 (circle) and S4 (black diamond) of the Scheldt estuary (1999-2001).

[a]: data source: T. Maris, University of Antwerp, Belgium, pers. comm.
[b]: data source: J. Middelburg, NIOO-CEME, The Netherlands, pers. comm.
[c]: data source: Tavernier s (1999; 2000; 2001)

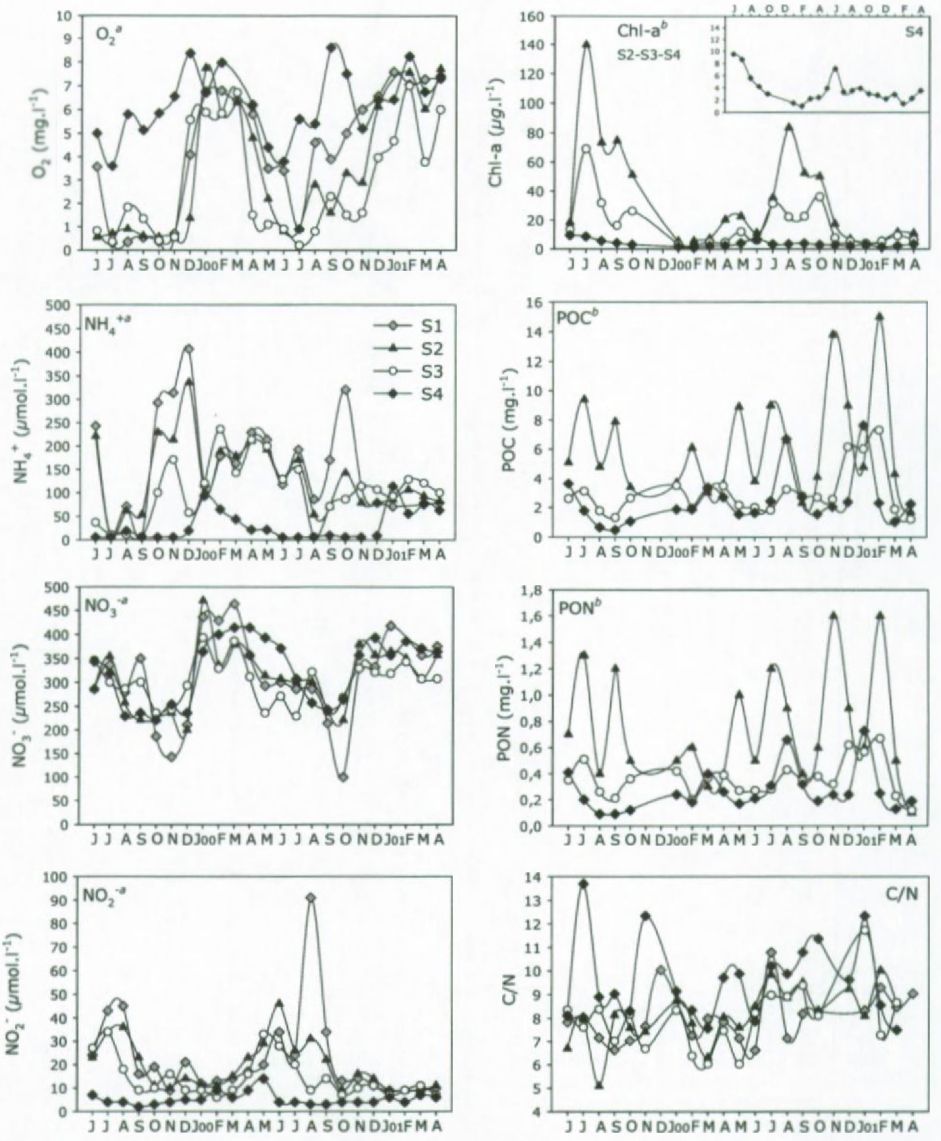

Figure 4.2: (continued)

4.3.2 Seasonal variation in copepod $\delta^{13}C$ and $\delta^{15}N$ signatures

4.3.2.1 $\delta^{15}N$ patterns of cyclopoid copepods

Cyclopoid copepod $\delta^{15}N$ signatures showed large seasonal variability at all stations (Fig. 4.3). A comparison between the general seasonal patterns of $\delta^{15}N$ of cyclopoid copepods ($\delta^{15}N_{cyc}$) showed that station S1 differed from other stations. At S1, we observed a gradual increase in $\delta^{15}N_{cyc}$ between early summer and winter with $\delta^{15}N_{cyc}$ values remaining relatively stable in winter (January-March 2000) and summer (June-September 2000). At stations S2, S3 and S4, $\delta^{15}N$ signatures of copepods were highest during summer and lowest during winter-early spring, but the summer increase was less pronounced at S2.

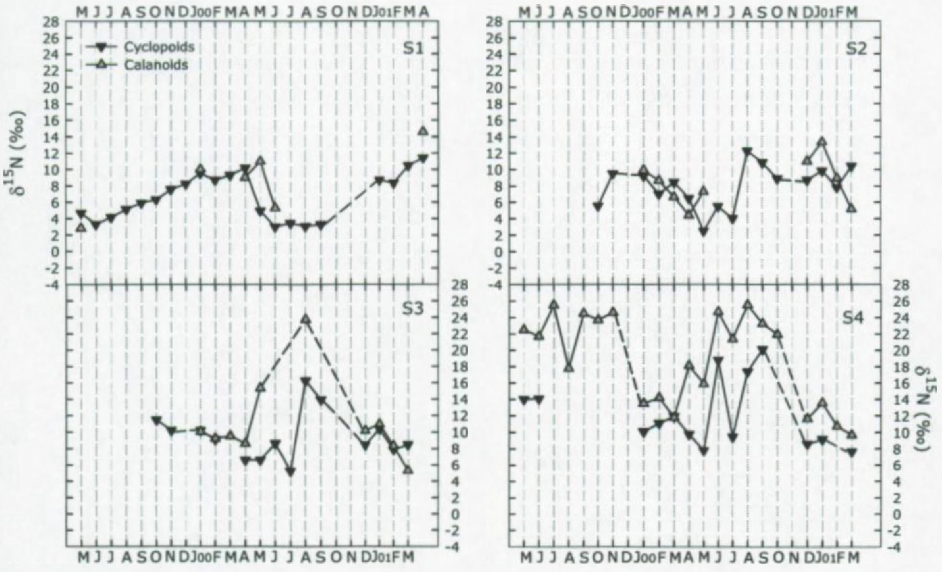

Figure 4.3: Seasonal variation in $\delta^{15}N$ of cyclopoid and calanoid copepods at stations S1 to S4 of the Scheldt estuary (1999-2001).

4.3.2.2 $\delta^{15}N$ patterns calanoid copepods

At S1 and S2, the $\delta^{15}N$ signatures of calanoid copepods ($\delta^{15}N_{cal}$) were similar to the ones of the cyclopoid copepods (Fig. 4.3). At S3 and S4, $\delta^{15}N_{cal}$ signatures were generally enriched in ^{15}N compared to $\delta^{15}N_{cyc}$. The general $\delta^{15}N$ pattern of calanoid copepods was quite similar to the one of cyclopoid copepods, but the increase in $\delta^{15}N$

started slightly earlier in the season; at S3 and S4, $\delta^{15}N_{cal}$ increased sharply during spring while $\delta^{15}N_{cyc}$ values increased only during summer. $\delta^{15}N_{cal}$ showed an overall decrease in autumn with minimum values reached in winter.

4.3.2.3 $\delta^{13}C$ patterns of cyclopoid and calanoid copepods

$\delta^{13}C$ values of copepods were highly variable at all stations (Fig. 4.4). The $\delta^{13}C$ signature of cyclopoid copepods ($\delta^{13}C_{cyc}$) did not show a consistent seasonal pattern, except at S4 where $\delta^{13}C_{cyc}$ and $\delta^{13}C_{cal}$ were clearly lowest during late-spring, early-summer. $\delta^{13}C$ signatures of calanoid copepods ($\delta^{13}C_{cal}$) were highest during winter and lowest during the growth season, which extends from spring to late summer at S1, S2 and S3 and from spring to early summer at S4 (Van Spaendonk et al., 1993; Kromkamp et al., 1995; Muylaert et al., 2000a).

At S1, $\delta^{13}C_{cal}$ values were slightly depleted compared to $\delta^{13}C_{cyc}$ values. At S3, $\delta^{13}C_{cal}$ values were highly enriched relative to $\delta^{13}C_{cyc}$ during the winter of the second year. During the summer of the second year at S4, the opposite was observed; here, $\delta^{13}C_{cyc}$ values were enriched relative to the ones of $\delta^{13}C_{cal}$.

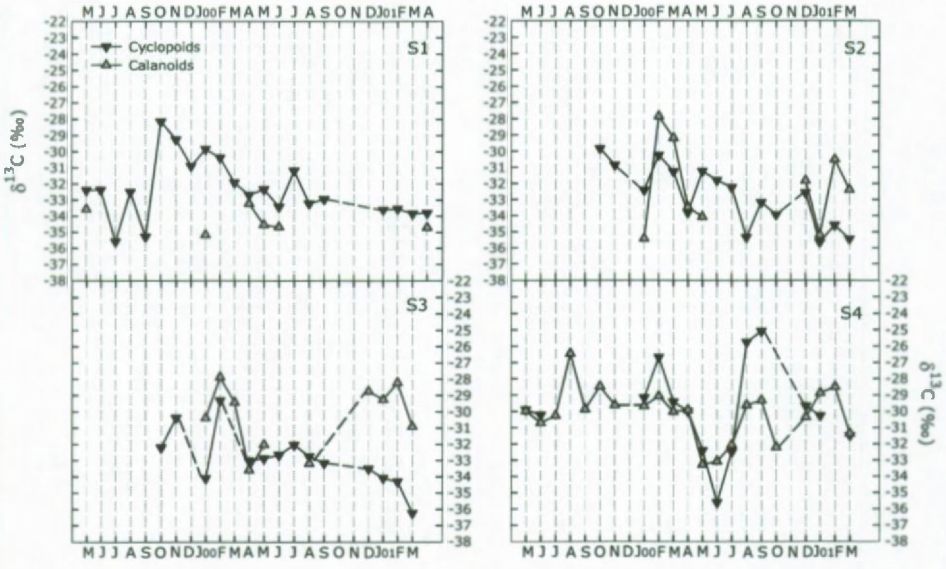

Figure 4.4: Seasonal variation in $\delta^{13}C$ of cyclopoid and calanoid copepods at stations S1 to S4 of the Scheldt estuary (1999-2001).

4.3.3 Seasonal patterns of $\delta^{15}N_{SPOM}$ and $\delta^{13}C_{SPOM}$ signatures

4.3.3.1 $\delta^{15}N_{SPOM}$

The $\delta^{15}N$ composition of SPOM showed considerable seasonal variation at all stations but the seasonal pattern differed between stations (Fig. 4.5; Table 4.2).

During the first year, $\delta^{15}N$ values at stations S1, S2 and S3 were initially low (June 1999) but increased to a maximum in September (S1), July (S2) or August-September (S3). At S1 and S3, $\delta^{15}N_{SPOM}$ values dropped sharply during October and remained low during winter. At S2, however, $\delta^{15}N_{SPOM}$ values decreased gradually between July and October. Station S4 differed from the other stations as $\delta^{15}N_{SPOM}$ values were initially high (June 1999), decreased slightly during July and remained relatively stable till November 1999.

During the second year, $\delta^{15}N_{SPOM}$ values at S1 first decreased to a minimum in April after which they gradually increased till September. At S2 and S3, $\delta^{15}N_{SPOM}$ values also decreased during late winter and reached a minimum in March, i.e. one month before the $\delta^{15}N_{SPOM}$ minimum at S1. At stations S2 and S3, however, $\delta^{15}N$ values did not increase gradually, but increased to a first maximum in April-May, decreased shortly during June and reached a second, higher maximum in September (S2) or August (S3). $\delta^{15}N_{SPOM}$ subsequently decreased at all three stations to a second minimum in October, after which values started to increase again. $\delta^{15}N_{SPOM}$ at stations S2 and S3 showed a winter maximum in January. At S1, this maximum was observed 2 months later in March. At station S4, $\delta^{15}N_{SPOM}$ values showed a different seasonal pattern: $\delta^{15}N_{SPOM}$ values increased gradually between January and June 2000, while the spring minimum was lacking. During July and August $\delta^{15}N_{SPOM}$ shortly decreased and a second, lower maximum was observed during September-October. On from November, values started to decrease again and remained stable till early spring of the next year.

4.3.3.2 $\delta^{13}C_{SPOM}$

$\delta^{13}C_{SPOM}$ values at stations S1, S2 and S3 were low during summer and increased between summer and winter (Fig. 4.5). At station S4, however, overall $\delta^{13}C_{SPOM}$ were higher and less variable. Here, only two clear $\delta^{13}C_{SPOM}$ maxima (January 2000 and March 2001) and one minimum (June 2000) were observed.

Table 4.2: Average and range of $\delta^{15}N_{SPOM}$ and $\delta^{13}C_{SPOM}$ signatures at stations S1, S2, S3 and S4 of the Scheldt estuary (1999-2001).

	$\delta^{15}N_{SPOM}$ (‰)		$\delta^{13}C_{SPOM}$ (‰)	
	average	**range**	**average**	**range**
S1	+4.8	-0.7 to +13.8	-29.1	-31.1 to -27.1
S2	+6.2	+0.5 to +14.6	-28.9	-30.8 to -27.1
S3	+6.0	+1.3 to +11.9	-28.3	-30.5 to -26.7
S4	+8.9	+2.3 to +15.1	-27.0	-29.3 to -23.7

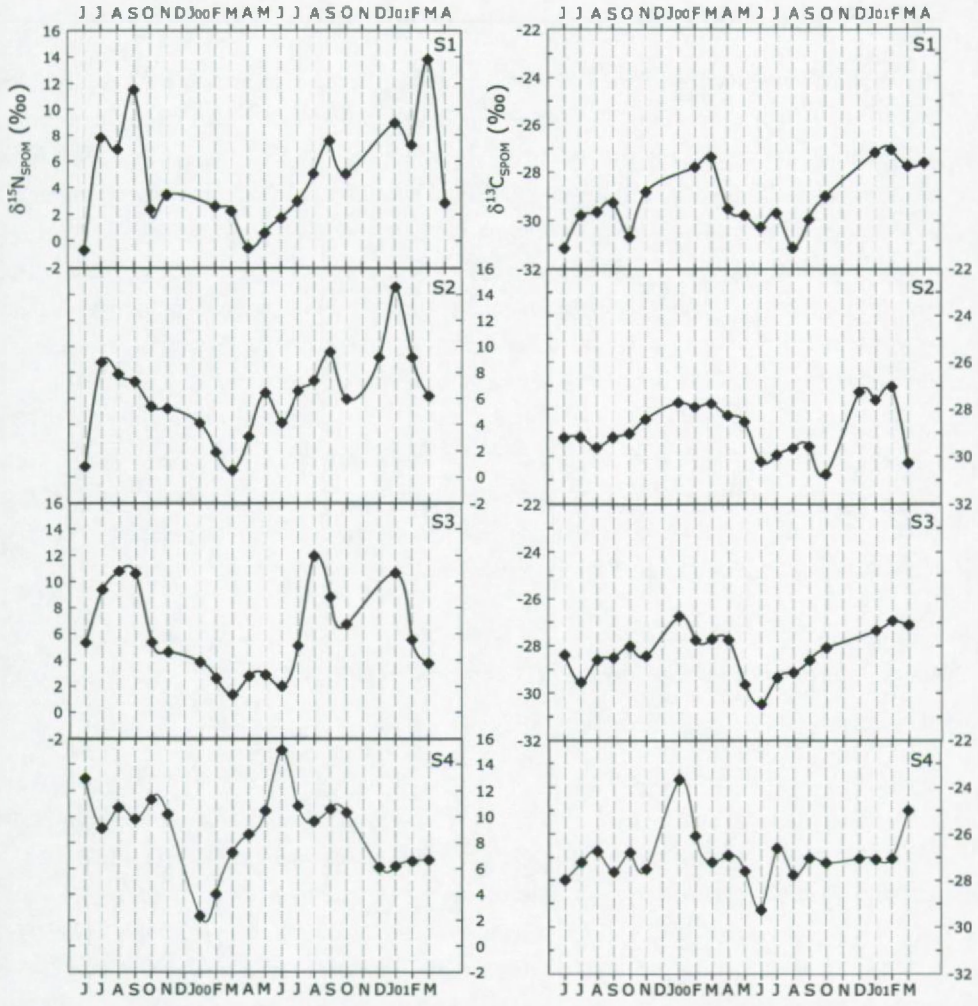

Figure 4.5: Seasonal variation in the $\delta^{15}N_{SPOM}$ (left) and $\delta^{13}C_{SPOM}$ (right) composition at stations S1, S2, S3 and S4 of the Scheldt estuary (1999-2001).

4.4 Discussion

In the following discussion, calanoid and cyclopoid copepod isotopic signatures are compared with the ones of bulk SPOM. In case isotopic signatures of copepods and SPOM show similar seasonal patterns, this reflects either that copepods select for a food source that also accounts for the seasonal variation in SPOM, or that copepods are omnivorous and have no selective feeding behavior. The latter possibility is, however, unlikely, since it has been shown that *Eurytemora affinis*, *Acartia tonsa* and *Acanthocyclops sp.*, the dominant calanoid and cyclopoid copepods in the Scheldt estuary, respectively, display selective feeding patterns (e.g. Gasparini and Castel, 1997; Rollwagen Bollens and Penry, 2003; Tackx et al., 2003).

Thus, for each station, we will first determine which component of the SPOM pool accounts for the major part of the seasonal variation in $\delta^{13}C_{SPOM}$ and $\delta^{15}N_{SPOM}$. Then, we will compare the seasonal patterns of the N and C isotopic signatures of SPOM, cyclopoid and calanoid copepods. Finally, we will investigate if copepod feeding preferences change along an estuarine gradient.

4.4.1 Sources of variation in $\delta^{15}N$ and $\delta^{13}C$ of SPOM

4.4.1.1 $\delta^{15}N_{SPOM}$

The seasonal patterns of $\delta^{15}N_{SPOM}$ at S1, S2 and S3 differed from the one at S4 and were mainly related to the variation in NH_4^+ (Spearman Rank, S1: -0.63; S2: -0.70; S3: -0.82; Table 4.3). At station S4 the variations in $\delta^{15}N$ of SPOM were significantly correlated with variations in the Chl-a concentration (Spearman Rank; Chl-a, 0.79; Table 4.3). Variations in phytoplankton biomass (Chl-a) explained only 54‰ of the variation in $\delta^{15}N_{SPOM}$ at S3 (Table 4.3) and did not correlate with $\delta^{15}N_{SPOM}$ at S2.

Table 4.3: Overview of the significant correlations (bold) between, $\delta^{15}N_{SPOM}$ and $\delta^{13}C_{SPOM}$ as revealed by a Spearman Rank correlation test.

$\delta^{15}N_{SPOM}$	S1			S2			S3			S4		
	p	*n*	*Rank*	*p*	*n*	*Rank*	*p*	*n*	*Rank*	*p*	*n*	*Rank*
NH_4^+	**	*18*	**-0.63**	***	*20*	**-0,70**	***	*19*	**-0,82**	**	*20*	**-0.66**
NO_3^-		*18*	-0.42		*20*	-0.43		*19*	-0.20	*	*20*	**-0.53**
Temperature		*19*	0.08		*20*	0.18	*	*19*	**0,48**	***	*20*	**0.69**
O_2		*19*	0.05		*19*	0.00		*19*	-0.20	*	*19*	**-0.49**
Chl-a	---	---	---		*19*	0.22	*	*19*	**0,54**	***	*19*	**0.79**
Discharge		*19*	0.02		*20*	0.03		*19*	-0.38	*	*20*	**-0.63**
Conductivity		*18*	-0.43		*20*	-0.27		*19*	0.26	***	*20*	**0.69**
SPM load	---	---	---	*	*19*	**0,48**		*18*	0.19		*19*	-0.18
C/N_{SPOM}		*19*	0.31	*	*20*	**0,49**	*	*19*	**0,49**		*20*	-0.04

$\delta^{13}C_{SPOM}$	S1			S2			S3			S4		
	p	*n*	*Rank*	*p*	*n*	*Rank*	*p*	*n*	*Rank*	*p*	*n*	*Rank*
Temperature	***	*19*	**-0.74**	***	*20*	**-0.69**	***	*19*	**-0.81**		*20*	-0.43
O_2	**	*19*	**0.64**		*19*	0.42	***	*19*	**0.72**	*	*19*	**0.55**
Chl-a	---	---	---	**	*19*	**-0.58**	**	*18*	**-0.60**	**	*19*	**-0.59**
Discharge	**	*19*	**0.65**		*20*	0.34	**	*19*	**0.61**	*	*20*	**0.45**
C/N_{SPOM}	*	*19*	**0.54**		*20*	-0.05		*19*	-0.02		*20*	-0.14
NO_2^-	***	*18*	**-0.82**		*20*	-0.38	**	*19*	**-0.60**		*20*	0.20
NO_3^-	*	*18*	**0.57**	**	*20*	**0.66**	**	*19*	**0.63**		*20*	-0.10
NH_4^+					*20*	0.14		*19*	0.20	**	*20*	**0.55**

* : p < 0.05; ** : p < 0.01; *** : p < 0.001; --- : no data

A detailed investigation of the variation of Chl-a and $\delta^{15}N_{SPOM}$ at S2 shows that the lack of correlation between Chl-a and $\delta^{15}N_{SPOM}$ results from the fact that high Chl-a concentrations coincide with low $\delta^{15}N_{SPOM}$ values in spring and with high $\delta^{15}N_{SPOM}$ in summer. Cifuentes et al. (1988) found that phytoplankton can decrease or increase the $\delta^{15}N$ composition of SPOM, depending on the history of processes acting on the NH_4^+ pool. Since NH_4^+ is the preferred N-source for phytoplankton in the Scheldt estuary (Mariotti et al., 1984; Middelburg and Nieuwenhuize, 2000; De Brabandere et al., 2002) and since $\delta^{15}N_{SPOM}$ correlates with NH_4^+ at all stations, processes acting on NH_4^+ will probably also determine the $\delta^{15}N_{SPOM}$ of the Scheldt estuary. NH_4^+ consuming processes such as microbial uptake and nitrification affect the $\delta^{15}N$ signature of NH_4^+ due to the large fractionation involved during NH_4^+ assimilation. Fractionation during phytoplankton uptake ranges between 5 and 30‰ in natural systems (Velinsky et al., 1991), tending towards the higher values when NH_4^+ concentrations are >20 $\mu mol.l^{-1}$ (Cifuentes et al., 1989; Pennock et al., 1996), as is mostly the case for the Scheldt estuary. During the spring bloom, NH_4^+ concentrations are high (Fig. 4.2) with $\delta^{15}NH_4^+$ signatures averaging +10‰ (Mariotti et al., 1984; Chapter 5). Under such conditions, fractionation is fully expressed and phytoplankton assimilating NH_4^+ would have $\delta^{15}N$ values as low as -20‰. The presence of phytoplankton in the suspended matter pool will consequently lower the $\delta^{15}N$ composition of SPOM, which has a value of approximately +3‰ in case allochthonous matter is the only component (Middelburg and Nieuwenhuize, 1998, Fisseha, 2000). However, $\delta^{15}NH_4^+$ can increase rapidly in closed or semi-closed systems due to the large fractionation related to uptake (Velinsky et al., 1991) and nitrification (Horrigan et al., 1990; Chapter 5). Such increase will be most pronounced during the growth season when the increasing N demand will exhaust the NH_4^+-pool. Phytoplankton assimilating this ^{15}N-rich NH_4^+ may then increase the $\delta^{15}N$ of SPOM.

At S3 and S4, where Chl a correlated significantly with $\delta^{15}N_{SPOM}$, NH_4^+ also correlated negatively but weakly with Chl a (Spearman Rank, R=-0.57; $p<0.01$ for both S3 and S4), indicating that phytoplankton blooms in most cases coincide with low ambient NH_4^+ concentrations. Phytoplankton will thus consistently draw from a reduced NH_4^+ pool so that the bloom periods at these stations will always be characterized by enriched $\delta^{15}N_{SPOM}$ signatures. The highest enrichments are found at S4 which is situated downstream from the main nitrification zone (de Bie et al., 2002a; Vanderborght et al., 2002) so that the NH_4^+ will be strongly reduced compared to the upstream stations (Fig. 4.2) and remnant NH_4^+ will be more enriched in ^{15}N. The low NH_4^+ concentrations at S4 also enhances the uptake of N-forms other than NH_4^+ as reflected in the correlation between $\delta^{15}N_{SPOM}$ and NO_3^- (rank -0.53, $p<0.05$; Table 4.3).

The importance of NO_3^- as an N-source for phytoplankton at S4 probably contributes to the fact that $\delta^{15}N_{SPOM}$ is only to a lesser degree correlated with NH_4^+.

Thus, the $\delta^{15}N$ signature of SPOM at stations S2, S3 and S4 may be mainly set by seasonal variations in the abundance and isotopic composition of phytoplankton. For completeness, it must be noted that $\delta^{15}N_{SPOM}$ was also positively correlated to the C/N ratio of SPOM at S2 and S3 (Spearman Rank: 0.49, $p<0.05$ for both stations, Table 4.3). Thornton and McManus (1994) and Owens (1985) reported an increase of $\delta^{15}N_{SPOM}$ coinciding with an increase in C/N_{SPOM} as a result of microbial mineralization of organic nitrogen (Owens, 1985). Thus, microbial mineralization could be an additional source of variation of $\delta^{15}N_{SPOM}$ at stations S2 and S3.

4.4.1.2 $\delta^{13}C_{SPOM}$

At S2 and S3, $\delta^{13}C_{SPOM}$ was mainly related to temperature and Chl-a with overall decreasing $\delta^{13}C_{SPOM}$ values as temperature and Chl-a increased (Table 4.3). At S4, $\delta^{13}C_{SPOM}$ was mainly related to Chl-a, although Chl-a explained as much of the variance of $\delta^{15}N_{SPOM}$ at S4 as it did at S2 and S3 (rank values are -0.59; -0.58 and -0.60, respectively; Table 4.3). The decrease in $\delta^{13}C_{SPOM}$ during the growth season resulted from the increasing importance of phytoplankton biomass, since phytoplankton has strongly depleted $\delta^{13}C$ signatures due to the continuous input of isotopically light CO_2 (Hellings et al., 2001) produced during heterotrophic processing of plant and phytoplankton detritus ($\delta^{13}C$ = -28.4‰; Hellings, 2000) and domestic sewage ($\delta^{13}C$ = -25.3‰; Fisseha, 2000) and due to the large isotope fractionation associated with CO_2 uptake. Indeed, the fractionation during phytoplanktonic CO_2 uptake has been reported to range between 10.9 – 11.7‰ (Boschker et al., 2005) and 23.0 ± 1.4‰ (Hellings, 2000) for the Scheldt estuary.

4.4.2 Evidence of selective feeding by calanoid and cyclopoid copepods

Trophic fractionation between copepods and their food sources averages 4±1‰ and 1±1‰ during N (ε_N) and C (ε_C) assimilation, respectively (Checkley and Entzeroth, 1985; Checkley and Miller, 1989; Goering et al., 1990; Montoya et al., 1991; 1992; del Giorgio and France, 1996; Wu et al., 1997 and Breteler et al., 2002). Correcting $\delta^{15}N$ and $\delta^{13}C$ of copepods for this trophic fractionation should give $\delta^{15}N$ and $\delta^{13}C$ values that approximate the ones of SPOM if copepods feed unselectively on bulk SPOM. However, after correction, $\delta^{15}N$ and $\delta^{13}C$ signatures of copepods still differed strongly from the ones of SPOM while strong seasonal variations were observed at all stations (Figs. 4.6 and 4.7). At S1 during summer, corrected $\delta^{15}N$ values of calanoid

and cyclopoid copepods were lower than $\delta^{15}N_{SPOM}$ after correction for trophic fractionation, while in spring $\delta^{15}N$ values of copepods were higher than $\delta^{15}N_{SPOM}$. At S2, corrected $\delta^{15}N$ values of calanoid and cyclopoid copepods were higher than $\delta^{15}N_{SPOM}$ during winter and lower than $\delta^{15}N_{SPOM}$ during the other seasons. At S3, corrected $\delta^{15}N$ values of calanoid and cyclopoid copepods mostly exceeded $\delta^{15}N_{SPOM}$, a pattern that was most pronounced for calanoid copepods. At S4, corrected $\delta^{15}N$ values of calanoid copepods largely exceeded $\delta^{15}N_{SPOM}$. The increase in $\delta^{15}N$ signatures of calanoids relative to $\delta^{15}N_{SPOM}$ reached its maximum during the summer months with $\delta^{15}N$ values of calanoids that were up to $4 \times \varepsilon_N$ higher than $\delta^{15}N_{SPOM}$ (July 1999). The deviation between corrected $\delta^{15}N$ values of cyclopoid copepods and $\delta^{15}N_{SPOM}$ was less pronounced than for calanoid copepods and both positive and negative deviations were observed. Corrected $\delta^{13}C$ values were much lower than $\delta^{13}C_{SPOM}$, a pattern almost consistently observed at the four stations.

Thus, the difference between the $\delta^{15}N$ and $\delta^{13}C$ signatures of copepods and SPOM differed significantly from what could be expected if bulk SPOM was the food source of copepods. This indicates that bulk SPOM as such, is not the food source of calanoid and cyclopoid copepods.

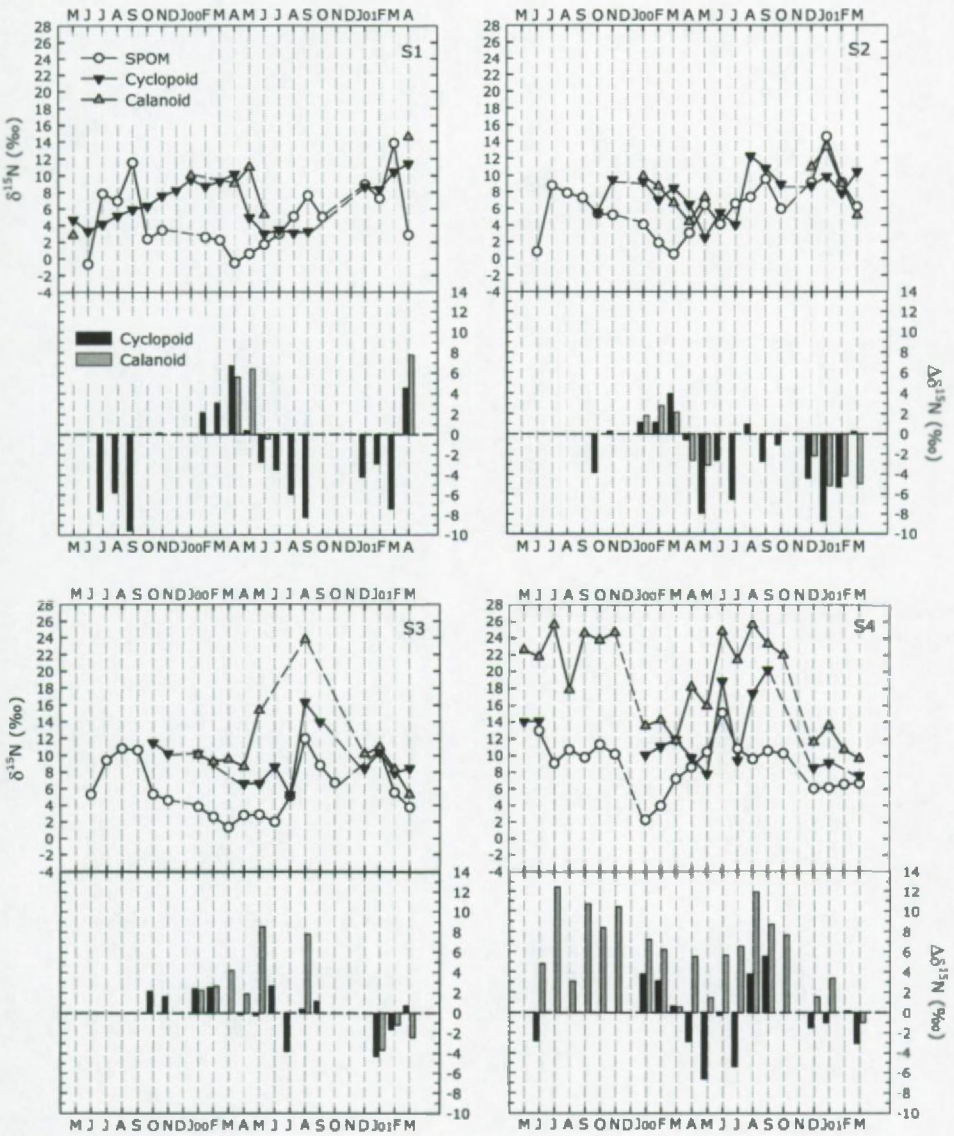

Figure 4.6: Upper half of each graph: Seasonal variation in $\delta^{15}N$ of SPOM, cyclopoid and calanoid copepods at stations S1 to S4 of the Scheldt estuary (1999-2001). Lower half: Difference between $\delta^{15}N$ of cyclopoid and calanoid copepods and $\delta^{15}N$ of SPOM at stations S1 to S4, after correction for trophic fractionation (4±1‰); i.e. $\Delta\delta^{15}N = (\delta^{15}N_{copepod} - \varepsilon_N) - \delta^{15}N_{SPOM}$.

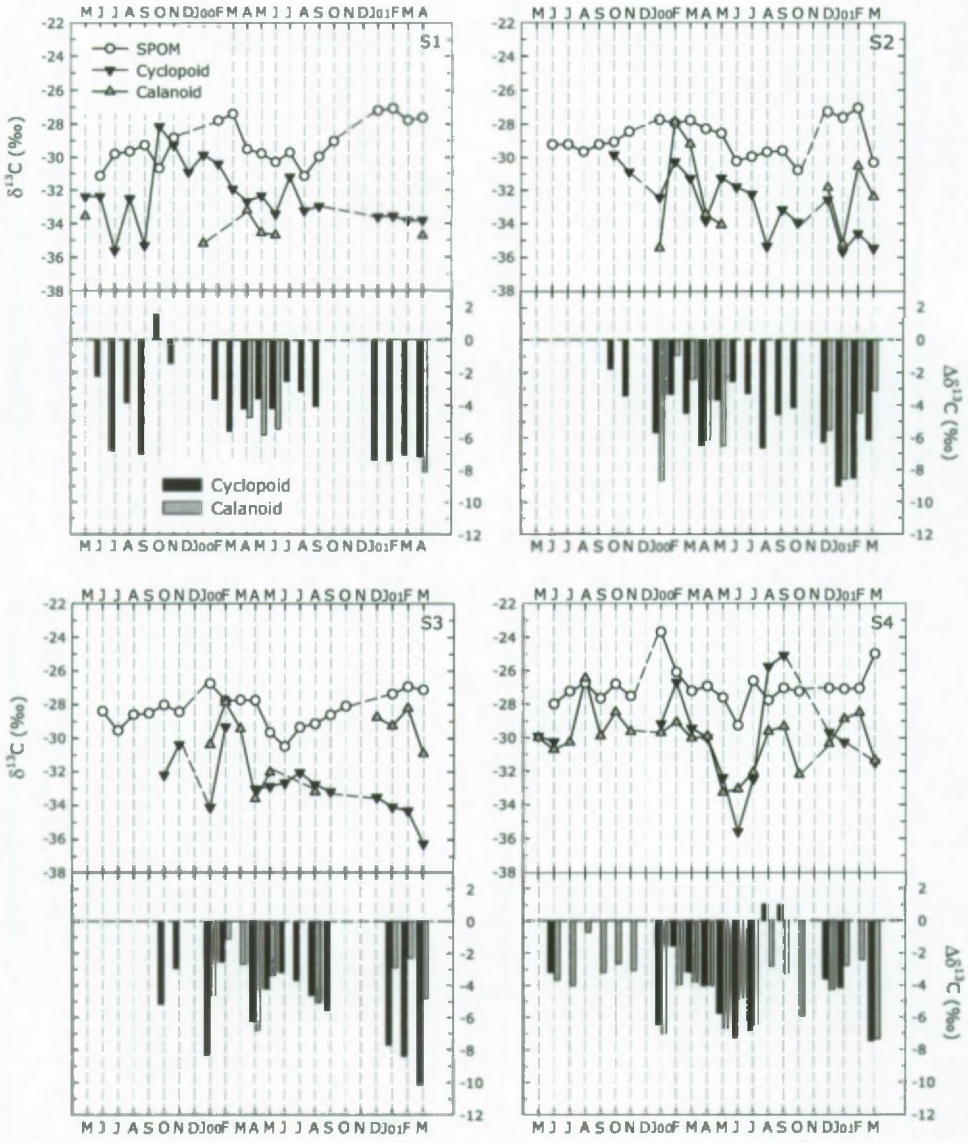

Figure 4.7: Upper half of each graph: Seasonal variation in $\delta^{13}C$ of SPOM, cyclopoid and calanoid copepods at stations S1 to S4 of the Scheldt estuary (1999-2001). Lower half: Difference between $\delta^{13}C$ of cyclopoid and calanoid copepods and $\delta^{13}C$ of SPOM at stations S1 to S4, after correction for trophic fractionation (1±1‰); i.e. $\Delta\delta^{13}C = (\delta^{13}C_{copepod} - \varepsilon_C) - \delta^{13}C_{SPOM}$.

4.4.3 Primary food sources of calanoid and cyclopoid copepods

Similarities between the seasonal patterns of the $\delta^{15}N$ signatures of SPOM and copepods may indicate that the ultimate food source of copepods is also the primary source of variation in $\delta^{15}N$ of the SPOM pool. Since we suggested that phytoplankton might be the main factor affecting the $\delta^{15}N$ signature of SPOM, parallelisms between $\delta^{15}N$ of SPOM and copepods would thus suggest that phytoplankton is the primary food source of copepods. However, heterotrophic bacteria will show a similar seasonal $\delta^{15}N$ pattern as phytoplankton when growing on phytoplankton-derived dissolved organic nitrogen (DON). These heterotrophic bacteria will probably be depleted in ^{15}N compared to phytoplankton since DON is depleted in ^{15}N relative to its substrate and bacteria preferentially assimilate ^{14}N-DON (Hoch et al., 1996). DON is mainly produced via sloppy feeding and passive release by zooplankton (Hoch et al., 1996; Van den Meersche et al., 2004), via bacteria processing detritus and via the passive release by living phytoplankton (Van den Meersche et al., 2004). DON concentrations can be high, especially at the end of a bloom period (Bronk and Glibert, 1993). The ^{15}N-depletion of bacteria will be even more pronounced if bacteria obtain DON from the processing of phytodetritus instead of via the passive release by phytoplankton. Indeed, successive generations of phytoplankton are increasingly enriched in ^{15}N due to a gradual exhaustion of the NH_4^+ pool and the enrichment of the NH_4^+ due to fractionating consumption processes.

Phytoplankton is strongly depleted in ^{13}C relative to SPOM (Hellings et al., 1999; Boschker et al., 2005) and heterotrophic bacteria growing on phytoplankton-derived dissolved organic carbon (DOC) will mimic this low $\delta^{13}C$ composition with an offset ranging between -2 and +2‰ (Coffin et al., 1989). Copepods depending on phytoplankton or heterotrophs as a primary food source will thus also have $\delta^{13}C$ signatures depleted in ^{13}C compared to SPOM since copepods reflect the $\delta^{13}C$ of their food source within a range of 1±1‰ (Checkley and Miller, 1989; Goering et al., 1990; del Giorgio and France, 1996; Breteler et al., 2002).

4.4.3.1 Oligohaline (S2, S3) and mesohaline (S4) stations

At stations S2, S3 and S4, $\delta^{15}N$ signatures of copepods roughly paralleled the ones of SPOM, although $\delta^{15}N_{SPOM}$ was only significantly correlated to $\delta^{15}N_{CAL}$ and $\delta^{15}N_{CYC}$ at S4 and S3, respectively (Table 4.4). In addition, $\delta^{15}N$ values of calanoids were highly enriched compared to the ones of the cyclopoid copepods at stations S3 and S4. At S3, this relative enrichment was restricted to late spring and summer while at S4, calanoid copepods were strongly enriched all year round, except in March 2000 and March 2001.

Tackx et al. (2003) showed that the calanoid *E. affinis* is mainly herbivorous and we may expect that the high selectivity for phytoplankton also holds for the period of our study (1999-2001). Tackx et al. (2003) calculated that *E. affinis* is able to obtain >80‰ of its diet from phytoplankton when phytoplankton-C/POC values exceed 0.05. When using a phytoplankton-C/Chl-a conversion factor of 50 (Tackx et al. 2003) we calculated that the phytoplankton-C/POC values almost always exceed 0.05, except during winter at S3 and during winter-early spring and August 2000 at S4 (Fig. 4.8), implying that *E. affinis* had the potential to feed selectively on phytoplankton. The selective feeding behavior of *E. affinis* is, however, negatively influenced when SPM concentrations increase to levels in the order of hunderds $mg.l^{-1}$, and in particular when the inorganic fraction in SPM increases (Gasparini et al., 1999). Gasparini et al. (1999) observed, however, no major impact of SPM concentrations on the selective feeding behavior of *E. affinis* in the Scheldt estuary since SPM concentrations rarely exceed 150 $mg.l^{-1}$ (Fig. 4.2) and the organic matter fraction in SPM of the Scheldt estuary is relatively high.

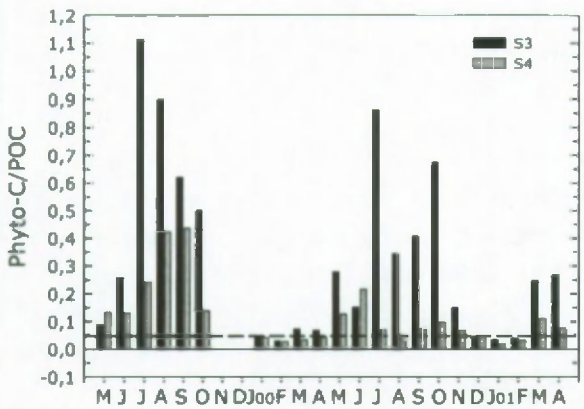

Figure 4.8: Seasonal variation in the phytoplankton-C/POC ratio at stations S3 and S4 of the Scheldt estuary (1999-2001). The dashed line indicates the 0.05 level.

Although we did not measure phytoplankton $\delta^{15}N$ values directly, we may expect that $\delta^{15}N$ of phytoplankton increases toward the mesohaline station. Indeed, the low NH_4^+ concentrations at this station (Fig. 4.2) suggest that NH_4^+ consuming processes will have exhausted the NH_4^+ pool while the fractionation associated with NH_4^+ consumption will have enriched it in ^{15}N (see discussion above). The $\delta^{15}N$ of calanoid copepods showed an overall increase in downstream direction (Fig. 4.3) which would be in agreement with a herbivorous feeding behavior.

We expect the cyclopoid *Acanthocyclops robustus* to show the highest enrichment in ^{15}N since this species has a carnivorous feeding behavior (Brandl, 1998). However, cyclopoid copepods have lower $\delta^{15}N$ signatures than the herbivorous calanoid copepods which might imply that phytoplankton, as such, is less important as a food source for the cyclopoid copepods. Since the seasonal pattern of $\delta^{15}N_{cyc}$ resembles the one of SPOM, heterotrophic bacteria utilizing phytoplankton-derived DON might be the primary food source of cyclopoid copepods.

The distinct $\delta^{15}N$ signatures of cyclopoid and calanoid copepods could thus indicate that calanoid copepods rely more on autotrophic organisms as a primary food source, while bacteria using DON derived from phytoplankton are the ultimate food source of cyclopoid copepods. The strong deviation between $\delta^{13}C$ of copepods and SPOM (Fig. 4.7) supports the idea that phytoplankton or phytoplankton-derived dissolved organic matter are the primary food sources of copepods, although the typical summer decrease in $\delta^{13}C_{SPOM}$ was only reflected in the $\delta^{13}C$ signatures of calanoid copepods at S2, S3 and S4 and in the one of cyclopoid copepods at station S4.

Table 4.4: Overview of significant correlations (bold) between copepod and SPOM isotopic signatures as revealed by Spearman Rank correlation statistics.

	$\delta^{15}N$				$\delta^{13}C$		
station	***n***	***Rank***	***p***	***station***	***n***	***Rank***	***p***
Calanoids				*Calanoids*			
S1	4	0.40	0.60	S1	4	-0.20	0.80
S2	9	0.63	0.07	S2	9	0.08	0.83
S3	9	0.35	0.36	S3	9	0.37	0.33
S4	**20**	**0.60**	**0.005**	S4	20	0.34	0.14
Cyclopoids				*Cyclopoids*			
S1	18	0.09	0.74	S1	18	-0.21	0.41
S2	16	0.34	0.20	S2	16	0.03	0.92
S3	**13**	**0.58**	**0.04**	**S3**	**13**	**-0.60**	**0.03**
S4	13	0.43	0.14	S4	13	0.23	0.46

4.4.3.2 Freshwater reaches (S1)

At S1, the discussion of the diet of copepods is restricted to the one of cyclopoid copepods since calanoid copepods were less abundant there and occurred only

occasionally in sufficiently high numbers for reliable analysis. This makes it difficult to draw hard conclusions about their diet.

In contrast to the oligohaline and mesohaline stations, the seasonal pattern of the $\delta^{15}N$ composition of cyclopoid copepods at S1 did not reflect the one of SPOM (Fig. 4.6). $\delta^{15}N$ of copepods gradually increased between spring and autumn, while $\delta^{15}N_{SPOM}$ clearly peaked during summer. If the $\delta^{15}N$ composition of SPOM at S1 also reflects the $\delta^{15}N$ composition of phytoplankton as is the case for the other stations (see discussion above), the lack of correlation between $\delta^{15}N_{CYC}$ and $\delta^{15}N_{SPOM}$ at S1 (Table 4.4) would suggests that in the freshwater reaches autochthonous phytoplankton or bacteria thriving on DON derived from this phytoplankton are not important as primary food sources of cyclopoid copepods. However, our results showed that cyclopoid copepods have strongly depleted $\delta^{13}C$ signatures compared to SPOM (Fig. 4.7), what points to phytoplankton or to heterotrophic bacteria using phytoplankton-derived organic matter as the ultimate food source of cyclopoid copepods. This apparent contradiction thus suggests that (1) $\delta^{15}N_{SPOM}$ does not reflect the $\delta^{15}N$ composition of phytoplankton or (2) if $\delta^{15}N_{SPOM}$ indeed reflects the $\delta^{15}N$ composition of phytoplankton, allochthonous phytoplankton sources with distinct $\delta^{15}N$ seasonal patterns, e.g. phytoplankton detritus advected from the tributaries (allochthonous phytodetritus), or heterotrophic bacteria processing this phytodetritus are the primary food source of cyclopoid copepods. Cyclopoid copepods would then be top-predators of the microbial loop, as has been suggested by Muylaert et al. (2000b).

4.5 Conclusions

The comparison between the seasonal evolution of $\delta^{15}N$ and $\delta^{13}C$ of SPOM and copepods at the oligohaline and mesohaline stations allowed us to propose possible pathways of matter transfer between the base of the food web and calanoid and cyclopoid copepods. The similarity between the seasonal patterns of $\delta^{15}N$ of cyclopoid and calanoid copepods at the oligohaline and mesohaline stations suggested that secondary production depended on phytoplankton for their C and N requirements, either directly (calanoid copepods) or indirectly via heterotrophic bacteria relying on phytoplankton (cyclopoid copepods).

At the freshwater station, however, it is clear that the interpretation of the relationship between the seasonal patterns of the $\delta^{15}N$ and $\delta^{13}C$ isotopic signature of cyclopoids and SPOM requires a better understanding of the relationship between $\delta^{15}N$ of SPOM and phytoplankton and on the seasonal $\delta^{15}N$ pattern of less abundant organic N compounds in the SPOM pool. Therefore, in the next chapter, we will (1) estimate

the $\delta^{15}N$ composition of phytoplankton at S1 and compare it with the $\delta^{15}N$ signature of SPOM and cyclopoid copepods in order to investigate the dependency of cyclopoid copepods on autochthonous phytoplankton sources and (2) try to reconstruct the $\delta^{15}N$ signature of non-algal nitrogen components of SPOM.

The complexity of trophic dependencies in the freshwater reaches

Chapter 5

5.1 Introduction

In chapter 4 we showed that a comparison between the seasonal patterns of the isotopic signatures of suspended particulate organic matter (SPOM) and copepods can provide indirect evidence of the primary food sources of copepods if the $\delta^{15}N$ and $\delta^{13}C$ signature of SPOM reflects the ones of these food sources. In the freshwater section of the estuary, the seasonal pattern of the $\delta^{15}N$ signature of cyclopoid copepods differed strongly from the one of SPOM, suggesting that the amount of nitrogen represented by the food source of cyclopoid copepods is negligible compared to the amount of nitrogen accounting for the seasonal $\delta^{15}N$ variation in SPOM. In the Scheldt estuary, the temporal and spatial variation in the $\delta^{15}N_{SPOM}$ signature largely reflects variation in the biomass and isotopic signature of phytoplankton (Mariotti et al., 1984; De Brabandere et al., 2002; Chapter 4), but the $\delta^{15}N$ signature of heterotrophic microorganisms (bacteria and fungi) colonizing detritus may also vary considerably if they take up ambient dissolved nitrogen (DN) to fulfill their N-demand (Zieman et al., 1984; Caraco et al., 1998). However, in the Scheldt estuary, the bacterial biomass is much lower than the one of phytoplankton (Goosen et al., 1999), so that their $\delta^{15}N$ signatures will be masked by the ones of phytoplankton. The difference between the seasonal $\delta^{15}N$ patterns of cyclopoid copepods and SPOM could thus indicate that microheterotrophs represent the major primary food source of cyclopoid copepods.

There are, to our knowledge, no existing seasonal records of phytoplankton or microbial $\delta^{15}N$ signatures for the freshwater estuary with which the ones of cyclopoid copepods can be compared. Since the analysis of algal and bacterial $\delta^{15}N$ signatures in SPOM is hampered by the presence of large amounts of terrestrial or sewage-derived nitrogen, group-specific biochemical compounds such as amino acids (Pelz et al., 1998) and nucleid acids (Coffin et al., 1990) are often used as an alternative tool to study algal and bacterial $\delta^{15}N$ signatures. In this study, however, we tried to reconstruct the seasonal variation of algal and microheterotrophic $\delta^{15}N$ by looking at the seasonal $\delta^{15}N$ variation of their potential N-substrates.

For phytoplankton, we hypothesized that the $\delta^{15}N$ of NH_4^+ would be the main factor setting $\delta^{15}N$ of phytoplankton since NH_4^+ is the preferred nutrient in the Scheldt estuary (Mariotti et al., 1984; Middelburg and Nieuwenhuize, 2000, De Brabandere et al., 2002). Therefore, our first objective was to investigate the seasonal $\delta^{15}N$ signature of NH_4^+ to reconstruct the $\delta^{15}N$ signature of autochthonous phytoplankton biomass in the Scheldt estuary (section 1). We investigated the pattern and the origin of the seasonal variation of $\delta^{15}NH_4^+$ and its relation to microbial NH_4^+ production and consumption. In addition, we investigated to which extent $\delta^{15}N$ of phytoplankton is reflected in the $\delta^{15}N$ of SPOM.

For bacteria, we distinguish two major potential N substrates: dissolved organic nitrogen (DON) derived from autochthonous phytoplankton and DON derived from organic matter present in flocs suspended in the water column. If DON derived from autochthonous phytoplankton would be the main bacterial N-substrate, bacterial $\delta^{15}N$ signatures would parallel the $\delta^{15}N$ signature of autochthonous phytoplankton (calculated in section 1). However, if bacteria derive their DON from organic matter associated with flocs, they may reflect the $\delta^{15}N$ of organic matter caught in the floc or the $\delta^{15}N$ of ambient dissolved nitrogen if the bioavailable N in flocs is low. Indeed, microheterotrophs are known to assimilate dissolved nitrogen from the ambient solution if the N-content of the organic substrate is not sufficient to meet the N requirements of microbial decomposers (Zieman et al., 1984; Caraco et al., 1998). Therefore, our second objective was to reconstruct the seasonal $\delta^{15}N$ signature of microheterotrophs associated with flocs by means of a decomposition experiment (section 2). We hypothesized that the seasonal $\delta^{15}N$ of microheterotrophs would (1) show only minor changes if organic substrate-N would be their main N-source and (2) reflect the seasonal $\delta^{15}N$ of ambient DN if DN assimilation would be important. Since flocs cannot be sampled without definitively changing their structure (Chen, 2003), we used submerged leaves as a proxy of organic matter in flocs in order to reconstruct the seasonal variation of $\delta^{15}N$ of microheterotrophs processing detritus.

5.2 Material and methods

5.2.1 Sampling and analytical protocols

The study was carried out at the freshwater station S1, situated below the confluence of the Scheldt River and the Dender tributary, at 121 km from the river mouth (Fig. 5.1) and lasted from 31 October 2001 till 24 April 2003 (18 months). Environmental parameters were monitored fortnightly between 31 October 2001 and 29 July 2002 and monthly between 23 August 2002 and 24 April 2003. The physico-chemical and biological parameters monitored included dissolved O_2, temperature, NH_4^+, NO_3^-, NO_2^-, Chlorophyll *a* (Chl-a) and suspended matter (SPM) concentration, $\delta^{15}N$ of suspended particulate organic matter (SPOM) and particulate organic carbon (POC) and particulate nitrogen (PN) concentrations of SPOM. Dissolved oxygen contents and temperature were measured in situ. Detailed descriptions of the sampling protocol and the analysis of nutrients, $\delta^{15}N_{SPOM}$, POC and PN concentrations in SPOM and Chl-a concentrations are presented in Chapter 3. Longitudinal profiles of

ammonium, nitrate and Chl-a concentrations for the km 155 to km 110 stretch were kindly provided by T. Maris (University of Antwerp).

Figure 5.1: Map of the Scheldt estuary and its major tributaries showing the sampling station S1 located in the freshwater section at km 121 from the mouth of the estuary.

5.2.2 $\delta^{15}NH_4^+$ analyses

$\delta^{15}NH_4^+$ signatures were determined using an original facilitated diffusion method (Brion et al., in prep). The sample was first diluted to reach an approximate concentration of 10 $\mu mol.l^{-1}$. A glass gas-washing bottle (Schott™) was filled with 250 ml of the diluted sample. The bottle holds an external gas inlet tube connected to a large gas diffusion disc located at the bottom. The gas outlet of the bottle is connected to an in-line INOX filter holder (Pall Life Sciences™), holding a 25 mm diameter GF/D glass-fiber membrane (Whatman™) impregnated with 50 μl $KHSO_4$ 2.5 $mol.l^{-1}$. After adding 1.5 ml KOH 80% to the sample, the bottle is immediately closed and respirable air is bubbled with controlled flow through the sample in order to strip the formed NH_3 out of the solution. When passing through the acidified filter, the NH_3 in the air flow is trapped. After extraction, the filter is removed and dried for 12 hours at 50°C. Trapped N and $\delta^{15}N$ are measured using IRMS as described in Chapter 3. Filters resulting from the extraction of Milli-Q water using the same protocol served as blank. Testing out this method showed that after 15 hours, more than 80% of the initial ammonium present in

the solution was trapped on the filter. Extractions made with a $^{15}N\text{-}NH_4^+$ standard solution showed that fractionation occurred with $\delta^{15}NH_4^+_{extracted} = \delta^{15}NH_4^+_{solution} - 2.4 \pm 1.6‰$. Measurements were thus corrected for this fractionation. The standard deviation of $\delta^{15}NH_4^+$ on triplicate sample extraction was 2.3‰.

5.2.3 Willow leaf decomposition: experimental setup

In autumn, at the onset of leaf fall, leaves were picked from willow trees growing on the riverbanks in the vicinity of the experimental site. In the laboratory, leaves were rinsed with distilled water to remove dust and attached organisms and dried at 50°C. Since the main focus lies on the study of the seasonal variation of the $\delta^{15}N$ composition of microbial decomposers, a litterbag with a small mesh size (300 μm) was chosen to exclude larger invertebrates. Fifty-seven nylon bags (size 10 × 10 cm) were filled with approximately 1 gram of willow leaves and hung in a stainless steel cage (120 × 80 × 80 cm; 4 cm mesh size). A sub-sample from the leaves of all bags was taken to have a reference value for the $\delta^{15}N$ signature, POC and PN concentration of the original leaf. The cage was attached to a floating pontoon at S1 station and positioned at approximately 1 m under the low tide water surface where the absence of light inhibited the growth of photo-autotrophs. Each month, three litterbags were recovered, transported to the laboratory in a cooling box and stored at -20°C until analysis.

5.2.4 Sample preparation

The litterbags were thawed in distilled water and opened carefully not to damage the content. Willow leaves were picked out manually or collected on a 300 μm net in case shredders had fragmented them. Willow leaves were sometimes covered with a considerable amount of gelatinous matrix or biofilm. The biofilm itself was not studied for its constituting components, but biofilms generally contain microorganisms, exoenzymes and detritus particles (Golladay and Sinsabaugh, 1991). Care was taken not to remove the biofilm while handling. In several cases, however, small amounts of leaf biofilm detached during thawing and had to be collected separately. On from May 2002, any biofilm covering the litterbag (referred to as Bag BioFilm 'BBF') was scraped, while detached fragments of leaf biofilm (referred to as Leaf BioFilm 'LBF') were collected separately on from August 2002. The leaf-biofilm complex (referred to as 'LBC') and the LBF and BBF samples were dried at 50°C and analyzed for their $\delta^{15}N$ composition. LBC samples were also analyzed for PN and POC concentrations (PN_{LBC}

and POC_{LBC}). These were expressed on an ash-free dry weight basis (550°C, 12h), since inorganic material (e.g. silt) trapped in the microbial mucilage may lead to underestimates of the PN and POC concentrations if expressed per gram dry weight.

5.2.5 Aluminium concentration

Aluminium concentrations of LBC and SPM were measured by digesting approximately 100 mg of LBC or one SPM filter with Aqua Regia (4ml HCl and 1ml HNO_3) in a microwave oven (CEM Mars 5) under controlled conditions of temperature and pressure: ramp to 160°C during 15 minutes (maximum pressure 200psi) and hold at 160°C during 15 minutes (maximum pressure 200psi). After digestion the samples were diluted to 50 ml with deionized water. Analysis of aluminium was performed by inductively coupled plasma atomic emission spectrometry ICP- AES (Thermo Optek, Iris).

5.2.6 Statistical analyses

Causal relationships between variables were tested by means of ordinary linear regressions (OLS), while bivariate least square regressions (BLS) were applied when errors on both independent and dependent variables were known (Riu and Rius, 1996). Correlations between variables were tested by means of a Spearman Rank correlation test. The standard deviation and percentile ranges associated with $\delta^{15}N$ of accumulated phytoplankton (section 5.5.5) were calculated using a Monte Carlo simulation.

5.3 Results: Water column characteristics

Water temperatures ranged between 5°C (late-December 2001) and 23°C (late-July 2002) and correlated inversely with O_2 concentrations (Fig. 5.2A). Generally, lowest O_2 concentrations were observed during summer-autumn with nearly anoxic conditions in September 2002 (O_2 concentrations as low as 0.9 $mg.l^{-1}$). During late autumn, winter and spring, O_2 concentrations were much higher with a maximum value of 9.1 $mg.l^{-1}$ observed in December 2001. Discharge at station S1 was calculated as the sum of the discharge of the Scheldt River measured at the head of the estuary (km 155) and the one of the Dender tributary. Discharge values ranged between 5 (September 2002) and 521 $m^3.s^{-1}$ (December 2002) and were generally higher during

winter-early spring (Fig. 5.2B). SPM concentrations generally fluctuated between 33 (February 2003) and 133 mg.l^{-1} (October 2002); (Fig. 5.2C). However, during late winter-early spring 2002 and late summer 2002, SPM concentrations were markedly higher with maximum values as high as 230 mg.l^{-1} (March 2002) and 201 (August 2002).

The Chl-a evolution marked a brief spring phytoplankton bloom and a longer lasting bloom during summer-early autumn (Fig. 5.3C). Spring Chl-a values of 137 ± 4 μg.l^{-1} and 70 ± 2 μg.l^{-1} were recorded in April 2002 and March 2003, respectively, while the summer bloom, lasting from June till October 2002, reached a maximum of 192 ± 11 μg.l^{-1} in September. $\delta^{15}N$ signatures of SPOM fluctuated around +3‰ during winter 2001-2002 and decreased to a value of −2.6‰ during the first spring bloom (Fig. 5.3D). $\delta^{15}N_{SPOM}$ subsequently increased to a maximum of +12.5‰ in July 2002 when high Chl-a levels coincided with lowest NH_4^+ concentrations (1 μmol.l^{-1}). In August, $\delta^{15}N_{SPOM}$ shortly decreased to +7.8‰ after which $\delta^{15}N_{SPOM}$ increased to a second maximum of +11.5‰ in September 2002. On from September, $\delta^{15}N$ of SPOM gradually decreased to reach a second minimum of −0.9‰ in March 2003. The summer increase in $\delta^{15}N_{SPOM}$ coincided with a steep increase in NO_2^- concentration which reached values up to 51 μmol.l^{-1} in June 2002 (Fig. 5.3A). NO_3^- concentrations were an order of magnitude higher than NO_2^- concentrations with a maximum of 535 μmol.l^{-1} observed in April 2002 and a minimum of 114 μmol.l^{-1} observed in December 2002 (Fig. 5.3A). NH_4^+ concentrations were approximately 3 times lower than NO_3^- concentrations (Fig. 5.3B). Largest NH_4^+ depletions were met in July and August 2002 (<1 μmol.l^{-1} in August 2002), while a maximum of 185 μmol.l^{-1} was observed in May 2002.

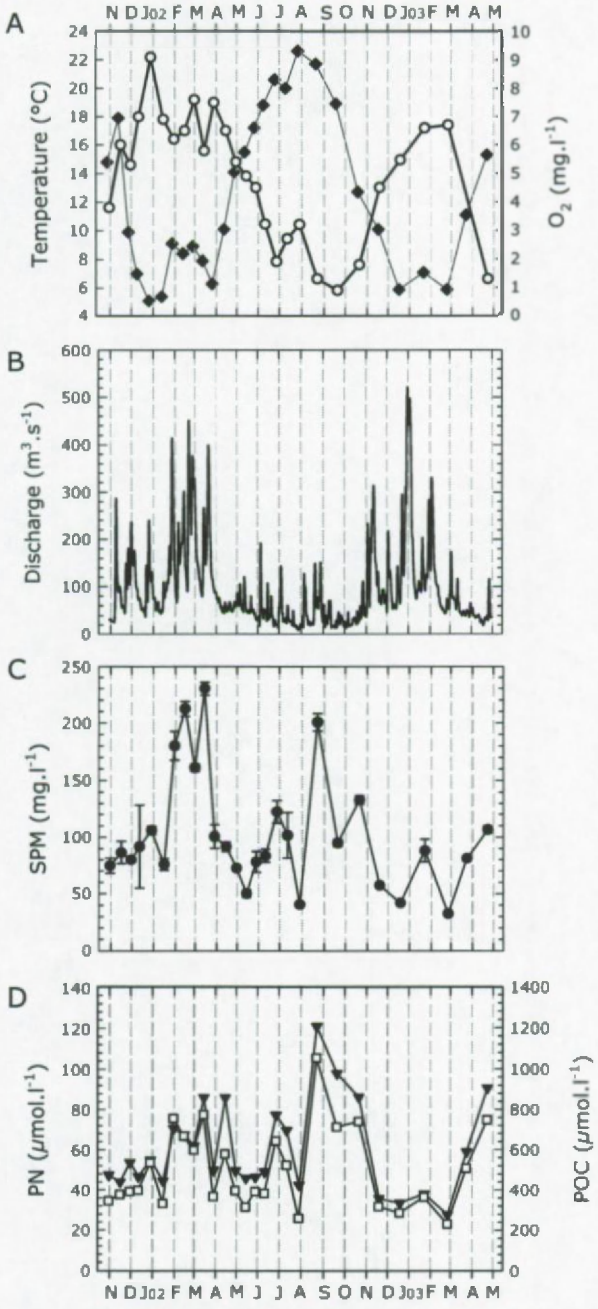

Figure 5.2: Seasonal variation of (A) temperature (diamonds) and O_2 concentrations (circles), (B) discharge (Tavernlers, 2001; 2002; 2003), (C) SPM (± 1SD) and (D) PN (triangles) and POC concentrations (squares) at the freshwater station S1 of the Scheldt estuary (2001-2003).

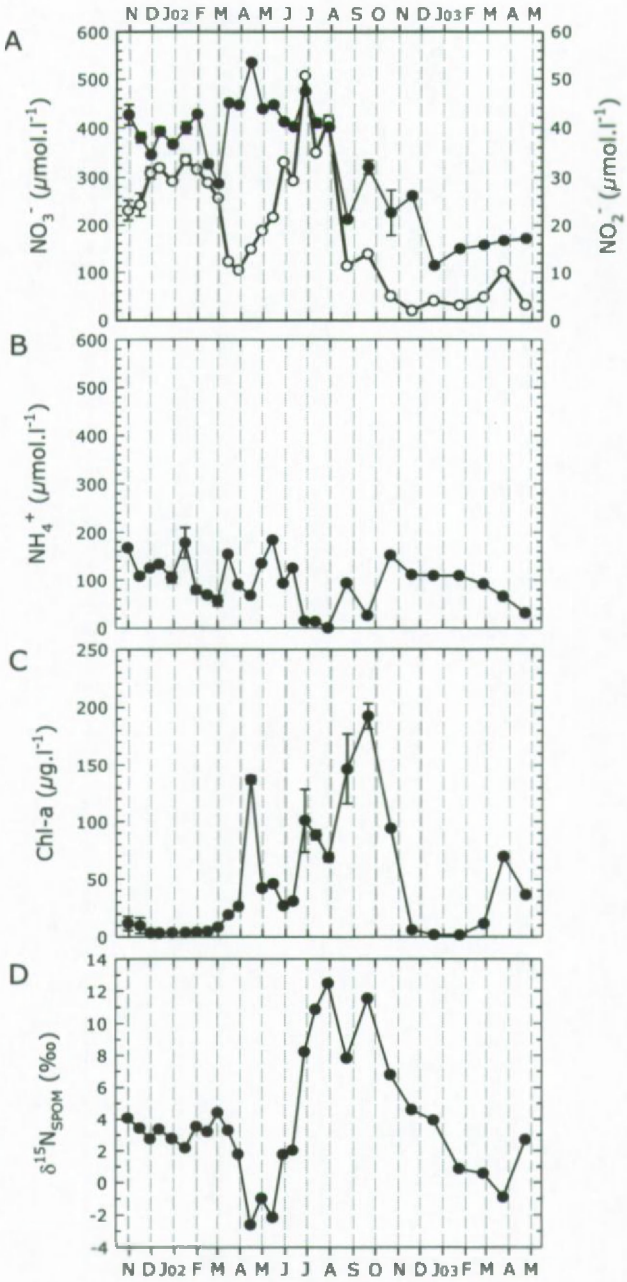

Figure 5.3: Seasonal variation of (A) NO_3^- (black) and NO_2^- (white), (B) NH_4^+, (C) Chl-a and (D) $\delta^{15}N_{SPOM}$ at the freshwater station S1 of the Scheldt estuary (2001-2003). Error bars = 1 standard deviation.

SECTION 1

5.4 Results: $\delta^{15}NH_4^+$

The $\delta^{15}N$ signature of NH_4^+ varied considerably over the course of the study period (Fig. 5.4). $\delta^{15}NH_4^+$ averaged +10‰ (SD=1‰) during winter (30 November 2001 till 19 February 2002). On from March 2002 $\delta^{15}NH_4^+$ values increased exponentially to a first maximum of +70‰ in mid-July. In August, $\delta^{15}NH_4^+$ sharply decreased to +31‰ after which a second maximum of +66‰ was reached in September. In October and November 2002, $\delta^{15}NH_4^+$ values decreased again but were higher than the average winter value of the previous year (i.e. +10‰). Generally, $\delta^{15}NH_4^+$ values were highly variable, sometimes changing dramatically within 2 weeks. For example, between June, 11th and June, 27th $\delta^{15}NH_4^+$ increased as much as 46‰.

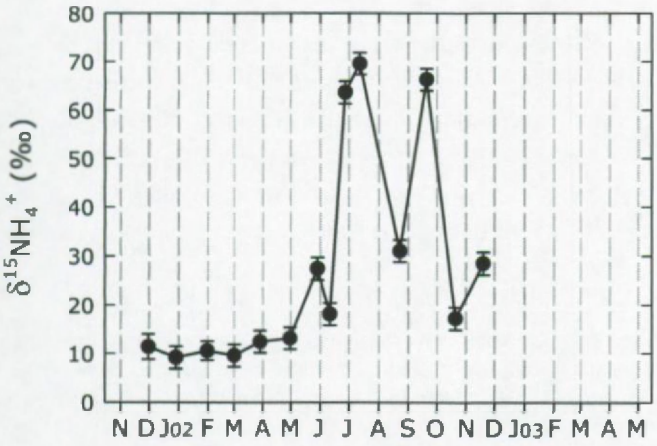

Figure 5.4: Seasonal variation in the $\delta^{15}N$ signature of NH_4^+ at the freshwater station S1 of the Scheldt estuary (2001-2003). Error bars = 1 standard deviation.

5.5 Discussion: $\delta^{15}NH_4^+$

5.5.1 Comparison of $\delta^{15}NH_4^+$ with literature data

$\delta^{15}NH_4^+$ values reported in literature range between +10‰ and +42‰ (Table 5.1). Aquatic systems characterized by low microbial activity or by high NH_4^+ concentrations typically have low $\delta^{15}NH_4^+$ values because fractionating processes will have little or no effect on the $\delta^{15}N$ composition of the NH_4^+ pool. Aquatic systems where high microbial NH_4^+ demands exhaust the NH_4^+ pool are characterized by high $\delta^{15}NH_4^+$ values.

$\delta^{15}NH_4^+$ values observed for the Scheldt estuary are much higher than reported for the Delaware estuary, which had similar initial $\delta^{15}NH_4^+$ values (Cifuentes et al., 1989; Velinsky et al., 1989; Table 5.1). The higher $\delta^{15}NH_4^+$ values observed during our study may result from a higher fractionation associated with processes draining the NH_4^+ pool in the Scheldt estuary compared to the Delaware estuary. Indeed, Cifuentes et al. (1989) modeled the fractionation during NH_4^+ consumption for open systems where isotopic signatures are not in steady-state (Delaware estuary, USA). They showed that a fractionation of 9‰ for phytoplanktonic NH_4^+ uptake can increase the $\delta^{15}NH_4^+$ from +11‰ till +40‰, while a fractionation of 20‰ would increase their $\delta^{15}NH_4^+$ values to +63‰, a value only slightly lower than the one observed in the Scheldt estuary. In addition, the fraction of NH_4^+ remaining in the NH_4^+ pool was larger in the Delaware estuary so that the $\delta^{15}N$ of NH_4^+ was still below its maximum. Indeed, $\delta^{15}NH_4^+$ values increase exponentially with decreasing fraction of NH_4^+ remaining in the NH_4^+ pool (equation 5.1, see below).

Table 5.1: Overview of $\delta^{15}N$ values of NH_4^+ reported in literature for polluted estuarine systems. $\delta^{15}NH_4^+$ marked as 'low' refer to aquatic systems were the NH_4^+ pool was not affected by microbial NH_4^+ consumption while $\delta^{15}NH_4^+$ marked as 'high' refer to systems where NH_4^+ consumption had reduced the NH_4^+ pool.

Estuary	$\delta^{15}NH_4^+$ (low)	$\delta^{15}NH_4^+$ (high)	Authors
Delaware estuary, USA	+11.2‰	+40‰	Cifuentes et al., 1989
Delaware estuary, USA	+12‰	+42‰	Velinsky et al., 1989
Chesapeake Bay, USA		+20‰	Horrigan et al., 1990
Thames estuary, UK	+14‰		Middelburg and Nieuwenhuize, 2001
Loire estuary, France		+17‰	Middelburg and Nieuwenhuize, 2001
Scheldt estuary, Belgium	+10‰	+29‰	Mariotti et al., 1984
Scheldt estuary, Belgium	**+10‰**	**+70‰**	**This study**

Our winter-spring average $\delta^{15}NH_4^+$ value (+10‰, SD=1‰) is equal to the one reported by Mariotti et al. (1984) for the upstream part of the Scheldt estuary during June-July 1982. Summer $\delta^{15}NH_4^+$ values measured in this study for the upstream reaches of the Scheldt estuary are up to 60‰ more enriched than the ones reported by Mariotti et al. (1984), which is probably a result of increased nitrification in this part of the Scheldt due to an improved water quality (de Bie et al., 2002a). However, the maximum value for $\delta^{15}NH_4^+$, reported for the downstream reaches of the Scheldt River where the intensity of the nitrification process increased due to improving O_2 conditions, was only +29‰ (Mariotti et al., 1984), which is still considerably lower than the +70‰ reported in this study. A value of +29‰ is, however, close to the value of +32‰ calculated by means of equation 5.1 (see below) for a situation where the fraction *f* equals 0.3, which is roughly the fraction of NH_4^+ remaining in the NH_4^+ pool during the summer of 1982 (Fig. 4 in Mariotti et al., 1984).

5.5.2 NH_4^+ consuming processes affecting $\delta^{15}NH_4^+$

In order to identify the nature of the NH_4^+ consuming processes (nitrification or uptake by phytoplankton) responsible for the seasonal variation in $\delta^{15}NH_4^+$, we compared the temporal pattern of $\delta^{15}NH_4^+$ with longitudinal profiles of NH_4^+, NO_3^- and Chl-a (Fig. 5.5). In general, a concomitant downstream decrease in NH_4^+ and increase in NO_3^- points to the presence of nitrification in the water column while increasing Chl-a concentrations reflect the presence of a growing phytoplankton community.

During winter, biological activity is suppressed by low water temperatures, which results in relatively constant NH_4^+, NO_3^- and Chl-a concentrations (winter longitudinal profiles resemble the profile of 2 April 2002; Fig. 5.5). The lack of biological activity is reflected in the $\delta^{15}NH_4^+$ signatures, which are relatively constant, averaging +10‰ (SD=1‰) (Fig. 5.4).

NH_4^+, NO_3^- and Chl-a concentrations were also relatively constant during the spring bloom (March and April 2002); (Fig. 5.5). Although NH_4^+ and NO_3^- did not change during early April, there is evidence that on from April, nitrification contributed to NH_4^+ consumption, since nitrification rates were relatively high at S1 in early April 2002 (0.3 $\mu mol.l^{-1}.h^{-1}$; Verlinden, 2002). The longitudinal profile of Chl-a for the second half of April is lacking, but the sharp increase in Chl-a between March, 29th and April, 15th (Fig. 5.3C) suggested the presence of a developing phytoplankton community whereby NH_4^+ may have served as the preferential N-substrate (Cohen and Fong, 2004). However, despite the contribution of both nitrification and phytoplankton uptake to total NH_4^+ consumption during the spring bloom, $\delta^{15}NH_4^+$ signatures increased only

slightly to a value of +13‰ (Fig. 5.4) which was probably because of the buffering capacity of the large NH_4^+ pool.

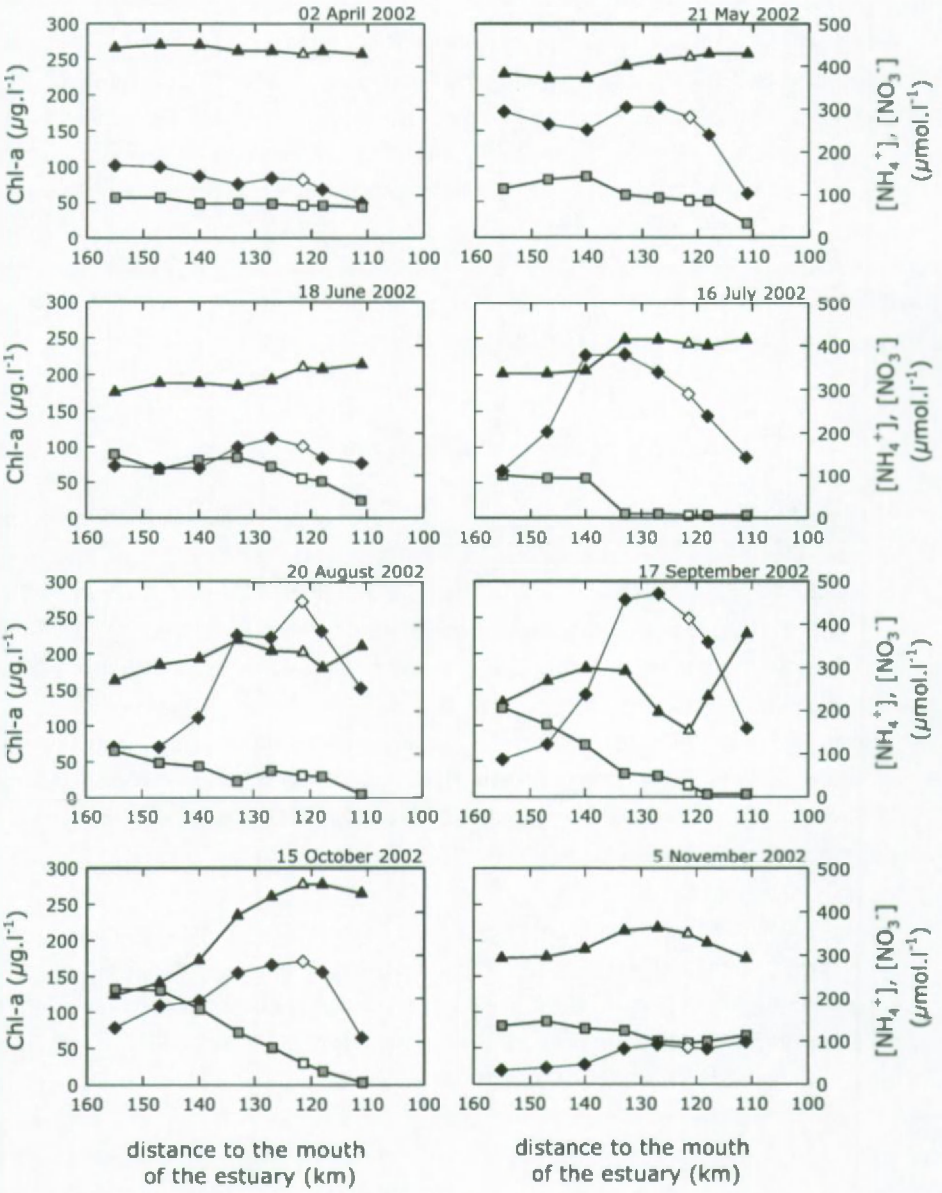

Figure 5.5: Longitudinal profiles of Chl-a (diamonds), NH_4^+ (squares) and NO_3^- (triangles) for the km 155 to km 110 stretch of the Scheldt estuary between April and November 2002 (T. Maris, University of Antwerp, pers. comm.). The white symbol indicates the location of station S1.

During the summer bloom (June to late September; Fig. 5.3C) $\delta^{15}NH_4^+$ values varied between +18‰ and +70‰ and were inversely correlated to the fraction of NH_4^+ remaining in the NH_4^+ pool at S1 (eq. 5.2; see below); (Fig. 5.6). Highest $\delta^{15}NH_4^+$ signatures (> +60‰) were observed during late June, July and September 2002 (Fig. 5.4) and coincided with periods of increased NH_4^+ consumption as shown by strongly reduced NH_4^+ pools (< 5% NH_4^+ remaining; Fig. 5.6). Indeed, during July 2002 Chl-a concentrations increased exponentially, while NH_4^+ decreases coincided with increases in NO_3^- (Fig. 5.5), indicating that both phytoplankton uptake and nitrification contributed to NH_4^+ consumption. The longitudinal profile of Chl-a for late June is lacking, but the sharp increase between June, 11th and June 27th (Fig. 5.3C), suggests that phytoplankton biomass increased during this period. During September, the decrease in NO_3^- (km 134 to km 118) and the low O_2 concentrations (0.9 mg.l^{-1}); (Fig 5.2A) suggested that denitrification dominated in the water column downstream from km 134. NH_4^+ concentrations decreased gradually, which was probably mainly due to phytoplankton uptake since Chl-a increased exponentially (Fig. 5.5) and the low O_2 concentrations would have suppressed nitrification activity (de Bie et al., 2002b).

$\delta^{15}NH_4^+$ values were significantly lower during May, early June and August 2002 (+27‰; +18‰ and +31‰, respectively) while the fractions of NH_4^+ remaining in the NH_4^+ pool were considerably higher (33 to 53%; Fig. 5.6). The elevated fractions of NH_4^+ remaining in the NH_4^+ pool during May and early June probably reflected a reduced NH_4^+ consumption compared to the other summer months. NH_4^+ and NO_3^- profiles reflected the presence of nitrification in the water column but phytoplanktonic NH_4^+ uptake was probably less important, given the lack of increase in Chl-a during these months. In August, on the contrary, the longitudinal profiles of NH_4^+, NO_3^- and Chl-a showed that phytoplankton uptake and nitrification both contributed to NH_4^+ removal, a situation similar to the one observed in July ($\delta^{15}NH_4^+$ = +70‰). Consequently, we expected NH_4^+ to be highly enriched in ^{15}N. The decrease in $\delta^{15}NH_4^+$ might have resulted from the mixing of NH_4^+ highly enriched in ^{15}N due to NH_4^+ consumption processes with NH_4^+ depleted in ^{15}N. The sharp increase in the PN and POC concentrations (Fig. 5.2D) and the decrease in the Chl-a/PN and Chl-a/POC ratios between July and August (data not shown) reflect the presence of a large amount of organic matter depleted in Chl-a. Potential sources of organic matter depleted in ^{15}N and Chl-a are phytoplankton detritus (see discussion below), terrestrial organic matter (+3‰, Middelburg and Nieuwenhuize, 1998) and sewage (+2‰, Fisseha, 2000). Heterotrophic bacteria processing this organic matter could subsequently have added NH_4^+ depleted in ^{15}N to the existing NH_4^+ pool.

After the summer bloom (October-November 2002), $\delta^{15}NH_4^+$ signatures were still relatively high (+17‰ and +29‰, respectively; Fig. 5.4). During this period,

phytoplanktonic NH_4^+ uptake (October) and nitrification (October and November) probably still accounted for NH_4^+ consumption (Fig. 5.5), although we may not exclude that the increased input a terrestrial organic matter during autumn introduced considerable amounts of $^{14}NH_4^+$ to the existing NH_4^+ pool.

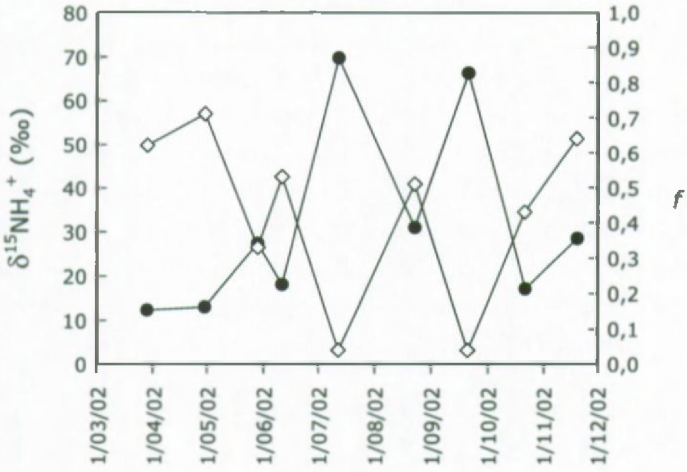

Figure 5.6: Seasonal variation between $\delta^{15}NH_4^+$ (circles) and the fraction of NH_4^+ remaining in the NH_4^+ pool (f) (diamonds) at the freshwater station S1 of the Scheldt estuary (2002).

5.5.3 Fractionation during NH_4^+ consumption

In the following sections we aim at reconstructing the $\delta^{15}N$ signature of phytoplankton. We will calculate the fractionation factor involved with NH_4^+ consumption followed by the calculation of the $\delta^{15}N$ signature of the accumulated phytoplankton pool (phytoplankton and phytodetritus).

For the calculation of the fractionation associated with NH_4^+ consumption, we assumed that a water body transported between the head of the estuary (km 155) and the sampling station S1 (km 121) operates in closed-system mode. Indeed, NH_4^+ concentrations between the head of the estuary and S1 are relatively constant during periods of low biological activity as shown by the longitudinal profile of NH_4^+ for April 2002, which represents a typical winter NH_4^+ profile, suggesting that in- and output of NH_4^+ are minimal over this transect. This allows us to use the Rayleigh fractionation equation to calculate the fractionation associated with NH_4^+ consumption.

The Rayleigh fractionation curve is described by the following equation (Mariotti, 1981; Fry, 2003; Chapter 2):

$$\delta^{15}NH_4^+ = \delta^{15}NH_4^+{}_{(i)} - \varepsilon \times \ln f \qquad \text{Eq. 5.1}$$

$\delta^{15}NH_4^+{}_{(i)}$ is the initial $\delta^{15}N$ signature of the NH_4^+ pool, ε is the fractionation associated with NH_4^+ consumption (nitrification and uptake) and *f* is the fraction of NH_4^+ remaining in the NH_4^+ pool. *f* is calculated as the ratio of NH_4^+ measured at S1 ($NH_4^+{}_{(f)}$) and the input NH_4^+ concentration ($NH_4^+{}_{(i)}$) at the head of the estuary:

$$f = \frac{NH_4^+(f)}{NH_4^+(i)} \qquad \text{Eq. 5.2}$$

However, NH_4^+ concentrations at the head of the estuary will only reflect input concentrations during winter months. Indeed, elevated water temperatures during non-winter months will increase the intensity of NH_4^+ consuming and producing processes so that NH_4^+ concentrations at the head of the estuary may under- or overestimate the input NH_4^+ concentration. However, since input NH_4^+ concentrations depend on the freshwater flow (Q) during periods of low biological activity (Fig. 5.7), we can use this relationship to calculate the theoretical input NH_4^+ concentration for the whole study period. We excluded months where the calculated fraction *f* was higher than 1 ($NH_4^+{}_{(f)} > NH_4^+{}_{(i)}$), as was the case for November 2001, because values >1 suggest that NH_4^+ production was important. Under such circumstances the evolution of $\delta^{15}NH_4^+$ cannot be described by the Rayleigh fractionation equation.

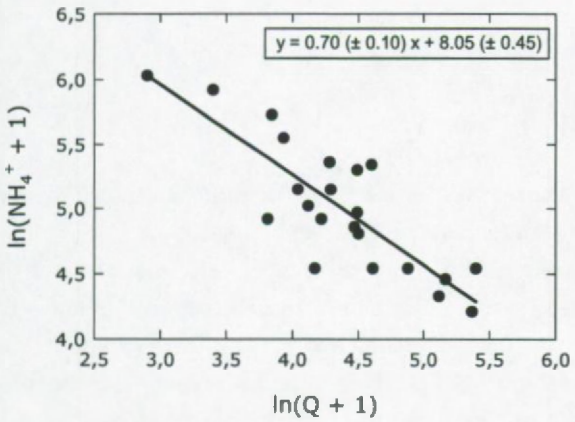

Figure 5.7: Linear relationship between the natural logarithm of discharge and NH_4^+ (r^2 = 0.69, $p<0.001$). NH_4^+ concentrations and discharge data are measured at the head of the estuary (km 155) during the winter period (December – April) of 1999, 2000, 2001 and 2002. [Source NH_4^+: S. Van Damme and T. Maris, (University of Antwerp), pers. comm.; source Q: Taverniers (1999; 2000; 2001; 2002)].

Conform to Rayleigh equation theory, $\delta^{15}NH_4^+$ values increased linearly with increasing values of ln *f* (Fig. 5.8), confirming that a water body transported between

the head of the estuary and S1 behaves as a closed system. The slope of this relationship, 18.4‰ (SE=1.2‰), represents the value of the fractionation factor (ε) associated with NH_4^+ consumption (= uptake and/or nitrification) in the Scheldt estuary. This value falls well within the ranges reported in literature: discrimination due to nitrification calculated for natural systems ranges between +13 and +16‰ (Horrigan et al., 1990) while fractionation due to phytoplankton uptake in natural systems has been reported to range between 5 and 30‰ (Cifuentes et al., 1989; Pennock et al., 1996).

The intercept of the Rayleigh equation graph (+9.6‰, SE=2.6‰) denotes the value for the input $\delta^{15}NH_4^+$ (eq. 5.1). This value includes our measured average value for the winter-early spring period (+10‰, SD=1‰).

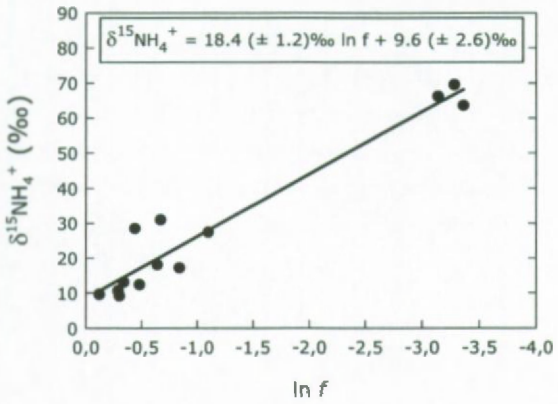

Figure 5.8: Scatter plot showing the linear relationship between ln *f* and $\delta^{15}N$ of NH_4^+ (r^2 = 0.97, $p<0.001$).

5.5.4 Relationship between $\delta^{15}NH_4^+$ and $\delta^{15}N_{SPOM}$

Winter $\delta^{15}N_{SPOM}$ values averaged +3‰, suggesting that SPOM consisted mainly of terrestrial detritus during winter (Middelburg and Nieuwenhuize, 1998).

During the spring and summer bloom (April to October; Fig. 5.3C), the $\delta^{15}N$ composition of SPOM first decreased (spring) and than increased (summer) relative to winter $\delta^{15}N$ values (Fig. 5.3D). In the following we will calculate the $\delta^{15}N$ of phytoplankton and compare it with the $\delta^{15}N$ of SPOM in order to investigate if changes in the $\delta^{15}N$ of SPOM can be related to the presence of phytoplankton. If we assume that NH_4^+ is the only N-source of phytoplankton, the $\delta^{15}N$ of accumulated phytoplankton can be calculated with the following equation (Mariotti et al., 1981; Fry, 2003):

$$\delta^{15}N_{acc} = \varepsilon \times \frac{f \ln f}{1-f} + \delta^{15}NH_4^{+}{}_{(i)} \qquad \text{Eq. 5.4}$$

$\delta^{15}N_{acc}$ is the $\delta^{15}N$ composition of the accumulated phytoplankton in the water column, ε is the fractionation associated with NH_4^+ uptake (18.4‰), f is the fraction NH_4^+ remaining in the water column (eq. 5.2) and $\delta^{15}NH_4^+{}_{(i)}$ is the initial $\delta^{15}N$ signature of NH_4^+ (+9.6‰). We may assume that the input $\delta^{15}NH_4^+$ signature is constant over the year since the summer $\delta^{15}NH_4^+$ reported by Mariotti et al. (1984) for a situation where NH_4^+ concentrations were not affected by NH_4^+ consumption, was similar to the one measured in winter during this study (i.e. +10‰).

If we assume that the organic matter fraction of the suspended matter consists entirely of in situ produced phytoplankton, the $\delta^{15}N$ composition of suspended matter will be similar to the $\delta^{15}N$ of accumulated phytoplankton. However, $\delta^{15}N$ signatures of accumulated phytoplankton for the spring and summer bloom period (April 15th till October 21st, Fig. 5.3C) were always lower than $\delta^{15}N$ signatures of bulk suspended matter (Fig. 5.9). Nevertheless, $\delta^{15}N_{acc}$ and $\delta^{15}N_{SPOM}$ were significantly correlated (Bivariate least square regression: $r^2 = 0.62$, $p<0.01$) indicating that phytoplankton biomass is largely responsible for the observed variation in $\delta^{15}N_{SPOM}$.

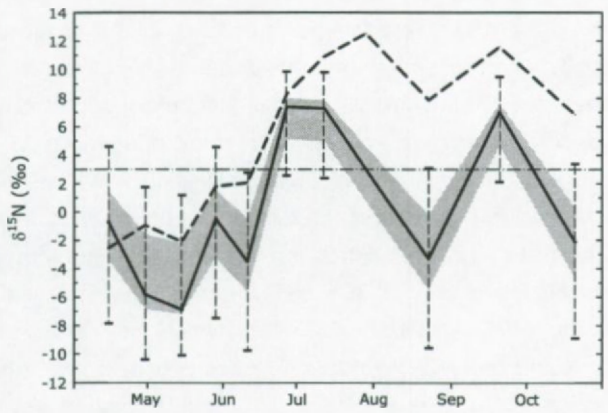

Figure 5.9: Comparison between $\delta^{15}N$ signatures of SPOM (dashed line) and calculated accumulated phytoplankton material (solid line) during the spring and summer phytoplankton bloom (April 2002 till October 2002). The grey area indicates the 25-75‰ interval range of the calculated $\delta^{15}N$ of accumulated phytoplankton, while the vertical dashed lines represent the 5-95% data range. The +3‰ line indicates the average $\delta^{15}N$ signature of terrestrial and sewage inputs. Uncertainty calculations were made using Monte Carlo simulations. During these simulations, only f-values < 1 ($NH_4^+{}_{(f)} < NH_4^+{}_{(i)}$) were taken into account because $\delta^{15}NH_4^+$ does not longer behave according to the Rayleigh fractionation theory in case of NH_4^+ production ($NH_4^+{}_{(f)} > NH_4^+{}_{(i)}$).

Several processes may contribute to the increase of $\delta^{15}N$ of bulk suspended matter compared to $\delta^{15}N$ of the accumulated phytoplankton pool. First, the presence of non-phytoplanktonic, ^{15}N-rich organic matter in the suspended matter pool could increase the overall $\delta^{15}N$ signature of SPOM. For instance, between mid-April and mid-June, the accumulated phytoplankton (range -6.9 to -0.5‰) could have mixed with terrestrial matter and sewage (averaging +2‰; Mariotti et al., 1984; Middelburg and Nieuwenhuize, 1998; Fisseha, 2000) resulting in a slightly higher value for bulk SPOM (range: -2.6 to +2.0‰). Second, the overall $\delta^{15}N$ signature of suspended matter can increase due to the assimilation of ^{15}N-rich dissolved N from the surrounding water by microbial decomposers (Caraco et al., 1998). Third, the actual standing stock of phytoplankton might not represent the real accumulated phytoplankton biomass if considerable loss of phytoplankton occurs. The calculated $\delta^{15}N_{acc}$ could then underestimate the actual $\delta^{15}N$ signature of phytoplankton since phytoplankton lost through sedimentation or through grazing is depleted in ^{15}N relative to new phytoplankton generations. Indeed, the $\delta^{15}N$ signature of the remnant NH_4^+ pool increases exponentially with decreasing fraction of NH_4^+ remaining in the NH_4^+ pool (Rayleigh equation 5.1, Chapter 2: Fig. 2.1) so that successive phytoplankton generations become increasingly enriched in ^{15}N. Fourth, the fractionation during NH_4^+ uptake decreases with decreasing NH_4^+ concentration (Hoch et al., 1992). The expression of fractionation is maximal (27‰) at NH_4^+ concentrations ranging between 100 and 1000 $\mu mol.l^{-1}$ (Hoch et al., 1992; Pennock et al., 1996). For NH_4^+ concentrations below 100 $\mu mol.l^{-1}$, fractionation can reach values as low as 4‰ (Hoch et al., 1992), especially when NH_4^+ demand is high due to high growth rates (Hoch et al., 1994). Thus, the relative enrichment in ^{15}N of the suspended matter pool during periods of reduced NH_4^+ (summer) may result from a increase in the $\delta^{15}N$ of phytoplankton due to a decrease in the fractionation against $^{15}NH_4^+$. The fractionation value of 18.4‰ (SE=1.2‰) calculated in this study could be considered as the intermediate value of a period of full expression of fractionation (spring bloom) when NH_4^+ concentrations are high (Fig. 5.3B) and a period of decreased fractionation (summer). Finally, the $\delta^{15}N$ signature of phytoplankton may increase due to the assimilation of other N-sources. NO_3^-, which is far more abundant than NH_4^+ (Fig. 5.3A, 5.3B), may represent an additional N-source for phytoplankton (Middelburg and Nieuwenhuize, 2000; Cohen and Fong, 2004). The $\delta^{15}N$ signature of NO_3^- in the Scheldt estuary averages +9‰ under oxic conditions ($\%O_2$ > 20%; Middelburg and Nieuwenhuize, 2001) and increases to +20‰ when denitrification is important (Mariotti et al., 1984) while fractionation during NO_3^- uptake ranges between 3 and 10‰ in natural systems (Cline and Kaplan, 1975; Wada, 1980; Altabet and Francois, 1994; Karsh et al., 2003). Thus, phytoplankton assimilating NO_3^- will have isotopic

signatures ranging between -1 and +6‰ under oxic conditions and between +10 and +17‰ under denitrifying conditions. The uptake of NO_3^- will thus mainly increase the $\delta^{15}N$ of phytoplankton under low oxygen conditions favoring denitrification.

SECTION 2

5.6 Results: Decomposition experiment

5.6.1 General decay patterns

Despite the small mesh size (300 μm) of the litterbags, presence of invertebrates (Oligochaeta and Hirudinea) inside the bags was noticed after 4 months (February 2002). After 5 months (March 2002) the first invertebrate shredders (Isopoda) turned up inside the litterbags, but effects of shredder activity on the leaf litter became only apparent after another 2 months (May 2002). Later, litterbags contained leaf litter in difference stages of decomposition, ranging from leaf skeletons to barely attacked leaves (Fig. 5.10). After 18 months, some bags contained litter of which the whole leaf structure was still recognizable although the leaf tissue was very fragile.

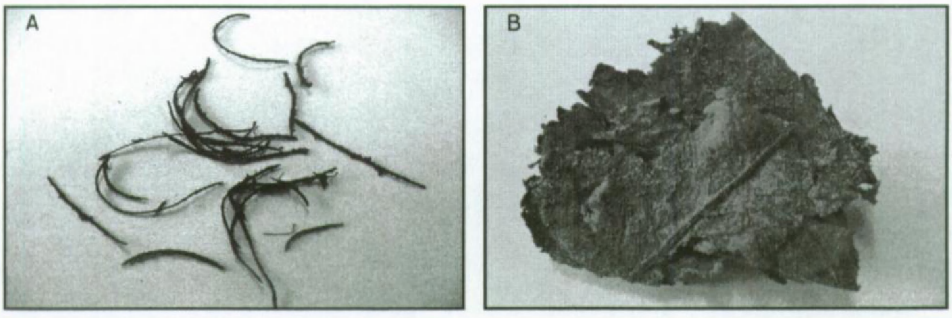

Figure 5.10: Willow leaves after 11 months (A) and 16 months (B) of decomposition at station S1 of the Scheldt River. (A) Shredders consuming leaf tissue have left only leaf skeletons in the litter bag. (B) Without shredder attack, leaf structure remained recognizable till the end of the incubation experiment.

5.6.2 Evolution of PN and POC concentrations of decomposing willow leaves

The PN and POC concentration of the LBC, expressed per ash-free dry weight (AFDW), increased gradually during the first four months of incubation. On from the 5th month (March 2002), PN_{LBC} and POC_{LBC} concentrations varied without clear seasonal

pattern (Fig. 5.11). The leaf-biofilm complex was consistently enriched in N compared to the original leaf. POC_{LBC} concentrations, on the contrary, were generally lower than the one of the original leaf, except during winter 2001 and early-summer 2002.

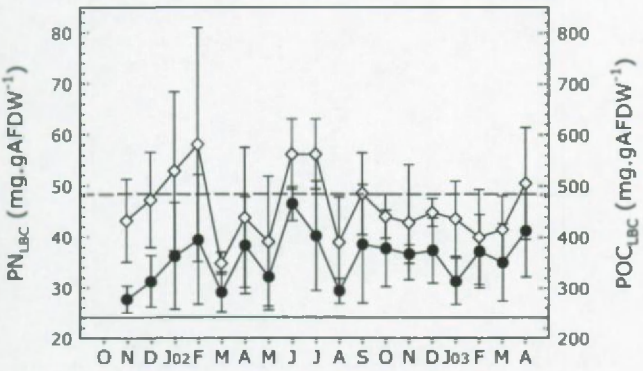

Figure 5.11: Seasonal variation in the PN (circle) and POC (diamond) concentrations of the leaf-biofilm complex, expressed per AFDW. The dashed line represents the POC concentrations of the original leaf, while the solid line represents the original PN concentration of the leaf. Error bars represent standard deviations of two or three replicates.

5.6.3 $\delta^{15}N$ variation of degrading leaves and associated biofilm

During the decomposition process, $\delta^{15}N$ of the LBC increased significantly compared to the original value of willow leaves (+7.1‰, SD=0.8‰) (t-test, $p < 0.05$) and showed a consistent temporal variation (Fig. 5.12). $\delta^{15}N$ values increased during the first three months of incubation (maximum of +10.5‰, SD=0.4‰, December 2001), but decreased sharply during February 2002 (+8.4‰, SD=0.8‰). Then, values increased steadily to a second maximum of +12.2‰ (SD=0.1‰) in October 2002 and decreased gradually to a second minimum in February 2003 (+10.4‰, SD=0.4‰), after which values started to increase again.

The $\delta^{15}N$ values of the LBF and BBF varied considerably over the season and between litterbags (Fig. 5.12). $\delta^{15}N$ values of BBF largely exceeded those of LBF, both showing lowest $\delta^{15}N$ values in winter-early spring and increasing $\delta^{15}N$ values towards autumn.

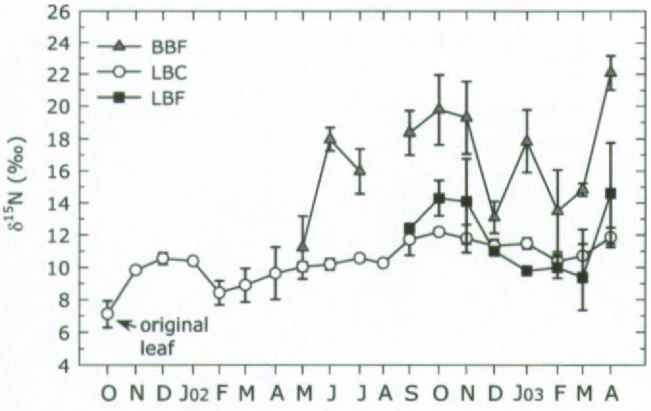

Figure 5.12: Seasonal changes in the $\delta^{15}N$ signature of the leaf-biofilm complex (LBC), the bag biofilm (BBF) and the leaf biofilm (LBF) over the course of the experiment. Error bars represent standard deviations of two or three replicates.

5.7 Discussion: Decomposition experiment

5.7.1 Contamination of the leaf-biofilm complex with suspended matter

Submerged organic surfaces are rapidly covered by a gelatinous biofilm secreted by microheterotrophic decomposers (Golladay and Sinsabaugh, 1991). These microorganisms thrive on nitrogen and carbon regenerated form the organic substrate, eventually complemented with nitrogen from the ambient solution if the bio-availability of the substrate-nitrogen is too low to cover their N-requirements (Suberkropp and Chauvet, 1995; Suberkropp, 1998; Grattan and Suberkropp, 2001). Microbial decomposers can considerably modify the POC and PN concentration of the leaf-biofilm complex through N-uptake, release of dissolved N- and C-compounds (Fogel and Tuross, 1999; Lehmann et al., 2002) and production of CO_2 (Findlay and Arsuffi, 1989; Baldy and Gessner, 1997). However, microbial modifications of the PN_{LBC} and POC_{LBC} concentration can be masked by the presence of suspended organic matter in the biofilm. Indeed, settled in the bags, decomposing leaves can become rapidly contaminated with suspended matter from the surrounding water trapped in the gelatinous matrix of the biofilm (Golladay and Sinsabaugh, 1991), a process even enhanced by the use of litter bags with fine mesh size, mainly because of reduced currents inside the bags (Hieber and Gessner, 2002). Thus, in order to investigate the changes in the PN and POC concentrations in the LBC induced by microbial activity, we had to correct for organic N and C from suspended origin trapped in the biofilm. We determined the degree of contamination by measuring the aluminium concentration in the LBC. The rationale behind this approach is as follows. First, Al can be considered a

good proxy of lithogenic material (Al = 8% of the aluminosilicate composition, taken to reflect clay material in the system; Bowen, 1979). Second, it is assumed that all Al comes from settled suspended matter consisting both of lithogenic material and particulate organic matter. Since the concentration of suspended solids in the suspended matter will alter seasonally (Van Damme et al., 1999), we measured the monthly variation in the aluminium concentration in the suspended matter and calculated the corresponding PN/Al and POC/Al ratios of SPM to correct for PN and POC of suspended matter origin trapped in the biofilm:

$$PN_{SPOM\,(LBC)} = \frac{PN_{(SPM)}}{Al_{(SPM)}} \times Al_{(LBC)} \qquad \text{Eq. 5.5}$$

$$POC_{SPOM\,(LBC)} = \frac{POC_{(SPM)}}{Al_{(SPM)}} \times Al_{(LBC)} \qquad \text{Eq. 5.6}$$

$PN_{SPOM(LBC)}$ and $POC_{SPOM(LBC)}$ denote the amount of PN and POC from suspended matter origin trapped in the leaf-biofilm complex. $PN_{(SPM)}/Al_{(SPM)}$ and $POC_{(SPM)}/Al_{(SPM)}$ denote the amount of PN and POC per unit of aluminium in the suspended matter (SPM) pool. $Al_{(LBC)}$ refers to the amount of aluminium trapped in the leaf-biofilm complex.

PN_{LBC} and POC_{LBC} concentrations decreased considerably after correction for the contamination with SPOM (Fig. 5.13). The decrease was most pronounced for PN_{LBC} values because SPOM is enriched in N (C/N: 6 to 11; data not shown) compared to willow leaves (C/N: 24). After correction, PN concentrations ($PN_{LBC,\ corr}$) fluctuated around the original PN concentration whereas $POC_{LBC,\ corr}$ concentrations were initially similar to the original value after which they slightly decreased. As a result, the C/N ratios of submerged willow leaves were slightly lower than the one of the original leaf (Fig. 5.14).

The decrease in the C/N ratio of the decomposing leaves suggested that C-containing compounds were removed preferentially during decomposition. However, literature data do not provide consistent information on the compound (C or N) preferentially released during plant litter decomposition. Caraco et al. (1998) and Lehmann et al. (2002), for instance, reported a preferential loss of N compounds during decomposition, while Fogel and Tuross (1999) concluded towards a preferential loss of C compounds. Alternatively, the colonization of the leaf by microbial organisms (low C/N) could have decreased the overall C/N ratio of the LBC (Lehmann et al., 2002). Furthermore, the microbial assimilation of dissolved N from the ambient (Suberkropp and Chauvet 1995; Grattan and Suberkropp, 1998; Suberkropp, 1998; Sanzone et al. 2001) could mask the loss of N-compounds. If the microorganisms

would assimilate dissolved N from the surrounding water, their $\delta^{15}N$ signature would reflect the one of NH_4^+ (Zieman et al., 1984; Caraco et al., 1998), since leaf-colonizing micro-organisms preferentially assimilate NH_4^+ if substrate-N becomes limiting (Sanzone et al., 2001). However, if the $PN_{SPOM(LBC)}$ provides the necessary N to the microbial community to compensate for the lack of bio-available N in the leaf, microorganisms would no longer assimilate dissolved N from the surrounding water and the $\delta^{15}N$ signature of the LBC would only be set by the $\delta^{15}N$ signatures of willow leaf and PN_{SPOM}. An investigation of the $\delta^{15}N$ signature of the LBC should thus give more information on the occurrence of microbial N-assimilation in the LBC.

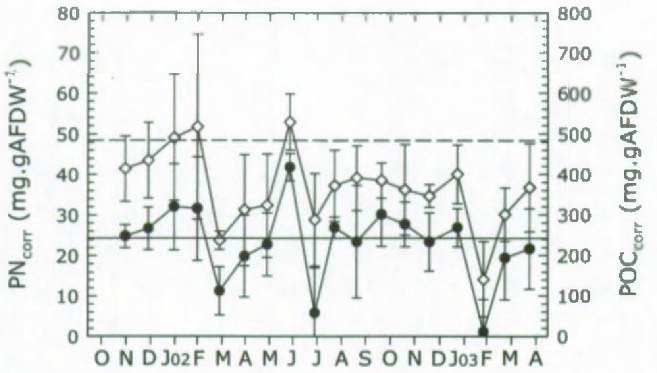

Figure 5.13: Seasonal variation in the PN (black) and POC concentration (white) of the leaf-biofilm complex after correction for contamination with PN and POC from the surrounding water. The dashed and solid lines represent the original $POC_{corr,LBC}$ and $PN_{corr,LBC}$ concentration, respectively, of the willow leaves. Error bars represent standard deviations of two or three replicates.

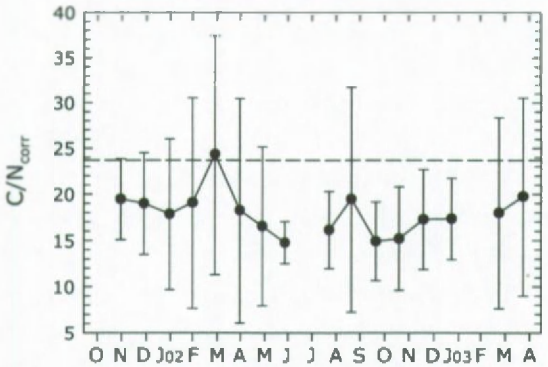

Figure 5.14: Seasonal variation in the C/N ratio of the leaf-biofilm complex, after correction for PN and POC trapped in the biofilm and originating from the surrounding water. The C/N ratios of July 2002 and January 2003 were considered as outliers (Massart et al., 1997). Error bars represent the calculated standard deviation of two or three replicates.

5.7.2 Microbial modification of the leaf-biofilm $\delta^{15}N$ signature

During the decomposition experiment, we measured the $\delta^{15}N$ composition of the leaf-biofilm complex and the biofilm on the willow leaves (LBF) and on the litter bags (BBF) (Fig. 5.12). The BBF was considerable enriched in ^{15}N compared to the LBF and LBC. This enrichment suggests that microorganisms in the LBC and LBF have access to an additional and ^{15}N-depleted N-source compared to microorganisms colonizing the BBF. This additional N-source is probably leaf-N ($\delta^{15}N$ = +7‰), because, in contrast to microorganisms colonizing the leaves, microorganisms in the BBF have no access to leaf-N but may only thrive on PN trapped in the biofilm and on dissolved N from the surrounding water.

The $\delta^{15}N$ signature of the BBF was significantly correlated with both the LBF and the LBC (Spearman Rank correlation, LBF: Rank 0.78, $p<0.05$; LBC: Rank 0.79, $p<0.01$) suggesting that the $\delta^{15}N$ pattern of the LBC is mainly set by variations in the $\delta^{15}N$ of the biofilm. Thus, other sources of variation of the $\delta^{15}N$ of the leaf substrate, such as hydrolysis of organic compounds (Lehmann et al., 2002) and the preferential loss of organic compounds with distinct isotopic signatures (Harvey et al., 1995; Fogel and Tuross, 1999; Lehmann et al., 2002) will probably have only a lesser impact on the overall $\delta^{15}N$ signature of the LBC.

If the microorganisms in the biofilms would thrive on nitrogen originating from SPOM trapped in the biofilm or on NH_4^+ from the ambient solution, the $\delta^{15}N$ signature of the LBC should correlate with the one of SPOM or NH_4^+, respectively. A Spearman Rank correlation test revealed, however, no significant correlation between $\delta^{15}N_{LBC}$ and $\delta^{15}N_{SPOM}$ or between $\delta^{15}N_{LBC}$ and $\delta^{15}NH_4^+$. Thus, neither the presence of PN_{SPOM} nor the assimilation of NH_4^+ affects the $\delta^{15}N$ composition of the LBC. We therefore suggest that the $\delta^{15}N$ signature of the biofilm is affected by the activity of the microbial organisms constituting it. The seasonal pattern of $\delta^{15}N_{LBC}$ could then be explained as follows. The initial increase in $\delta^{15}N$ of the LBC (Fig. 5.15) could result from a combination of leaching and microbial assimilation of ^{15}N-depleted N-compounds from the leaf tissue (Lehmann et al., 2002). Loss of microbial organisms could subsequently contribute to a net removal of ^{15}N-depleted organic. On from the third month, the development of a biofilm and the increasing amount of PN_{SPOM} trapped in it may have counteracted the increase in $\delta^{15}N_{LBC}$ since PN_{SPOM} is depleted in ^{15}N during winter compared to willow leaves (Fig.5.3D). Between March 2002 and October 2002, microbial processing of the nitrogen in the biofilm would again increase the $\delta^{15}N$ of the LBC. Uptake processes fractionating against ^{15}N could enrich the remnant N-substrates (DON, NH_4^+, NO_3^-) in ^{15}N, which in turn could increase the $\delta^{15}N$ of successive generations of microorganisms. These fractionating processes could occur all over the biofilm. Indeed, biofilms typically constitute of an oxic top layer while the underlying layers become gradually more

anoxic (Golladay and Sinsabaugh, 1991; Simon et al., 2002). The oxic layer could support a community of nitrifiers enriching the available NH_4^+ through the preferential assimilation of $^{14}NH_4^+$. Similarly, a community of denitrifiers could increase the $\delta^{15}N$ of the NO_3^- in the anaerobic subsurface layers through the preferential assimilation of $^{14}NO_3^-$. $\delta^{15}N_{LBC}$ values decreased gradually on from November 2002, probably as a result of the continuous trapping of ^{15}N-depleted PN from the water column and a suppressed microbial activity due to decreasing water temperatures. In February 2003, the minimum $\delta^{15}N$ value coincided with a maximum PN_{SPOM} trapped in the biofilm. Finally, on from March 2003, $\delta^{15}N_{LBC}$ started to increase again. Here, the same processes as the ones described for the spring of the previous year may apply.

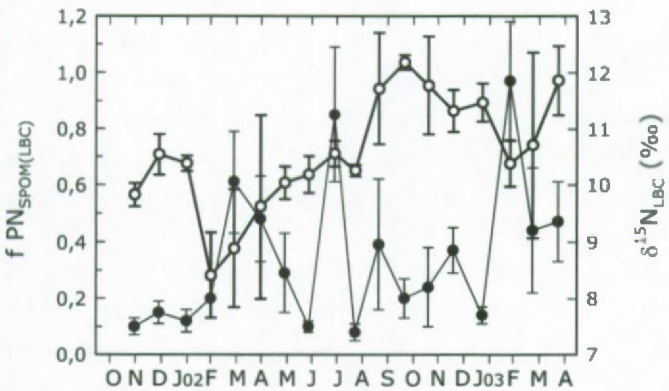

Figure 5.15: Comparison between the seasonal patterns of $\delta^{15}N_{LBC}$ (white) and the fraction f of PN originating from SPOM (black) in the LBC. Error bars represent the calculated standard deviations of two or three replicates.

The results of this incubation experiment do not allow us to draw conclusions about the relative importance of organic substrate-N or ambient DN in setting the $\delta^{15}N$ of microbial organisms. The relatively N-rich suspended matter trapped in the biofilm may have provided the necessary additional nitrogen for the microbial decomposers in case substrate-N would have become limiting. We were thus not able to reconstruct the $\delta^{15}N$ signature of heterotrophs assimilating dissolved N from the ambient. Instead, our results suggest that the $\delta^{15}N$ signature of microbial heterotrophs in the biofilm of decomposing leaves reflects the microbial activity in the biofilm.

5.8 General discussion

The main objective of this study was to investigate the $\delta^{15}N$ signature of the microbial (phytoplankton + bacteria) community in the freshwater section of the Scheldt estuary to verify if the local cyclopoid copepod community relies ultimately on autotrophic or heterotrophic food sources. Based on the calculated fractionation factor for NH_4^+ uptake and the calculated input $\delta^{15}NH_4^+$ we can now calculate the $\delta^{15}N$ signature of phytoplankton at S1 for the period 1999-2001, during which also copepod sampling was undertaken. Heterotrophs assimilating phytoplankton-derived DOM should then parallel the $\delta^{15}N$ signal of phytoplankton (Benner et al., 1997). The results of a Spearman Rank correlation test showed, however, that $\delta^{15}N$ of the accumulated phytoplankton and $\delta^{15}N$ of cyclopoid copepods were not significantly correlated ($p<0.05$). This excluded in situ produced phytoplankton or heterotrophs thriving on DOM derived from this phytoplankton as a food source for cyclopoid copepods. The strongly depleted $\delta^{13}C$ signatures of cyclopoid copepods relative to $\delta^{13}C_{SPOM}$ (Fig. 5.16) suggest, however, that the heterotrophic primary producers obtain at least part of their C-sources from phytoplankton organic matter. Indeed, phytoplankton is the only component of the SPOM pool with highly depleted $\delta^{13}C$ signatures ($\delta^{13}C$ green algae: ± -45‰, $\delta^{13}C$ diatoms ± -35‰; Boschker et al., 2005 compared to terrestrial and sewage mater: $\delta^{13}C$ approximately -27‰; Hellings, 2000; Fisseha, 2002). As a consequence, it is likely that bacteria also obtain part of their N-sources from phytoplankton.

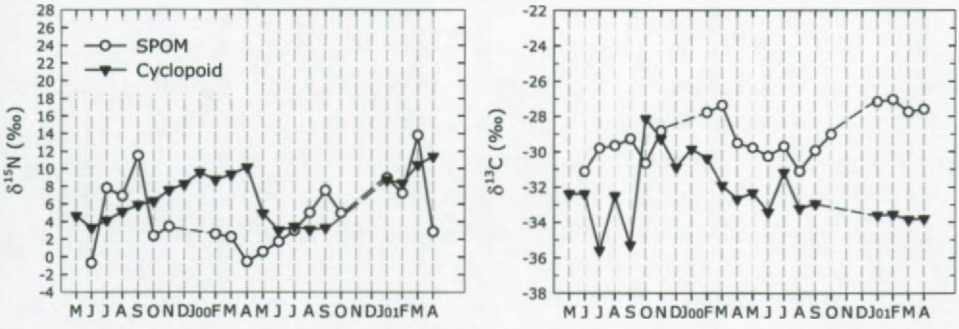

Figure 5.16: Seasonal variation in the $\delta^{15}N$ and $\delta^{13}C$ signature of SPOM and cyclopoid copepods at station S1 for the period 1999-2001.

Unfortunately, our data do not provide enough information to solve this apparent contradiction. However, we can propose three scenarios where cyclopoid copepods could simultaneously reflect the $\delta^{13}C$ of phytoplankton and still have a $\delta^{15}N$ signature that differs from the calculated $\delta^{15}N$ signature of phytoplankton.

First, green algae could act as a substrate for bacteria at the base of the food web. Indeed, the phytoplankton community in the freshwater section under study consists mainly of active diatoms and decaying green algae imported from tributaries (Muylaert et al., 2001; Boschker et al., 2005). Since green algae are not growing in the estuary proper, their $\delta^{15}N$ signature may differ from the one of diatoms if they grow under N-conditions that differ from the ones in the Scheldt estuary.

Second, variations in the $\delta^{15}N$ of cyclopoid copepods due to variations in their trophic position could interfere with the seasonal variations imposed by the food sources. Indeed, cyclopoid copepods can have trophic positions ranging between 2 and 5 (bacteria - ciliates - carnivorous ciliates – rotifers – copepods) due to the complexity of the heterotrophic food web in the freshwater section of the Scheldt estuary (Muylaert et al., 2000b). Moreover, if cyclopoid copepods occupy a high trophic position, the time-lag between the incorporation of N at the basis of the food web and the incorporation of this N in the tissue of the cyclopoid copepods may cause this cyclopoids to be 'out of phase' compared to the seasonal $\delta^{15}N$ pattern of the primary food sources.

Third, cyclopoids may be grazing on microorganisms associated with flocs in the water column. Concentrations of bacteria and microzooplankton in the flocs can be 10 (microzooplankton) to 100 (bacteria) times higher than in the water column (Muylaert, 1999) and may thus attract cyclopoid copepods (Simon et al., 2002). Flocs also contain substantial amounts of phytoplankton (Muylaert, 1999; Chen, 2003) that may serve as a food substrate for bacteria which may explain the depleted $\delta^{13}C$ signature of cyclopoid copepods. Flocs consist of organic and inorganic particles sticking together by the polysaccharide-rich secretion of microorganisms (Chen, 2003) and may thus have a similar layered structure with an oxic-anoxic gradient as the biofilm on the leaves. If similar microbial processes occur in the floc-biofilm as in the leaf-biofilm, $\delta^{15}N$ signature of bacteria may be strongly modified and thus no longer reflect the $\delta^{15}N$ of phytoplankton.

5.9 Conclusion

This study aimed at reconstructing the $\delta^{15}N$ signature of the potential primary food sources of cyclopoid copepods in the freshwater section of the Scheldt estuary. In particular, we aimed at understanding how the $\delta^{13}C$ signatures of cyclopoid copepods could point to a phytoplankton-derived food substrate, while this was not the case for $\delta^{15}N$ signatures.

$\delta^{15}NH_4^+$ measurements allowed us to calculated the fractionation value associated with NH_4^+ uptake (18.4‰, SE=1.2‰) and the value of the initial $\delta^{15}NH_4^+$ (+9.6‰, SE=2.6‰). These values were subsequently used to reconstruct the $\delta^{15}N$ of phytoplankton for the period 1999 – 2001, during which also cyclopoid copepods were sampled. The lack of correlation between these values and the $\delta^{15}N_{cyc}$ showed that cyclopoid copepods do not graze on locally produced phytoplankton and thus probably rely on heterotrophic bacteria as a primary food source.

We tried to reconstruct the seasonal pattern of the $\delta^{15}N$ signature of heterotrophic microorganisms in the suspended matter pool for a situation where they have access to both substrate-N and dissolved nitrogen from the ambient solution. We used submerged leaves as a proxy of organic matter substrates in flocs, assuming that the factors setting the $\delta^{15}N$ pattern of heterotrophic decomposers in the biofilm of submerged leaves would be similar to microheterotrophs in the suspended matter pool. The results suggested, however, that the $\delta^{15}N$ signature of submerged leaves mainly reflected microbial activity in the biofilm covering the leaf, while external additions of nitrogen were only of minor importance in setting the seasonal pattern of $\delta^{15}N$. Therefore, we were not able to reconstruct the $\delta^{15}N$ of heterotrophs colonizing organic matter, and thus no direct comparisons with $\delta^{15}N_{cyc}$ could be made.

Finally, we proposed three scenarios to explain the $\delta^{13}C$ and $\delta^{15}N$ pattern of cyclopoid copepods. In the first two scenarios we assumed that the $\delta^{15}N$ signature of the food source does not reflect the actual $\delta^{15}NH_4^+$ at the study site. Scenario 1 assumed a preference for detritus of green algae grown in the tributaries rather than in the estuary proper, while scenario 2 assumed that the $\delta^{15}N$ pattern of cyclopoids reflects other variations than the one of the primary food sources. The third scenario assumed that cyclopoid copepods feed on flocs and their associated microorganisms whereby the $\delta^{15}N$ signature of bacteria is modified by the microbial processes in the biofilm of the flocs.

Acknowledgments

We thank Natacha Brion for the analysis of $\delta^{15}NH_4^+$, Marc Elskens for statistical support and Martine Leermakers for the analysis of Al concentrations.

Variation in $\delta^{15}N$ and $\delta^{13}C$ of suspended particulate matter and copepods along the estuarine gradient

Chapter 6

6.1. Introduction

In chapter 4 we looked at the monthly variation of $\delta^{15}N$ and $\delta^{13}C$ of SPOM in order to examine the organic matter sources controlling the seasonal variation in SPOM at the freshwater to mesohaline reaches of the Scheldt estuary. From that study, we concluded that phytoplankton biomass was most likely the main factor setting the isotopic composition of SPOM. In this chapter, we concentrate on the general spatial trends in the isotopic signatures of SPOM and extend our study area to the marine reaches of the estuary in order to have a full picture of the spatial variation in the isotopic signature along the estuary.

Several studies show that the spatial pattern in SPOM C and N isotopic signatures cannot be explained by the mixing of freshwater, terrestrial and marine organic matter, but that autochthonous sources (Mariotti et al., 1984; Owens, 1985; Cai et al., 1988; Coffin and Cifuentes, 1999; Fichez et al., 1993), diagenetic alteration of organic matter (Thornton and McManus, 1994) and the resuspension of sediment organic matter (Fichez et al., 1993) contribute significantly to the variation in $\delta^{15}N$ and $\delta^{13}C$. In general, biogeochemical processes are considered to influence the isotopic distribution along the estuary to a greater extent than physical mixing (Cifuentes et al., 1988). Deviations from the mixing relationship between freshwater and marine particulate organic matter (POM) are generally more pronounced for nitrogen than for carbon isotopes (Thornton and McManus, 1994) and are most apparent in macrotidal estuaries with long residence times (Mariotti et al., 1984; Owens, 1985; Cifuentes et al., 1988; Thornton and McManus, 1994). Indeed, variations in the $\delta^{15}N$ and $\delta^{13}C$ signature of SPOM were only minor in the non-tidal Po estuary (Martinotti et al., 1997).

Our objective was to investigate the main factors accounting for the spatial variation in $\delta^{15}N_{SPOM}$ and $\delta^{13}C_{SPOM}$ over the whole estuarine gradient. In addition, we looked at the general spatial $\delta^{15}N$ and $\delta^{13}C$ patterns of cyclopoid and calanoid copepods and discuss them in the light of two major applications of stable isotopes: the study of the diet of planktivorous fish and the tracing of migration in the estuary.

6.2. Material and methods

Freshwater, oligohaline and upper mesohaline reaches have been sampled between May 1999 and April 2001 (Chapter 4). During February, May and July 2001, we collected SPOM and zooplankton at 3 additional stations in the mesohaline to marine reaches of the Scheldt estuary: stations S5 (mesohaline), S6 and S7 (marine); (Fig. 6.1). Descriptions of the sampling protocol and the analysis of SPOM and copepods can be found in Chapters 3 and 4.

Annual mean $\delta^{15}N$ and $\delta^{13}C$ signatures of SPOM and cyclopoid and calanoid copepods were calculated for the periods May 1999 – April 2000 and May 2000 – April 2001 for the stations S1, S2, S3 and S4 and for February to July 2001 for stations S5, S6 and S7. In the text below, the abbreviations SPOM, CYC, CAL refer to suspended particulate organic matter, cyclopoid and calanoid copepods, respectively, while the suffixes I, II and III refer to the period May 1999 – April 2000 (I), May 2000 – April 2001 (II) and February-July 2001 (III).

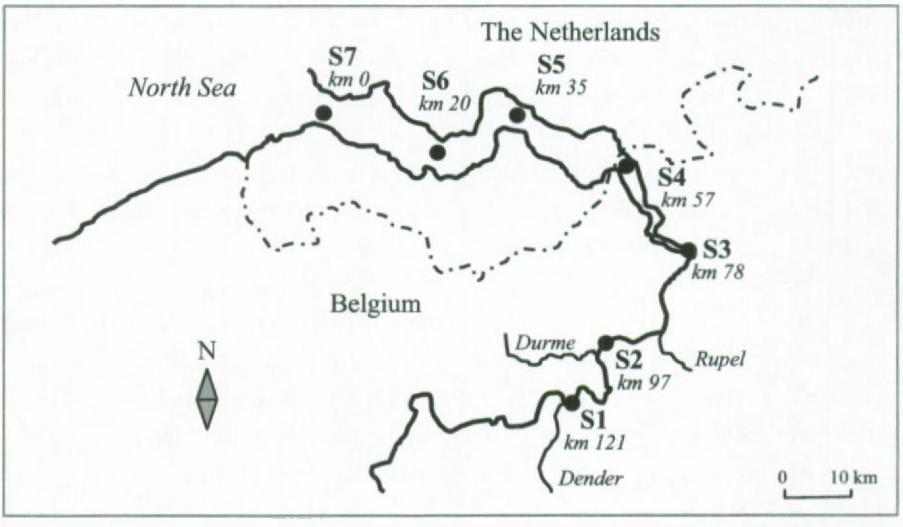

Figure 6.1: Map of the Scheldt estuary showing the sampling stations and their respective distance to the mouth of the estuary.

6.3. Results and Discussion

6.3.1. Factors controlling spatial variation in $\delta^{15}N_{SPOM}$ and $\delta^{13}C_{SPOM}$

6.3.1.1. $\delta^{13}C$ SPOM

Annual mean $\delta^{13}C_{SPOM}$ values increased in downstream direction (Fig. 6.2), a pattern frequently observed in temperate estuaries (Cai et al., 1988; Fichez et al., 1993; Thornton and McManus, 1994; Savoye et al., 2003; Martineau et al., 2004).

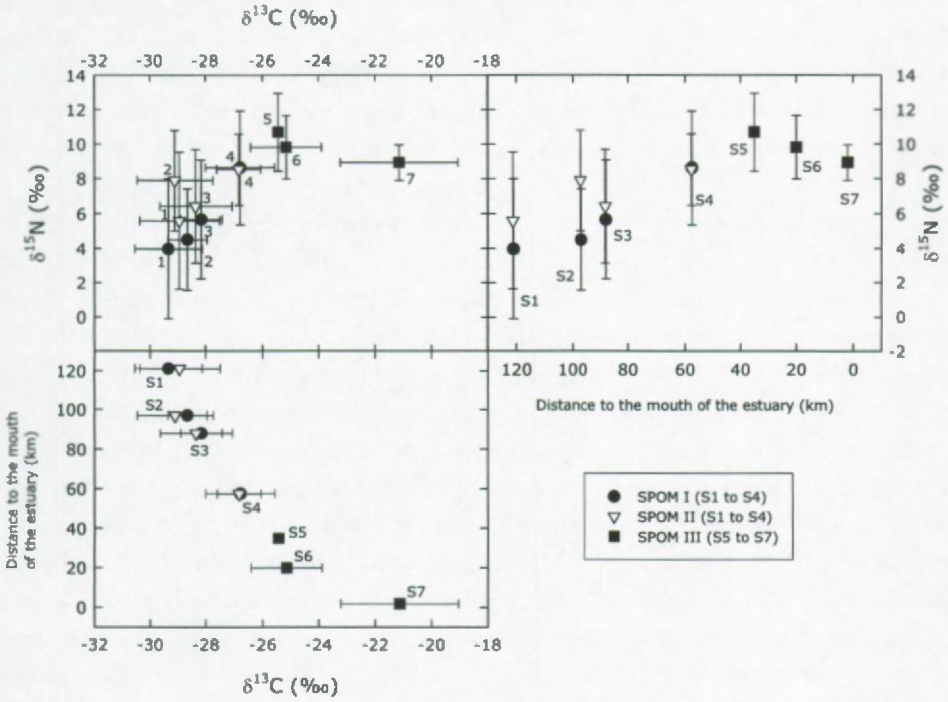

Figure 6.2: Dual isotope plot and longitudinal profiles of annual mean $\delta^{13}C$ and $\delta^{15}N$ values of SPOM I (May 1999 – April 2000), SPOM II (May 2000 – April 2001), and SPOM III (2001). Error bars = 1 SD.

A comparison between the $\delta^{13}C$ of SPOM and dissolved inorganic carbon (DIC) should provide more information on the organic carbon source controlling the $\delta^{13}C$ of SPOM (Chanton and Lewis, 1999; Coffin and Cifuentes, 1999). No $\delta^{13}C_{DIC}$ data are available for the period covered by the present study (1999-2001) but a comparison between $\delta^{13}C_{DIC}$ data for the period 1996-1998 (Hellings et al., 2001) and 2002-2003

(OMES, unpublished results) for stations S1 to S4 revealed no significant long term changes (Mann-Whitney U, $p>0.05$). This justifies that average $\delta^{13}C_{DIC}$ values obtained for different years can be considered to apply also for 1999-2001 when the present study was undertaken. For stations S5, S6 and S7, $\delta^{13}C_{DIC}$ data were too scarce (only February 1997 and April 2002) to allow reliable statistical significance testing. We assumed that the lack of long-term changes observed for the S1 to S4 stretch also apply for the S5 to S7 section and used the average $\delta^{13}C_{DIC}$ of February 1997 and April 2002 as a proxy of the $\delta^{13}C_{DIC}$ for the present period of study (1999-2001). $\delta^{13}C_{DIC}$ and $\delta^{13}C_{SPOM}$ were positively and highly significantly linearly correlated (bivariate least square regression; $r^2 = 0.98$, $p<0.001$; Fig. 6.3). Since phytoplankton is the only SPOM compound of which the $\delta^{13}C$ signature is set by the $\delta^{13}C$ of DIC (Chanton and Lewis, 1999; Hellings et al., 2001), the correlation between $\delta^{13}C_{DIC}$ and $\delta^{13}C_{SPOM}$ may indirectly result from the presence of phytoplankton in the SPOM pool. We may thus conclude that phytoplankton biomass is the main factor controlling the longitudinal variation in $\delta^{13}C_{SPOM}$.

If DIC is the only factor controlling the phytoplankton composition, the slope of a regression between $\delta^{13}C_{DIC}$ and $\delta^{13}C$ of phytoplankton should be 1 (Chanton and Lewis, 1999). Thus, if we assume that phytoplankton is the only component in the SPOM pool, the slope between $\delta^{13}C_{DIC}$ and $\delta^{13}C_{SPOM}$ should also be 1 (Coffin and Cifuentes, 1999). The slope of the linear regression between $\delta^{13}C_{DIC}$ and $\delta^{13}C_{SPOM}$ was 0.72 (SE=0.04), which implies that other carbon sources than phytoplankton also contribute to the variation in $\delta^{13}C_{SPOM}$ (Coffin and Cifuentes, 1999). In the Scheldt estuary, these carbon sources are most likely sewage and terrestrial matter. The dashed line in Fig. 6.3 represents the $\delta^{13}C$ value of SPOM if SPOM would consist purely of phytoplankton (i.e. $\delta^{13}C_{SPOM} = \delta^{13}C_{phytoplankton}$). The $\delta^{13}C$ of phytoplankton is calculated assuming a marine end-point $\delta^{13}C$ value for phytoplankton of -20‰ (Boschker et al., 2005) and a fractionation value between phytoplankton and DIC of 19.2‰. The latter is the sum of the average fractionation value relative to dissolved CO_2 for CO_2 uptake by phytoplankton for the Scheldt estuary (11.2‰; Boschker et al., 2005) and the fractionation factor for the conversion of CO_2 to DIC (8‰); (O'Leary, 1981). The increasing deviation between the $\delta^{13}C$ of phytoplankton and the observed $\delta^{13}C_{SPOM}$ toward to upper reaches (Fig. 6.3) points to an increasing importance of non-algal carbon sources.

However, the slope of the regression between $\delta^{13}C_{DIC}$ and $\delta^{13}C_{phytoplankton}$ may vary due to systematic variations in the degree of fractionation during CO_2 uptake (Chanton and Lewis, 1999). Chanton and Lewis (1999) reported a decrease in the slope from 1 to 0.6 for a situation where the fractionation during CO_2 uptake increased with increasing salinities. They attributed this decrease to a gradual shift in the species

composition (Chanton and Lewis, 1999). Recently, Boschker et al. (2005) have shown that the opposite is true for the Scheldt estuary. They reported that the magnitude of the fractionation during CO_2 uptake decreases in downstream direction, probably resulting from a combination of a downstream increase in the growth rate of phytoplankton and a downstream decrease of the dissolved CO_2 concentration. Consequently, for the Scheldt estuary, the slope of the regression between $\delta^{13}C_{DIC}$ and $\delta^{13}C_{phytoplankton}$ would be higher than 1. The arrow in Fig. 6.3 shows the direction in which the $\delta^{13}C$ of phytoplankton would shift if the fractionation during CO_2 uptake would decrease in downstream direction. Such decrease would only increase the deviation between $\delta^{13}C_{phytoplankton}$ and the observed $\delta^{13}C_{SPOM}$, which would further stress the increasing importance of non-algal C sources in the SPOM pool in upstream direction.

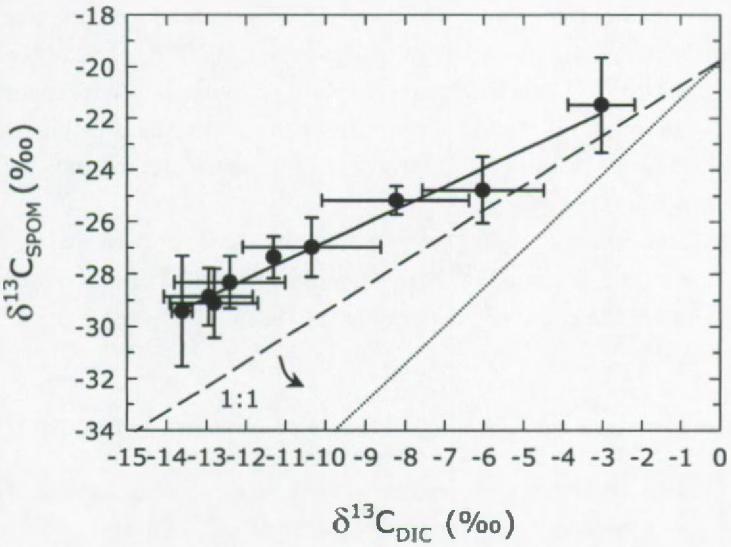

Figure 6.3: Regression between $\delta^{13}C_{DIC}$ averaged over the periods 1996-1998 and 2002-2003 and $\delta^{13}C_{SPOM}$ signatures (this study). Error bars = 1 SD. The slope of the equation for the obtained regression is 0.72 (SE=0.04) and the intercept is -19.60 (SE=0.44)‰. The dashed line denotes the theoretical value of $\delta^{13}C_{SPOM}$ if SPOM would consist only of phytoplankton and if fractionation during CO_2 uptake remains constant. The arrow indicates the direction in which the dashed line would shift if the fractionation associated with CO_2 uptake would increase in upstream direction. The dotted line shows the theoretical value of $\delta^{13}C_{SPOM}$ if SPOM would consist only of phytoplankton and if fractionation in the upper reaches would increase with e.g. 5‰ compared to the lower reaches.

6.3.1.2. $\delta^{15}N_{SPOM}$

Mean $\delta^{15}N_{SPOM}$ signatures first increased in downstream direction, peaked in the mesohaline reaches of the estuary and declined again in seaward direction (Fig. 6.2). Earlier studies have shown that mid-estuarine maxima in the $\delta^{15}N_{SPOM}$ signature can result from two processes. First, an increase in the heterotrophic microbial activity, favored by the enhanced residence time of suspended matter in the maximum turbidity zone (MTZ) (Owens, 1985) can enrich organic matter in ^{15}N (Owens, 1985; Thornton and McManus, 1994). Second, the presence of phytoplankton grown on an N-source previously enriched in ^{15}N following uptake and/or nitrification processes may enrich the overall SPOM $\delta^{15}N$ (Mariotti et al., 1984; Cifuentes et al., 1988).

In the Scheldt estuary, maximum values were recorded downstream of the MTZ, which stretches roughly between km 58 and km 100 (i.e. between S2 and S4; Chen, 2003). If microbial activity would have dominated the increase in $\delta^{15}N_{SPOM}$, highest $\delta^{15}N_{SPOM}$ values should have been found in the MTZ. Since this is not the case, the strong enrichment of the $\delta^{15}N_{SPOM}$ values might have resulted from the presence of ^{15}N-rich phytoplankton following uptake of NH_4^+ enriched in ^{15}N due to the preferential consumption of $^{14}NH_4^+$ in the upstream regions. Alternatively, the overall $\delta^{15}N$ signature of SPOM could be relatively enriched in the mid-estuary compared to the upper and lower reaches if the ^{15}N-rich phytoplankton represents a larger part of the bulk SPOM pool in the mid-estuary.

$\delta^{15}N_{SPOM}$ decreased again in the lower marine reaches of the estuary, probably as a result of the mixing of estuarine organic matter with marine organic matter with a $\delta^{15}N$ value of +9‰ (Middelburg and Nieuwenhuize, 1998).

6.3.2. The use of copepod $\delta^{15}N$ and $\delta^{13}C$ signatures to study the diet of fish

Stable C and N isotopes are increasingly used to identify food sources and trophic positions in aquatic ecosystems because they offer advantages over more conventional methods such as the analyses of stomach contents. Gut content analyses may be misleading if the gut contents are not assimilated (Kling et al., 1992) and if food sources, in particular planktonic organisms, are not detectable by inspection of ingested material (Grey et al., 2001). The strength of the stable isotope technique is that they reflect the actual assimilated as opposed to ingested food (Kling et al., 1992).

The use of stable isotopes to identify food sources and trophic positions is based on the assumption that consumers and their prey differ by ±3‰ and ±1‰ in their $\delta^{15}N$ and $\delta^{13}C$ signatures, respectively (DeNiro and Epstein, 1978; Fry and Sherr, 1984; Minagawa and Wada, 1984; Vander Zanden and Rasmussen, 2001). If stable isotopes

are to be used as indicators of the trophic position of large aquatic consumers we need to know the isotopic signatures at the base of the food web to compare consumer isotopic signatures with. However, phytoplankton or primary consumers are generally not considered as useful baseline indicators because of their high sensitivity to changes in the isotopic signature of their food substrates. Large consumers, in contrast, are less sensitive to variations in isotopic signatures than their prey because of the slower turnover rate of their tissue, and integrate the isotopic signatures of their food sources over a certain time period (Cabana and Rasmussen, 1996; Post, 2002). This may result in a considerable time lag between changes in the isotopic signature of large consumers and their prey. Thus, in case isotopic signatures of prey are highly variable, variations in the difference between isotopic signatures of consumer and prey could erroneously be interpreted as variations in the trophic position of consumers. Therefore, longer-living prey are preferred as an indicator of baseline isotopic signatures of the system (Cabana and Rasmussen, 1996; Post, 2002).

Since both phytoplankton and copepods have highly variable isotopic signatures in the Scheldt estuary (Hellings et al., 1999; De Brabandere et al., 2002; Chapter 4 and 5), they may not be adequate isotopic baseline indicators. However, copepods are a direct food source for many fish species in the Scheldt estuary (Maes et al., 2003), which makes direct comparisons between fish tissue and copepods inevitable. To circumvent the problem of the different response time of fish and copepods to changing isotopic signature of their food substrate, annual mean isotopic signatures were calculated (Cabana and Rasmussen, 1996; Post, 2002). As such, we can provide a baseline isotopic signature with which future studies on the diet of fish can be compared.

The longitudinal patterns of the annual mean $\delta^{13}C$ and $\delta^{15}N$ signatures of copepods ($\delta^{15}N_{cop}$ and $\delta^{13}C_{cop}$) resembled the ones of SPOM (Figs. 6.4 and 6.5; Table 6.1); $\delta^{15}N_{cop}$ signatures were highest in the mesohaline zone of the estuary (stations S4 and S5) and decreased toward the upper and lower reaches, while $\delta^{13}C_{cop}$ signatures increased downstream. However, $\delta^{13}C_{cop}$ signatures were generally shifted toward more negative values compared to $\delta^{13}C_{SPOM}$, while $\delta^{15}N_{cop}$ were shifted toward more positive values, although the shift in $\delta^{15}N$ was less pronounced for cyclopoid copepods. The shifts in the isotopic signatures of the copepods relative to SPOM are in agreement with the preference of copepods for phytoplankton or heterotrophs thriving on phytoplankton derived dissolved organic matter, which are generally depleted in ^{13}C and mostly enriched in ^{15}N compared to SPOM (Chapter 4 and 5).

Table 6.1: Annual mean and standard deviation (SD) of $\delta^{13}C$ and $\delta^{15}N$ signatures of SPOM, calanoid and cyclopoid copepods.

	I (May 1999- April 2000)				II (May 2000 – April 2001)				III (February – July 2001)			
	$\delta^{13}C$ (‰)		$\delta^{15}N$ (‰)		$\delta^{13}C$ (‰)		$\delta^{15}N$ (‰)		$\delta^{13}C$ (‰)		$\delta^{15}N$ (‰)	
	mean	(SD)	mean	(SD)	mean	(SD)	mean	(SD)	mean	(SD)	mean	(SD)
SPOM												
S1	-29.3	(1.2)	+4.0	(4.0)	-28.9	(1.4)	+5.6	(4.0)				
S2	-28.6	(0.7)	+4.5	(2.9)	-29.1	(1.4)	+7.9	(2.9)				
S3	-28.1	(0.7)	+5.6	(3.4)	-28.3	(1.3)	+6.4	(3.3)				
S4	-26.8	(1.2)	+8.6	(3.3)	-26.8	(0.8)	+8.5	(2.1)				
S5									-25.4	(0.2)	+10.7	(2.3)
S6									-25.2	(1.3)	+9.8	(1.8)
S7									-21.1	(2.1)	+8.9	(1.0)
CALANOIDS												
S1	-34.0	(1.0)	+7.3	(3.9)	-34.6	(0.1)	+10.3	(4.7)				
S2	-31.5	(3.6)	+7.4	(2.4)	-32.8	(1.9)	+9.2	(3.2)				
S3	-30.3	(2.4)	+9.4	(0.6)	-30.3	(1.8)	+12.0	(6.0)				
S4	-29.5	(1.2)	+19.8	(5.0)	-30.2	(1.4)	+16.7	(6.2)				
S5									-28.0		+16.0	
S6									-25.4	(0.8)	+17.0	(1.6)
S7									-22.2	(2.4)	+12.6	(1.1)
CYCLOPOIDS												
S1	-31.8	(2.2)	+6.9	(2.3)	-33.1	(0.9)	+6.3	(3.4)				
S2	-31.4	(1.5)	+7.7	(1.6)	-33.6	(1.6)	+8.1	(3.2)				
S3	-31.8	(1.9)	+9.5	(1.8)	-33.2	(1.6)	+9.5	(3.3)				
S4	-29.2	(1.3)	+11.8	(1.9)	-29.4	(2.9)	+11.9	(4.9)				
S5									-29.1		+11.4	

The shifts between SPOM and consumer isotopic signatures are also in agreement with a study of Martineau et al. (2004), who compared data of $\delta^{15}N$ and $\delta^{13}C$ of SPOM and consumers between different estuaries (Table 6.2). They found that consumers tend to be enriched in $\delta^{15}N$ relative to SPOM. However, the enrichment between SPOM and consumer $\delta^{15}N$ observed in the Scheldt system is much higher than the one observed in other estuaries (maximum of 11.2‰ for calanoids at station S4). Martineau et al. (2004) observed a maximum enrichment between *Eurytemora affinis* and SPOM of 8.5‰. They attributed this high enrichment to a high trophic position of *E. affinis* owing to its selectivity for microzooplankton. In the Scheldt system, where *E. affinis* is assumed to have a herbivorous feeding behavior (Tackx et al., 2003), the high enrichment between calanoids and SPOM $\delta^{15}N$ is probably mainly due to the strong ^{15}N enrichment of phytoplankton following uptake of ^{15}N-enriched NH_4^+ (Chapter

5). A comparative study of $\delta^{13}C$ signatures, on the contrary, showed that primary consumers can be both enriched and depleted relative to $\delta^{13}C_{SPOM}$ (Table 6.2). Large offsets between $\delta^{13}C$ of primary consumers and SPOM were related to selective feeding behaviour of consumers (Martineau et al., 2004). In the Scheldt estuary, copepods were consistently depleted in ^{13}C relative to SPOM, resulting from the selectivity for phytoplankton or for heterotrophic organisms thriving on phytoplankton-derived dissolved organic matter.

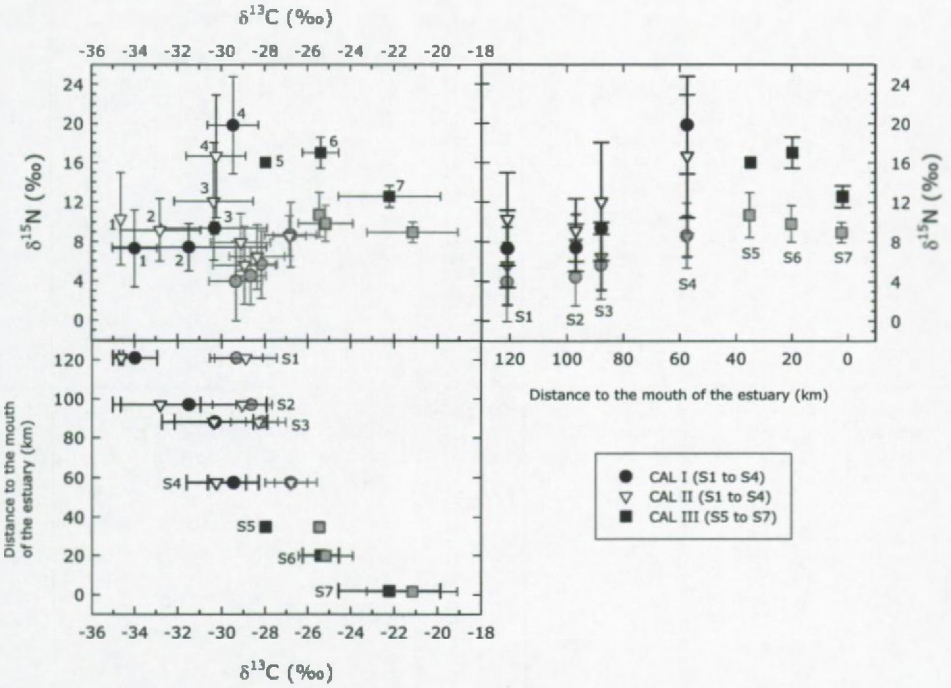

Figure 6.4: Dual isotope plot and longitudinal profiles of $\delta^{13}C$ and $\delta^{15}N$ signatures of calanoid copepods: CAL I (May 1999 – April 2000), CAL II (May 2000 – April 2001) and CAL III (2001). Error bars = 1 SD. Grey-scaled symbols represent the data for SPOM (see Fig. 6.2 for symbol legend of SPOM).

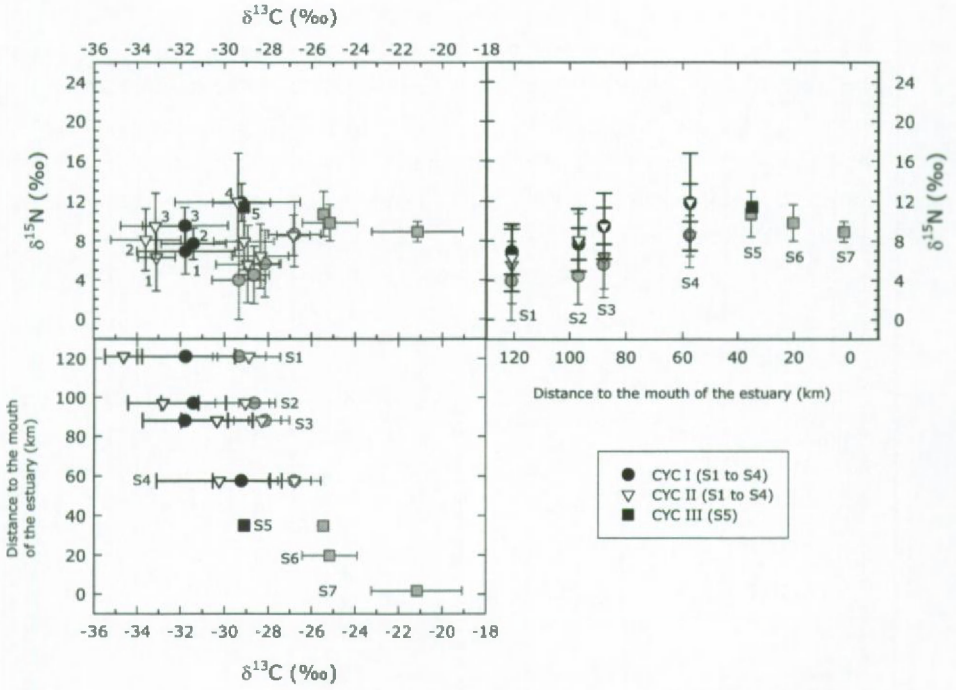

Figure 6.5: Dual isotope plot and longitudinal profiles of $\delta^{13}C$ and $\delta^{15}N$ signatures of cyclopoid copepods: CYC I (May 1999 – April 2000), CYC II (May 2000 – April 2001) and CYC III (2001). Error bars = 1 SD. Grey-scaled symbols represent the data for SPOM (see Fig. 6.2 for symbol legend of SPOM).

Table 6.2: Intersystem comparison between the $\delta^{15}N$ and $\delta^{13}C$ signatures of SPOM and primary consumers and the difference between primary producers and SPOM isotopic signatures ($\Delta\delta^{15}N = \delta^{15}N_{primary\ producer} - \delta^{15}N_{SPOM}$; $\Delta\delta^{13}C = \delta^{13}C_{primary\ producer} - \delta^{13}C_{SPOM}$). (Modified from Martineau et al., 2004).

Site	Environment	SPOM	Primary consumers	delta
		$\delta^{15}N$ (‰)	$\delta^{15}N$ (‰)	$\Delta\delta^{15}N$ (‰)
Tijuana Estuary[a]	Estuary	+10.9	+14.1	3.2
Plum Island Sound[b]	Upper estuary	+6.7	+7.6	0.9
Plum Island Sound[b]	Middle estuary	+5.6	+7.7	2.1
Plum Island Sound[b]	Lower estuary	+6.7	+7.6	0.9
Ria de Arosa[c]	Estuary	+7.0	+9.8	2.8
St.Lawrence River[d]	Estuarine MTZ	+5.9	+7.3	1.4

Site	Environment	SPOM	Primary consumers	delta
		$\delta^{13}C$ (‰)	$\delta^{13}C$ (‰)	$\Delta\delta^{13}C$ (‰)
Avon-Heathcote[e]	Estuary	-24.4	-20.0	4.4
Tijuana Estuary[a]	Estuary	-20.8	-21.8	-1.0
Plum Island Sound[b]	Upper estuary	-27.9	-26.5	1.4
Plum Island Sound[b]	Middle estuary	-21.6	-24.3	-2.7
Plum Island Sound[b]	Lower estuary	-21.9	-22.4	-0.5
Marennes-Oléron Bay[f]	Estuary plume	-23.5	-20.3	3.2
Ria de Arosa[c]	Estuary	-24.2	-14.5	9.7
St. Lawrence River[d]	Estuarine MTZ	-27.0	-21.0	6.0

[a]Kwak and Zedler (1997), [b]Deegan and Garritt (1997), [c]Page and Lastra (2003), [d]Martineau et al. (2004), [e]Stephenson and Lyon (1982), [f]Riera and Richard (1997)

6.3.3. The use of stable isotopes to study fish migration in the Scheldt estuary

Earlier studies have shown that many marine fish species use the Scheldt estuary as a nursery area or as a refuge for predators and that diadromous species use the Scheldt as a route to migrate between freshwater and marine environments (Maes et al., 1998a). Several studies have show that geographic isotope differences can be used to trace migration (e.g. Hesslein et al., 1991; Hansson at al., 1997; Doucett et al., 1999; McCarthy and Waldron, 2000). Marine $\delta^{13}C$ and $\delta^{15}N$ signatures are enriched compared to the ones of freshwater ecosystems (e.g. France, 1994; Peterson and Fry, 1987). Estuarine habitats display intermediate values for $\delta^{13}C$ (Cai et al., 1988; Fichez

et al., 1993; Thornton and McManus, 1994; Savoye et al., 2003), while $\delta^{15}N$ signatures are depleted, enriched or intermediate, depending on the biogeochemical processes acting on the substrates of primary producers (Mariotti et al., 1984; Owens, 1985; Cifuentes et al., 1988; Thornton and McManus, 1994). Adult fish migrating between habitats need some time to equilibrate their tissue isotope composition with that of the local food because of their slow tissue turnover rates. Migration can thus be traced when fish tissue is not in equilibrium with the isotopic signatures of the local food sources (Hansson et al., 1997).

In the Scheldt estuary, $\delta^{15}N$ and $\delta^{13}C$ signatures of copepods are highly variable and show considerable overlap at the different stations along the Scheldt estuary (Chapter 4). Therefore, we will investigate if the annual mean isotopic signatures of the food sources at the endpoints are sufficiently distinct to allow migration studies based on N and C isotopes. We used Mann-Whitney U statistics to test for significant differences between average $\delta^{15}N$ or $\delta^{13}C$ signatures of calanoid and cyclopoid copepods at the different stations. The results of the Mann-Whitney U test are presented in Figs. 6.6 and 6.7. Stations sharing grey-scaled blocks may sustain zooplanktivorous fish with significantly different $\delta^{15}N$ and/or $\delta^{13}C$ signatures. As a result, stable isotopes can only be used to trace migration between stations sharing grey-scaled blocks.

The $\delta^{13}C$ signatures of calanoid copepods at S4 differed significantly from the ones at the freshwater station S1 and the marine stations S6 and S7 (Fig. 6.6). During the second year, the oligohaline and marine stations also differed significantly in $\delta^{13}C_{Cal}$ signatures. During the first year, $\delta^{15}N$ of calanoid copepods differed significantly between stations S4 and the freshwater and oligohaline stations. During the second year, however, $\delta^{15}N_{Cal}$ at S4 differed only from $\delta^{15}N_{Cal}$ at S2. It must be noted, however, that the results of the Mann-Whitney U test for the stations S5, S6 and S7 have to be interpreted with care, given the low number of data ($\leq$ 3). The $\delta^{15}N$ and $\delta^{13}C$ signatures of cyclopoid copepods at S4 differed significantly from the ones at the upstream stations (Fig. 6.7). This suggests that $\delta^{13}C$ and $\delta^{15}N$ can mostly be used to trace migration of zooplanktivorous fish between mid-estuarine and upstream stations. $\delta^{13}C$ of calanoid copepods also allow tracing migration between mid-estuarine and lower reaches. In the Scheldt estuary, migratory behavior of fish is largely restricted to the marine and mesohaline reaches of the estuary because of the severe oxygen depletion in the upstream reaches (Maes et al., 1998b). Thus, since the mesohaline and marine reaches differ only in their $\delta^{13}C_{Cal}$ signature, fish migration between marine and mesohaline reaches can only by traced based on their $\delta^{13}C$ signatures and only if calanoid copepods comprise an important part of the diet of fish. These results are in

contrast to other studies which successfully applied $\delta^{15}N$ and/or $\delta^{13}C$ as a tracer of migration (Hesslein et al., 1991; Hansson at al., 1997; Doucett et al., 1999; McCarthy and Waldron, 2000). These studies were, however, carried out in systems which display only minor seasonal $\delta^{15}N$ and $\delta^{13}C$ variation at the base of the food web. We hypothesize that in eutrophic systems where enhanced microbial activity results in highly variable $\delta^{15}N$ and $\delta^{13}C$ signatures of the substrates of primary producers (Chapter 5), $\delta^{15}N$ and $\delta^{13}C$ will be less useful to study migration.

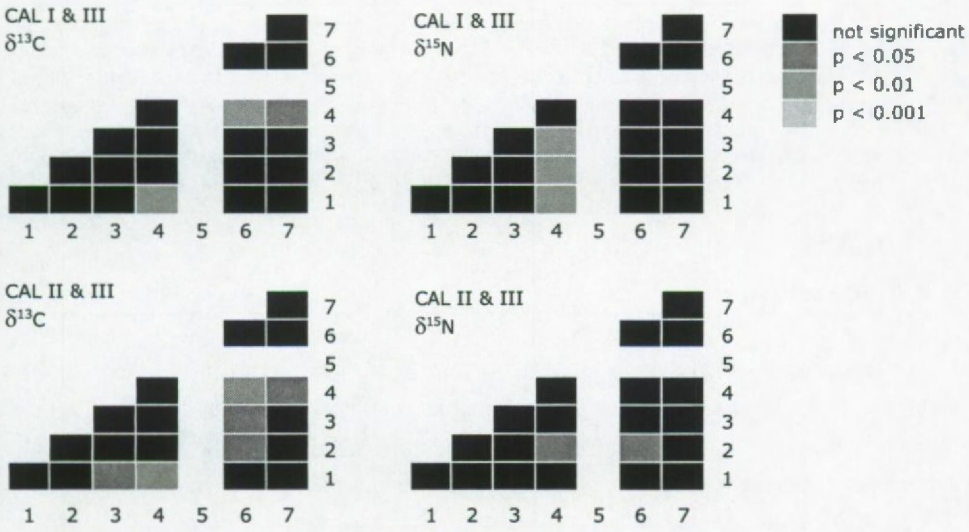

Figure 6.6: Schematic representation of the significant differences between the $\delta^{15}N_{cal}$ or $\delta^{13}C_{cal}$ signatures of the different stations along the estuarine gradient. The grey-scale of the boxes indicates the significance level based on which stations can be distinguished. In each row, $\delta^{15}N_{CAL}$ or $\delta^{13}C_{CAL}$ values of one particular station are compared to the ones of the other stations. Mean $\delta^{15}N$ and $\delta^{13}C$ values of CAL I and II (S1 to S4) are each compared with CAL III (S5 to S7) to cover the full estuarine gradient, despite the fact that they cover different years. Significant differences between stations are tested by means of a Mann-Whitney U test. Calanoid copepods were only once recorded at station S5. As a result, no significance tests could be performed.

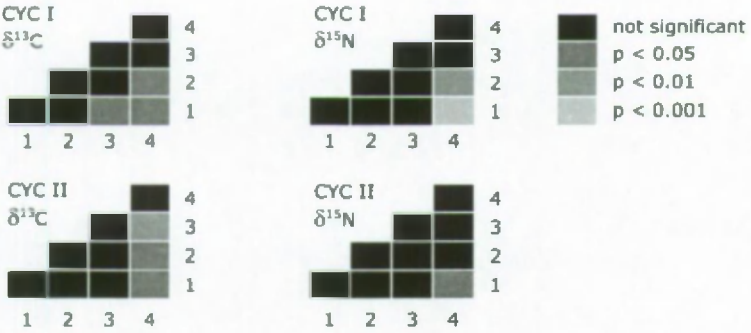

Figure 6.7: Schematic representation of the significant differences between the $\delta^{15}N_{cyc}$ or $\delta^{13}C_{cyc}$ signatures of the different stations along the estuarine gradient. The grey-scale of the boxes indicates the significance level based on which stations can be distinguished. In each row, $\delta^{15}N_{cyc}$ or $\delta^{13}C_{cyc}$ values of one particular station are compared to the ones of the other stations. Significant differences between stations are tested by means of a Mann-Whitney U test. Cyclopoid copepods were only present at stations S1 to S5, although cyclopoid copepods were only recorded once recorded at station S5 so that no significance tests could be performed.

6.4. Conclusions

The longitudinal patterns of $\delta^{13}C_{SPOM}$ and $\delta^{15}N_{SPOM}$ were mainly related to the variation in the C and N sources of phytoplankton. $\delta^{13}C_{SPOM}$ increased in downstream direction due to the presence of phytoplankton with gradually increasing $\delta^{13}C$ signatures. The relative importance of non-algal carbon sources increased in upstream direction. $\delta^{15}N_{SPOM}$ peaked in the mid-estuary due to the presence of phytoplankton assimilating NH_4^+ enriched in ^{15}N due to the fractionation associated with NH_4^+ consumption in the upper reaches. The spatial patterns of $\delta^{15}N_{SPOM}$ and $\delta^{13}C_{SPOM}$ were reflected in the $\delta^{15}N$ and $\delta^{13}C$ composition of the calanoid and cyclopoid copepods, with $\delta^{15}N$ values of copepods being enriched and $\delta^{13}C$ values being depleted relative to the ones of SPOM as a result of selective feeding of copepods on phytoplankton or phytoplankton-derived dissolved organic matter.

Marine and mid-estuarine stations displayed significantly different $\delta^{13}C_{cal}$ signatures, suggesting that stable C isotopes can be used to trace fish migration between the mid-estuary and the North Sea. Stable N isotopes, on the contrary, were not considered a useful tool to investigate fish migration between the mid-estuary and the North Sea since they did not discriminate between mesohaline and marine stations. Both $\delta^{15}N$ and $\delta^{13}C$ signatures can, however, be used to trace migration between the mesohaline station S4 and the upper reaches, but neither $\delta^{15}N$ nor $\delta^{13}C$ can be used to trace fish migrations over the full estuarine gradient.

General conclusions

The main objective of this study was to investigate the relative importance of heterotrophic and autotrophic primary food sources sustaining the secondary production at different salinity conditions in the highly eutrophic Scheldt estuary. In particular, we investigated the primary food sources of calanoid and cyclopoid copepods since these represent an important intermediate for the transfer of energy and matter to the higher trophic levels. First, we studied the factors accounting for the monthly variation (April 1999 - April 2001) of the $\delta^{15}N$ and $\delta^{13}C$ signature of suspended particulate organic matter (SPOM) in the fresh to mesohaline reaches. Second, we investigated the nature of the primary food sources (bacteria or phytoplankton) of calanoid and cyclopoid copepods, with particular emphasis on the organic substrate of heterotrophic microorganisms. Finally, we extended our study area to the marine reaches of the estuary to investigate the factors controlling the spatial variation in SPOM isotopic signatures and to provide baseline isotope values for future food web research.

Seasonal variations in the $\delta^{15}N$ and $\delta^{13}C$ signatures of SPOM were linked to variations in the relative contribution of phytoplankton to the total SPOM pool and to variations in the isotopic signature of phytoplankton. Increased contribution of phytoplankton to SPOM was marked by a decrease in the overall $\delta^{13}C$ signature of SPOM. The presence of phytoplankton either decreased or increased the $\delta^{15}N$ of SPOM, depending on the ambient NH_4^+ concentration. Highest enrichments were typically found under low NH_4^+ concentrations.

At the oligohaline and mesohaline stations, the seasonal variation of the $\delta^{15}N$ and $\delta^{13}C$ signatures of calanoid copepods paralleled the one of SPOM, but with an offset mostly exceeding the one commonly accepted for trophic fractionation. The seasonal variation of the $\delta^{15}N$ and $\delta^{13}C$ signatures of cyclopoid copepods of the oligohaline and mesohaline reaches also paralleled the one of SPOM, but their summer $\delta^{15}N$ signatures showed strong ^{15}N depletion relative to the ones of calanoid copepods. It is thought that these patterns reflect a dependency of calanoid copepods on phytoplankton while cyclopoid copepods ultimately depend on heterotrophic bacteria using phytoplankton derived dissolved organic matter (DOM) as a food substrate.

In contrast, the seasonal patterns of the $\delta^{15}N$ and $\delta^{13}C$ signatures of the cyclopoid copepods at the freshwater station were very different from the ones of SPOM suggesting no dependency of cyclopoid copepods on in situ produced phytoplankton or on heterotrophs thriving on DOM derived from this phytoplankton. This was confirmed by the discrepancy between the seasonal $\delta^{15}N$ pattern of cyclopoids and the modeled $\delta^{15}N$ pattern of in situ produced phytoplankton. It was therefore suggested that allochthonous phytoplankton advected from the tributaries represents

the food substrate of heterotrophs on which cyclopoid copepods feed. We tried to reconstruct the seasonal $\delta^{15}N$ signature of heterotrophs thriving on detritus to compare the $\delta^{15}N$ of cyclopoid copepods with. We investigated if heterotrophic microorganisms associated with flocs reflect the $\delta^{15}N$ composition of organic matter trapped in flocs or the dissolved nitrogen from the ambient solution. This was tested by means of a decomposition experiment where the $\delta^{15}N$ pattern of decomposing willow leaves and associated decomposers was used as a proxy for the $\delta^{15}N$ of heterotrophs associated with flocs. However, due to significant contamination of the biofilm by trapped suspended matter, incorporation of dissolved nitrogen was insignificant and the $\delta^{15}N$ of the submerged willow leaf-biofilm complex probably reflected mainly microbial activity in the biofilm, rather than the $\delta^{15}N$ of the N-source.

$\delta^{15}NH_4^+$ signatures observed in the Scheldt estuary were very high (up to +70‰) and highly variable. Such high $\delta^{15}NH_4^+$ signatures were related to the combined effect of fractionation during algal NH_4^+ uptake and nitrification. $\delta^{15}NH_4^+$ was used to model the seasonal $\delta^{15}N$ variation of phytoplankton. The strong correlation between modeled $\delta^{15}N$ of phytoplankton and the $\delta^{15}N$ of SPOM confirmed that phytoplankton was the main factor setting the seasonal variation in $\delta^{15}N_{SPOM}$. Finally, we showed that phytoplankton biomass is also a major factor controlling the spatial variation in SPOM isotopic signatures. We calculated an isotope baseline with which future studies on the diet of zooplanktivorous fish can be compared and we questioned the use of stable N isotopes to study fish migration in the Scheldt estuary since endpoint habitats mostly do not differ sufficiently in their $\delta^{15}N$ signature.

To conclude, calanoid and cyclopoid copepod communities were shown to represent different food webs. Calanoid copepods depended ultimately on phytoplankton for their C and N requirements, while cyclopoid copepods relied ultimately on heterotrophic bacteria. The organic substrate for the heterotrophs in the oligohaline and mesohaline reaches differed from the one in the freshwater reaches. Heterotrophic bacteria from the oligohaline and mesohaline reaches probably utilized dissolved organic matter derived from autochthonous phytoplankton, while freshwater bacteria probably depended on allochthonous phytoplankton sources. Although previous studies already suggested that nowadays, heterotrophic and autotrophic food webs are both present in the oligo-and mesohaline reaches, our study is the first to show that both food webs are actually linked. The fate of phytoplankton in the freshwater reaches is, however, still unclear.

Our observations highlight a very different ecosystem functioning for the freshwater part compared to the oligo- and mesohaline waters of the estuary proper. A conceptual model of the energy transfer from primary food sources to the higher trophic levels in the freshwater versus oligo-and mesohaline reaches is presented in Figure 1.

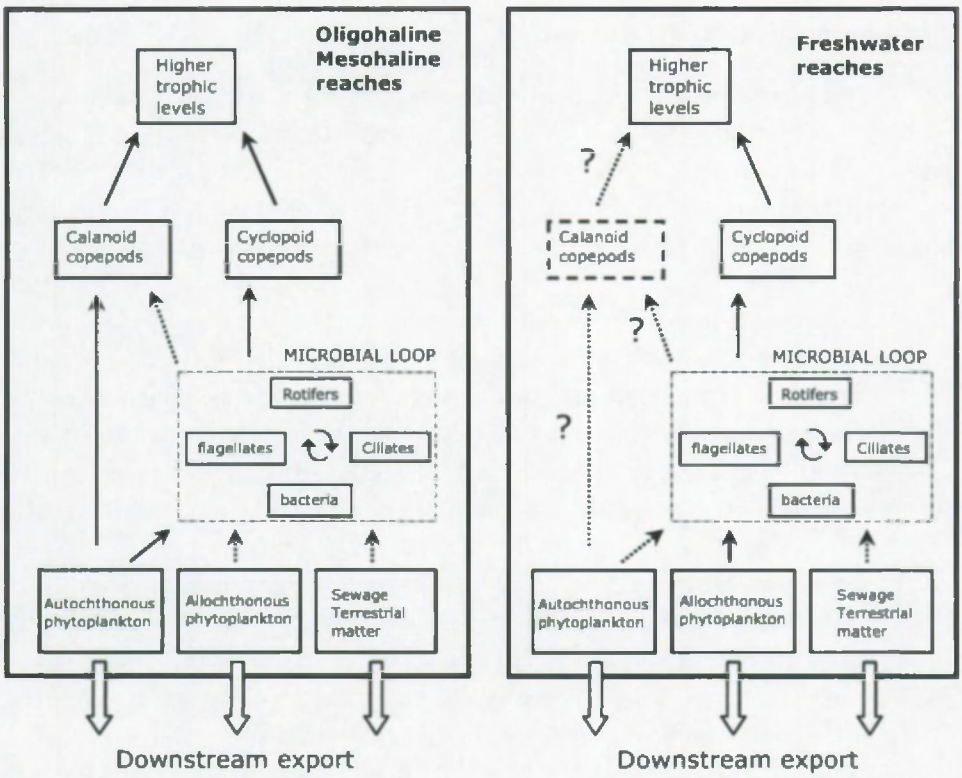

Figure 1: Conceptual model of the (simplified) food web in the oligohaline to mesohaline reaches (left) and the freshwater reaches (right) of the Scheldt estuary. Both the algal-grazer and the decomposer pathway are presented. In the freshwater reaches, calanoid copepods were only occasionally observed and were therefore not studied for their primary food sources. In the meso- and oligohaline reaches, calanoid and cyclopoid copepods represent autotrophic and heterotrophic food webs, respectively. The heterotrophic food web is linked to the autotrophic food web via the microbial processing of locally produced algal-derived organic matter. In the freshwater reaches, the heterotrophic food web is probably mainly fuelled by allochthonous phytoplankton inputs. Solid arrows indicate trophic linkages between groups, while dotted arrows indicated potential linkages between groups.

Our results show that the secondary production in oligohaline to mesohaline estuaries may be fuelled by autotrophic organic matter sources. A large part of this autotrophic organic matter reaches the higher trophic levels via the decomposer

pathway. In the freshwater reaches, however, allochthonous autotrophic organic matter sources may be more important in fuelling secondary production. Although organic matter inputs from wastewater constitute an important fraction of the labile organic matter pool in the Scheldt estuary, autotrophic organic matter represented the major energy source for heterotrophs.

Recommendations for future research

Although our results were helpful in delineating the major energy pathways to secondary production in the Scheldt estuary, it also raised some questions about the fate of autochthonous phytoplankton in the freshwater reaches and the fate of allochthonous organic matter in the oligo- to mesohaline reaches. Therefore, we give some recommendations for future research to solve above-mentioned questions.

- The C- and N-sources at the base of the heterotrophic food web are still poorly understood. Therefore, future research should focus on the seasonal $\delta^{15}N$ and $\delta^{13}C$ pattern of bacterial organisms. To date, bacterial isotopic signatures can be accurately measured by compound-specific analysis of bacterial biomarkers such as nucleid acids (Coffin et al., 1990; Créach et al., 1999), amino acids (Pelz et al., 1998; McClelland et al., 2003) and polar lipid-derived fatty acids (Boschker et al., 1998; 2005).
- Some potential N- and C-sources for heterotrophs and primary producers were not addressed in this study, being dissolved organic nitrogen en carbon, NO_3^- and allochthonous phytoplankton. The study of the $\delta^{15}N$ and $\delta^{13}C$ of these sources could provide additional insight in the processes driving the $\delta^{15}N$ and $\delta^{13}C$ of heterotrophs and autotrophs in the Scheldt estuary.
- The study of the seasonal $\delta^{15}N$ and $\delta^{13}C$ pattern of size-fractionated suspended matter components may help to investigate the $\delta^{15}N$ and $\delta^{13}C$ of minor SPOM components. Indeed, recent studies combining flow-cytometric cell sorting and isotope-ratio mass spectrometry to measure the $\delta^{13}C$ of fatty acids of specific plankton groups (Pel et al., 2003), have shown that bulk SPOM is a heterogeneous mixture of different size-fractions with their specific isotopic signature.
- Finally, this study focused on the pelagic food web, but benthic food webs may also contribute significantly to secondary production in the estuary. Therefore, more research is needed to study the coupling between benthic and pelagic production along the estuary.

Reference List

Abelson P. and Hoering T.C. (1961) Carbon isotope fractionation in formation of amino acids by photosynthetic organisms. Proceedings of the National Academy of Sciences 47:623-632

Abril G., Etcheber H., Borges A.V. and Frankignoulle M. (2000) Excess atmospheric carbon dioxide transported by rivers into the Scheldt estuary. Earth and Planetary Sciences 330:761-768

Abril G. and Frankignoulle M. (2001) Nitrogen-alkalinity interactions in the highly polluted Scheldt basin (Belgium). Water Research 35:844-850

Abril G., Nogueira M., Etcheber H., Cabecadas G., Lemaire E. and Brogueira M.J. (2002) Behaviour of organic carbon in nine contrasting European estuaries. Estuarine Coastal and Shelf Science 54(2):241-262

Altabet M.A. and Francois R. (1994) Sedimentary nitrogen isotopic ratio as a recorder for surface ocean nitrate utilization. Global Biogeochemical Cycles 8:103-116

Appeltans W., Hannouti A., Van Damme S., Soetaert K., Vanthomme R. and Tackx M. (2003) Zooplankton in the Schelde estuary (Belgium The Netherlands). The distribution of *Eurytemora affinis*: effect of oxygen? Journal of Plankton Research 25(11):1441-1445

Azam F., Fenchel T., Field J.G., Gray J.S., Meyer-Reil L.A. and Thingstadt F. (1983) The ecological role of water column microbes in the sea. Marine Ecology Progress Series 10:257-263.

Bada J.L., Schoeninger M.J. and Schimmelmann A. (1989) Isotopic fractionation during peptide-bond hydrolysis. Geochimica et Cosmochimica Acta 53:3337-3341

Baeyens W., Van Eck B., Lambert C., Wollast R. and Goeyens L. (1998) General description of the Scheldt estuary. Hydrobiologia 366:1-14

Baldwin D.S. (1999) Dissolved organic matter and phosphorus leached from fresh and 'terrestrially' aged river red gum leaves: implications for assessing river-floodplain interactions. Freshwater Biology 41:675-685

Baldy V. and Gessner M.O. (1997) Towards a budget of leaf litter decomposition in a first-order woodland stream. Comptes Rendus de l'Academie des Sciences Serie III-Sciences de la Vie-Life Sciences 320(9):747-758

Bender M.M. (1971) Variations in the $^{13}C/^{12}C$ ratios of plants in relation to the pathway of photosynthesis carbon dioxide fixation. Phytochemistry 10:1239-1244

Benner R., Biddanda B., Black B. and McCarthy M. (1997) Abundance, size distribution, and stable carbon and nitrogen isotopic compositions of marine organic matter isolated by tangential-flow ultrafiltration. Marine Chemistry 57:243-263

Berry J.A. (1989) Studies of mechanisms affecting the fractionation of carbon isotopes in photosynthesis. In: P.W. Rundel J.R.E. and Nagy K.A. (eds) Stable Isotopes in Ecological Research. Springer-Verslag, New York, pp 82-94

Billen G., Joiris C., Wijnant J. and Gillain G. (1980) Concentration and microbiological utilisation of small organic-molecules in the Scheldt estuary, the Belgian coastal zone of the North-Sea and the English-Channel. Estuarine and Coastal Marine Science 11:279-294

Billen G., Somville M., Debecker E. and Servais P. (1985) A nitrogen budget of the Scheldt hydrographical basin. Netherlands Journal of Sea Research 19:223-230

Borges A.V. and Frankignoulle M. (2002) Distribution and air-water exchange of carbon dioxide in the Scheldt plume off the Belgian coast. Biogeochemistry 59:41-67

Boschker H.T.S., Nold S.C., Wellsbury P., Bos D., de Graaf W., Pel R., Parkes R.J. and Cappenberg T.E. (1998) Direct linking of microbial populations to specific biogeochemical processes by ^{13}C-labelling of biomarkers. Nature 392:801-805

Boschker H.T.S., Kromkamp J.C. and Middelburg J.J. (2005) Biomarker and carbon isotopic constraints on bacterial and algal community structure and functioning in a turbid, tidal estuary. Limnology and Oceanography 50(1):70-80

Bouillon S. (2002) Organic carbon in a southeast Indian mangrove ecosystem: sources and utilization by different faunal communities. Ph. D. Thesis, Vrije Universiteit Brussel, Belgium

Bowen H.M.J. (1979) Environmental chemistry of the elements. Academic Press, London, UK

Brandl Z. (1998) Feeding strategies of planktonic cyclopoids in lacustrine ecosystems. Journal of Marine Systems 15(1-4):87-95

Breteler W.C.M.K., Grice K., Schouten S., Kloosterhuis H.T. and Damste J.S.S. (2002) Stable carbon isotope fractionation in the marine copepod *Temora longicornis* : unexpectedly low $\delta^{13}C$ value of faecal pellets. Marine Ecology Progress Series 240:195-204

Brion N. (2002) Book of Abstracts ECSA

Bronk D.A. and Glibert P.M. (1993) Application of a ^{15}N tracer method to the study of dissolved organic nitrogen uptake during spring and summer in Chesapeake Bay. Marine Biology 115(3):501-508

Bunn S.E., Loneragan N.R. and Kempster M.A. (1995) Effects of acid washing on stable isotope ratios of C and N in penaeid shrimp and seagrass: Implications for food-web studies using multiple stable isotopes. Limnology and Oceanography 40:622-625

Burkhardt S., Riebesell U. and Zondervan I. (1999a) Effects of growth rate, CO_2 concentration, and cell size on the stable carbon isotope fractionation in marine phytoplankton. Geochimica et Cosmochimica Acta 63:3729-3741

Burkhardt S., Riebesell U. and Zondervan I. (1999b) Stable carbon isotope fractionation by marine phytoplankton in response to daylength, growth rate, and CO_2 availability. Marine Ecology Progress Series 184:31-41

Cabana G. and Rasmussen J.B. (1996) Comparison of aquatic food chains using nitrogen isotopes. Proceedings of the National Academy of Science of the USA 93:10844-10847

Cai D.L., Tan F.C. and Edmond J.M. (1988) Sources and transport of particulate organic carbon in the Amazon River and Estuary. Estuarine, Coastal and Shelf Science 26:1-14

Caraco N.F., Lampman G., Cole J.J., Limburg K.E., Pace M.L. and Fischer D. (1998) Microbial assimilation of DIN in a nitrogen rich estuary: implications for food quality and isotope studies. Marine Ecology Progress Series 167:59-71

Chanton J.P. and Lewis F.G. (1999) Plankton and dissolved inorganic carbon isotopic composition in a river-dominated estuary: Apalachicola Bay, Florida. Estuaries 22(3A):575-583

Checkley D.M. Jr. and Entzeroth L.C. (1985) Elemental and isotopic fractionation of carbon and nitrogen by marine, planktonic copepods and implications to the marine nitrogen cycle. Journal of Plankton Research 7(4):553-568

Checkley D.M. and Miller C.A. (1989) Nitrogen isotope fractionation by oceanic zooplankton. Deep-Sea Research Part a - Oceanographic Research Papers 36(10):1449-1456

Chen M.S. (2003) Suspended matter and flocculation in the estuarine environment. Ph. D. Thesis, Vrije Universiteit Brussel, Belgium.

Cifuentes L.A., Sharp J.H. and Fogel M.L. (1988) Stable carbon and nitrogen isotope biogeochemistry in the Delaware estuary. Limnology and Oceanography 33:1102-1115

Cifuentes L.A., Fogel M.L., Pennock J.R. and Sharp J.H. (1989) Biogeochemical factors that influence the stable nitrogen isotope ratio of dissolved ammonium in the Delaware Estuary. Geochimica et Cosmochimica Acta 53(10):2713-2721

Claessens J. (1988) Het hydraulisch regime van de Schelde. Water 43:163-169

Cline J.D. and Kaplan I.R. (1975) Isotopic fractionation of dissolved nitrate during denitrification in the eastern tropical north pacific ocean. Marine Chemistry 3:271-299

COFFIN R.B., FRY B., PETERSON B.J. AND WRIGHT R.T. (1989) Carbon isotopic compositions of estuarine bacteria. Limnology and Oceanography 34(7):1305-1310

COFFIN R.B., VELINSKY D.J., DEVEREUX R., PRICE W.A. AND CIFUENTES L.A. (1990) Stable carbon isotope analysis of nucleic-acids to trace sources of dissolved substrates used by estuarine bacteria. Applied and Environmental Microbiology 56(7):2012-2020

COFFIN R.B. AND CIFUENTES L.A. (1999) Stable isotope analysis of carbon cycling in the Perdido Estuary, Florida. Estuaries 22(4):917-926

COHEN, R.A. AND FONG P. (2004) Nitrogen uptake and assimilation in *Enteromorpha intestinalis* (L.) Link (Chlorophyta): using ^{15}N to determine preference during simultaneous pulses of nitrate and ammonium. Journal of Experimental Marine Biology and Ecology 309(1):67-77

COULL B.C. (1999) Role of meiofauna in estuarine soft-bottom habitats. Australian Journal of Ecology 24(4):327-343

CRÉACH V., SCHRICKE M.T., BERTRU G. AND MARIOTTI A. (1997) Stable isotopes and gut analysis to determine feeding relationships in saltmarsh macroconsumers. Estuarine, Coastal and Shelf Science 44:599-611

DAM H.G. AND PETERSON W.T. (1988) The effect of temperature on the gut clearance rate-constant of planktonic copepods. Journal of Experimental Marine Biology and Ecology 123(1):1-14

DE BIE M.J.M., STARINK M., BOSCHKER H.T.S., PEENE J.J. AND LAANBROEK H.J. (2002a) Nitrification in the Schelde estuary: methodological aspects and factors influencing its activity. FEMS Microbiology Ecology 42:99-107

DE BIE M.J.M., MIDDELBURG J.J., STARINK M. AND LAANBROEK H.J. (2002b) Factors controlling nitrous oxide at the microbial community and estuarine scale. Marine Ecology Progress Series 240:1-9

DE BRABANDERE L., DEHAIRS F., VAN DAMME S., BRION N., MEIRE P. AND DARO N. (2002) $\delta^{15}N$ and $\delta^{13}C$ dynamics of suspended organic matter in freshwater and brackish waters of the Scheldt estuary. Journal of Sea Research 48:1-15

DEEGAN L.A. AND GARRITT R.H. (1997) Evidence for spatial variability in estuarine food webs. Marine Ecology Progress Series 147:31-47

DEGENS E.T., GUILLARD R.R.L., SACKETT W.M. AND HELLEBUST J.A. (1968) Metabolic fractionation of carbon isotopes in marine phytoplankton - I. Temperature and respiration experiments. Deep-Sea Research 15:1-9

DEL GIORGIO P.A. AND FRANCE R.L. (1996) Ecosystem-specific patterns in the relationship between zooplankton and POM or microplankton $\delta^{13}C$. Limnology and Oceanography 41(2):359-365

DENIRO M.J. AND EPSTEIN S. (1978) Influence on the distribution of carbon isotopes in animals. Geochimica et Cosmochimica Acta 42:495-506

DESCOLAS-GROS C. AND FONTUGNE M. (1990) Stable carbon isotope fractionation by marine phytoplankton during photosynthesis. Plant, Cell and Environment 13:207-218

DE WILDE H.P.J. AND DE BIE M.J.M. (2000) Nitrous oxide in the Schelde estuary: production by nitrification and emission to the atmosphere. Marine Chemistry 69:203-216

DHONDT K., BOECKX P., VAN CLEEMPUT O. AND HOFMAN G. (2003) Quantifying nitrate retention processes in a riparian buffer zone using the natural abundance of ^{15}N in NO_3^-. Rapid Communications in Mass Spectrometry 17(23):2597-2604

DOUCETT R.R.; HOOPER W. AND POWER G. (1999) Identification of anadromous and nonanadromous adult brook trout and their progeny in the Tabusintac River, New Brunswick, by means of multiple-stable-isotope analysis. Transactions of the American Fisheries Society 128:278-288

FARQUHAR G.D., EHLERINGER J.R. AND HUBICK K.T. (1989) Carbon isotope discrimination and photosynthesis. Annual Review of Plant Physiology and Plant Molecular Biology 40:503-537

FAURE G. (1986) Principles of isotope geology J. Wiley, New York

FERNANDEZ I., MAHIEU N. AND CADISCH G. (2003) Carbon isotopic fractionation during decomposition of plant materials of different quality. Global Biogeochemical Cycles 17(3) art. no. 1075, doi:10.1029/2001CB001834

FICHEZ R., DENNIS P., FONTAINE M.F. AND JICKELLS T.D. (1993) Isotopic and biochemical-composition of particulate organic-matter in a shallow-water estuary (Great Ouse, North-Sea, England). Marine Chemistry 43:263-276

FINDLAY S.E.G. AND ARSUFFI T.L. (1989) Microbial-growth and detritus transformations during decomposition of leaf litter in a stream. Freshwater Biology 21(2):261-269

FINDLAY S., PACE M.L., LINTS D., COLE J.J., CARACO N.F. AND PEIERLS B. (1991) Weak-coupling of bacterial and algal production in a heterotrophic ecosystem - The Hudson River estuary. Limnology and Oceanography 36(2):268-278

FISSEHA R. (2000) Use of stable isotopes as a tracer of domestic sewage pollution in the Woluwe Brook-Woluwe sewer collector system. Master Thesis in Environmental Science and Technology, Vrije Universiteit Brussel, Belgium

FOCKEN U. AND BECKER K. (1998) Metabolic fractionation of stable carbon isotopes: implications of different proximate compositions for studies of the aquatic food webs using $\delta^{13}C$ data. Oecologia 115:337-343

FOGEL M.L. AND CIFUENTES L.A. (1993) Isotope fractionation during primary production. In: Engel M.H. and Macko S.A. (eds) Organic Chemistry, pp 77-98

FOGEL M.L. AND TUROSS N. (1999) Transformation of plant biochemicals to geological macromolecules during early diagenesis. Oecologia 120:336-346

FOUILLAND E., DESCOLAS-GROS C., COLLOS Y., VAQUER A., SOUCHU P., GASC A., BIBENT B. AND PONS V. (2002) Influence of nitrogen enrichment on size-fractionated in vitro carboxylase activities of phytoplankton from Thau Lagoon (Coastal Mediterranean Lagoon, France). Journal of Experimental Marine Biology and Ecology 275:147-171

FRANCE R.L. (1994) Nitrogen isotopic composition of marine and freshwater invertebrates. Marine Ecology Progress Series 115:205-207

FRANKIGNOULLE M., BOURGE I. AND WOLLAST R. (1996) Atmospheric CO_2 fluxes in a highly polluted estuary (the Scheldt). Limnology and Oceanography 41:365-369

FRANKIGNOULLE M., ABRIL G., BORGES A., BOURGE I., CANON C., DELILLE B., LIBERT E. AND THEATE J.M. (1998) Carbon dioxide emission from European estuaries. Science 282:434-436

FRY B. AND SHERR E.B. (1984) $\delta^{13}C$ measurements as indicators of carbon flow in marine and fresh-water ecosystems. Contributions in Marine Science 27:13-47

FRY B. (2003) Steady state models of stable isotopic distributions. Isotopes in Environmental and Health Studies 39:219-232

FUJIWARA M. AND HIGHSMITH R.C. (1997) Harpacticoid copepods: potential link between inbound adult salmon and outbound juvenile salmon. Marine Ecology Progress Series 158:205-216

GANNES L.Z., O'BRIEN D.M. AND MARTÍNEZ DEL RIO C. (1997) Stable isotopes in animal ecology: assumptions, caveats, and a call for more laboratory experiments. Ecology 78(4):1271-1276

GASPARINI S. AND CASTEL J. (1997) Autotrophic and heterotrophic nanoplankton in the diet of the estuarine copepods *Eurytemora affinis* and *Acartia bifilosa*. Journal of Plankton Research 19(7):877-890

GASPARINI S., CASTEL J. AND IRIGOIEN X. (1999) Impact of suspended particulate matter on egg production of the estuarine copepod, *Eurytemora affinis*. Journal of Marine Systems 22:195-205

GOERING J., ALEXANDER V. AND HAUBENSTOCK N. (1990) Seasonal variability of stable carbon and nitrogen isotope ratios of organisms in a North Pacific Bay. Estuarine, Coastal and Shelf Science 30:239-260

GOLLADAY S.W. AND SINSABAUGH R.L. (1991) Biofilm development on leaf and wood surfaces in a boreal river. Freshwater Biology 25:437-450

GOOSEN N.K., VAN RIJSWIJK P. AND BROCKMANN U. (1995) Comparison of heterotrophic bacterial production rates in early spring in the turbid estuaries of the Scheldt and the Elbe. Hydrobiologia 311:31-42

GOOSEN N.K., VAN RIJSWIJK P., KROMKAMP J. AND PEENE J. (1997) Regulation of annual variation in heterotrophic bacterial production in the Schelde estuary (SW Netherlands). Aquatic Microbial Ecology 12:223-232

GOOSEN N.K., KROMKAMP J., PEENE J., VAN RIJSWIJK P. AND VAN BREUGEL P. (1999) Bacterial and phytoplankton production in the maximum turbidity zone of three European estuaries: the Elbe, Westerschelde and Gironde. Journal of Marine Systems 22:151-171

GRATTAN R.M. AND SUBERKROPP K. (2001) Effects of nutrient enrichment on yellow poplar leaf decomposition and fungal activity in streams. Journal of the North American Benthological Society 20(1):33-43

GREY J., JONES R.I. AND SLEEP D. (2001) Seasonal changes in the importance of the source of organic matter to the diet of zooplankton in Loch Ness, as indicated by stable isotope analysis. Limnology and Oceanography 46(3):505-513

HAMERLYNCK O., MEES J., CRAEYMEERSCH J.A., SOETAERT K., HOSTENS K., CATTRIJSSE A. AND VAN DAMME P.A. (1993) The Westerschelde estuary: two food webs and a nutrient rich desert. Progress in Belgian Oceanographic Research:217-234

HANSSON S., HOBBIE J.E., ELMGREN R., LARSSON U., FRY B. AND JOHANSSON S. (1997) The stable nitrogen isotope ratio as a marker of food-web interactions and fish migration. Ecology 78(7):2249-2257

HARVEY H.R., TUTTLE J.H. AND BELL J.T. (1995) Kinetics of phytoplankton decay during simulated sedimentation - Changes in biochemical-composition and microbial activity under oxic and anoxic conditions. Geochimica et Cosmochimica Acta 59(16):3367-3377

HAYES J.M. (1993) Factors controlling ^{13}C contents of sedimentary organic compounds: Principles and evidence. Marine Geology 113:111-125

HEIP C. AND HERMAN P.M.J. (1995) Major biological processes in European tidal estuaries - a synthesis of the JEEP-92 Project. Hydrobiologia 311:1-7

HEIP C.H.R., GOOSEN N.K., HERMAN P.M.J., KROMKAMP J., MIDDELBURG J.J. AND SOETAERT K. (1995) Production and consumption of biological particles in temperate tidal estuaries. In: Ansell A.D., Gibson R.N. and Barnes M. (eds) Oceanography and Marine Biology: an Annual Review 1995. UCL Press, pp 1-149

HELLINGS L., DEHAIRS F., TACKX M., KEPPENS E. AND BAEYENS W. (1999) Origin and fate of organic carbon in the freshwater part of the Scheldt estuary as traced by stable carbon isotope composition. Biogeochemistry 47(2):167-186

HELLINGS L. (2000) Origin and fate of dissolved inorganic and particulate organic carbon in a highly polluted estuary (The Scheldt) as traced by stable isotopes. Ph. D. Thesis, Vrije Universiteit Brussel, Belgium

HELLINGS L., DEHAIRS F., VAN DAMME S. AND BAEYENS W. (2001) Dissolved inorganic carbon in a highly polluted estuary (the Scheldt). Limnology and Oceanography 46:1406-1414

HERMAN P.M.J. AND HEIP C.H.R. (1999) Biogeochemistry of the MAximum TURbidity Zone of Estuaries (MATURE): some conclusions. Journal of Marine Systems 22:89-104

HESSLEIN R.H., CAPEL M.J., FOX D.E. AND HALLARD K.A. (1991) Stable isotopes of sulfur, carbon and, nitrogen as indicators of trophic level and fish migration in the Lower Mackenzie River Basin, Canada. Canadian Journal of Fisheries and Aquatic Sciences 48:2258-2265

HIEBER M. AND GESSNER M.O. (2002) Contribution of stream detrivores, fungi, and bacteria to leaf breakdown based on biomass estimates. Ecology 83(4):1026-1038

HINGA K.R., ARTHUR M.A., PILSON M.E.Q. AND WHITAKER D. (1994) Carbon isotope fractionation by marine phytoplankton in culture: the effects of CO_2 concentration, pH, temperature, and species. Global Biogeochemical Cycles 8:91-102

HOBSON K.A. AND CLARK R.G. (1992) Assessing avian diets using stable isotopes. 2. Factors influencing diet-tissue fractionation. Condor 94:189-197

HOBSON K.A., ALISAUSKAS R.T. AND CLARK R.G. (1993) Stable-nitrogen isotope enrichment in avian-tissues due to fasting and nutritional stress - Implications for isotopic analyses of diet. Condor 95:388-394

HOCH M.P., FOGEL M.L. AND KIRCHMAN D.L. (1992) Isotope fractionation associated with ammonium uptake by a marine bacterium. Limnology and Oceanography 37:1447-1459

HOCH M.P., FOGEL M.L. AND KIRCHMAN D.L. (1994) Isotope fractionation during ammonium uptake by marine microbial assemblages. Geomicrobiology Journal 12:113-127

HOCH M.P., SNYDER R.A., CIFUENTES L.A. AND COFFIN R.B. (1996) Stable isotope dynamics of nitrogen recycled during interactions among marine bacteria and protists. Marine Ecology Progress Series 132:229-239

HOPKINSON C.S. AND VALLINO J.J. (1995) The relationships among man's activities in watersheds and estuaries - A model of runoff effects on patterns of estuarine community metabolism. Estuaries 18(4):598-621

HORRIGAN S.G., MONTOYA J.P., NEVINS J.L. AND MCCARTHY J.J. (1990) Natural isotopic composition of dissolved inorganic nitrogen in the Chesapeake Bay. Estuarine, Coastal and Shelf Science 30:393-410

HOWARTH R.W., SCHNEIDER R. AND SWANEY D. (1996) Metabolism and organic carbon fluxes in the tidal freshwater Hudson River. Estuaries 19(4):848-865

HUGHES J.E., DEEGAN L.A., PETERSON B.J., HOLMES R.M. AND FRY B. (2000) Nitrogen flow through the food web in the oligohaline zone of a New England estuary. Ecology 81(2):433-452

HUMMEL H., MOERLAND G. AND BAKKER C. (1988) The concomitant existence of a typical coastal and a detritus food chain in the Westerschelde Estuary. Hydrobiological Bulletin 22:35-41

IGAMBERDIEV A.U., IVLEV A.A., BYKOVA N.V., THRELKELD C.N., LEA P.J. AND GARDESTROM P. (2001) Decarboxylation of glycine contributes to carbon isotope fractionation in photosynthetic organisms. Photosynthesis Research 67:177-184

IVLEV A.A., BYKOVA N.V. AND IGAMBERDIEV A.U. (1996) Fractionation of carbon ($^{13}C/^{12}C$) isotopes in glycine decarboxylase reaction. FEBS Letters 386:174-176

KARSH K.L., TRULL T.W., LOUREY A.J. AND SIGMAN D.M. (2003) Relationship of nitrogen isotope fractionation to phytoplankton size and iron availability during the Southern Ocean Iron RElease Experiment (SOIREE). Limnology and Oceanography 48:1058-1068

KEELEY J.E. AND SANDQUIST D.R. (1992) Carbon: freshwater plants. Plant, Cell and Environment 15:1021-1035

KEIL R.G. AND KIRCHMAN D.L. (1991) Contribution of dissolved free amino-acids and ammonium to the nitrogen requirements of heterotrophic bacterioplankton. Marine Ecology Progress Series 73:1-10

KLING G.W., FRY B. AND O'BRIEN W.J. (1992) Stable isotopes and planktonic trophic structure in arctic lakes. Ecology 73(2):561-566

KOSKI M., VIITASALO M. AND KUOSA H. (1999) Seasonal development of mesozooplankton biomass and production on the SW coast of Finland. Ophelia 50(2):69-91

KROMKAMP J., PEENE J., VAN RIJSWIJK P., SANDEE A. AND GOOSEN N. (1995) Nutrients, light and primary production by phytoplankton and microphytobenthos in the eutrophic, turbid Westerschelde estuary (The Netherlands). Hydrobiologia 311:9-19

KROOPNICK P. (1974) Correlations between ^{13}C and CO_2 in surface waters and atmospheric CO_2. Earth and Planetary Science Letters 22:397-403

KWAK T.J. AND ZEDLER J.B. (1997) Food web analysis of southern California coastal wetlands using multiple stable isotopes. Oecologia 110(2):262-277

LAWS E.A., BIDIGARE R.R. AND POPP B.N. (1997) Effect of growth rate and CO_2 concentration on carbon isotopic fractionation by the marine diatom *Phaeodactylum tricornutum*. Limnology and Oceanography 42:1552-1560

LEBOULANGER C., DESCOLAS-GROS C., FONTUGNE M.R., BENTALEB I. AND JUPIN H. (1995) Interspecific variability and environmental influence on particulate organic carbon $\delta^{13}C$ in cultured marine phytoplankton. Journal of Plankton Research 17:2079-2091

LEGGETT M.F., SERVOS M.R., HESSLEIN R., JOHANNSSON O., MILLARD E.S. AND DIXON D.G. (1999) Biogeochemical influences on the carbon isotope signatures of Lake Ontario biota. Canadian Journal of Fisheries and Aquatic Sciences 56(11):2211-2218

LEHMANN M.F., BERNASCONI S.M., BARBIERI A., AND MCKENZIE J.A. (2002) Preservation of organic matter and alteration of its carbon and nitrogen isotope composition during simulated and in situ early sedimentary diagenesis. Geochimica et Cosmochimica Acta 66:3573-3584

LEMAIRE E., ABRIL G., DE WIT R. AND ETCHEBER H. (2002) Distribution of phytoplankton pigments in nine European estuaries and implications for an estuarine typology. Biogeochemistry 59:5-23

LORENZEN C.J. (1967) Determination of chlorophyll and phaeopigments: spectrophotometric equations. Limnology and Oceanography 12:343-346

LOUREY M.J., TRULL T.W. AND SIGMAN D.M. (2003) Sensitivity of $\delta^{15}N$ of nitrate, surface suspended and deep sinking particulate nitrogen to seasonal nitrate depletion in the Southern Ocean. Global Biochemical Cycles 17(3) art. no. 1081, doi:10.1029/2002GB001973

MABERLY S.C. AND SPENCE D.H.N. (1983) Photosynthetic inorganic carbon use by freshwater plants. Journal of Ecology 71:705-724

MABERLY S.C., RAVEN J.A. AND JOHNSTON A.M. (1992) Discrimination between ^{12}C and ^{13}C by marine plants. Oecologia 91:481-492

MACKO S.A., FOGEL ESTEP M.L., ENGEL M.H. AND HARE P.E. (1986) Kinetic fractionation of stable nitrogen isotopes during amino acid transamination. Geochimica et Cosmochimica Acta 50:2143-2146

MACKO S.A., FOGEL M.L., HARE P.E. AND HOERING T.C. (1987) Isotopic fractionation of nitrogen and carbon in the synthesis of amino acids by microorganisms. Chemical Geology 65:79-92

MACLEOD N.A. AND BARTON D.R. (1998) Effects of light intensity, water velocity, and species composition on carbon and nitrogen stable isotope ratios in periphyton. Canadian Journal of Fisheries and Aquatic Sciences 55:1919-1925

MAECKELBERGHE H. (1997) De kwaliteit van de Schelde in 1994. Water 94:107-112

MAES J., TAILLIEU A., VAN DAMME P.A., COTTENIE K. AND OLLEVIER F. (1998a) Seasonal patterns in the fish and crustacean community of a turbid temperate estuary (Zeeschelde Estuary, Belgium). Estuarine, Coastal and Shelf Science 47:143-151

MAES J., VAN DAMME P.A., TAILLIEU A. AND OLLEVIER F. (1998b) Fish communities along an oxygen-poor salinity gradient (Zeeschelde Estuary, Belgium). Journal of Fish Biology 52:534-546

MAES J., DE BRABANDERE L., OLLEVIER F. AND MEES J. (2003) The diet and consumption of dominant fish species in the upper Scheldt estuary, Belgium. Journal of the Marine Biological Association of the United Kingdom 83:603-612

MARGUILLIER S. (1998) Stable isotope ratios and food web structure of aquatic ecosystems. Ph. D. Thesis, Vrije Universiteit Brussel, Belgium

MARIOTTI A., GERMON J.C., HUBERT P., KAISER P., LETOLLE R., TARDIEUX A. AND TARDIEUX P. (1981) Experimental determination of nitrogen kinetic isotope fractionation: some principles; illustration for the denitrification and nitrification processes. Plant and Soil 62:413-430

MARIOTTI A. (1983) Atmospheric nitrogen is a reliable standard for natural ^{15}N abundance measurements. Nature 303:685-687

MARIOTTI A., LANCELOT C. AND BILLEN G. (1984) Natural isotopic composition of nitrogen as a tracer of origin for suspended matter in the Scheldt estuary. Geochimica et Cosmochimica Acta 48:549-555

MARTINEAU C., VINCENT W.F., FRENETTE J.J. AND DODSON J.J. (2004) Primary consumers and particulate organic matter: Isotopic evidence of strong selectivity in the estuarine transition zone. Limnology and Oceanography 49(5):1679-1686

MARTINOTTI W., CAMUSSO M., GUZZI L., PATROLECCO L. AND PETTINE M. (1997) C, N and their stable isotopes in suspended and sedimented matter from the Po estuary (Italy). Water Air and Soil Pollution 99:325-332

MASSART D.L., VANDEGINSTE B.G.M., BUYDENS L.M.C., DE JONG S., LEWI P.J. AND SMEYERS-VERBEKE J. (1997) Handbook of Chemometrics and Qualimetrics: Part A. Data Handling in Science and Technology 20A. Elsevier

MCCARTHY I.D. AND WALDRON S. (2000) Identifying migratory *Salmo trutta* using carbon and nitrogen stable isotope ratios. Rapid Communications in Mass Spectrometry 14(15):1325-1331

MCCLELLAND J.W., HOLL C.M. AND MONTOYA J.P. (2003) Relating low $\delta^{15}N$ values of zooplankton to N_2-fixation in the tropical North Atlantic: insights provided by stable isotope ratios of amino acids. Deep-Sea Research Part I-Oceanographic Research Papers 50(7):849-861

MIDDELBURG J.J. AND NIEUWENHUIZE J. (1998) Carbon and nitrogen stable isotopes in suspended matter and sediments from the Scheldt estuary. Marine Chemistry 60:217-225

MIDDELBURG J.J. AND NIEUWENHUIZE J. (2000) Uptake of dissolved inorganic nitrogen in turbid, tidal estuaries. Marine Ecology Progress Series 192:79-88

MIDDELBURG J.J. AND NIEUWENHUIZE J. (2001) Nitrogen isotope tracing of dissolved inorganic nitrogen behaviour in tidal estuaries. Estuarine, Coastal and Shelf Science 53(3):385-391

MINAGAWA M. AND WADA E. (1984) Stepwise enrichment of ^{15}N along food chains: Further evidence and the relation between $\delta^{15}N$ and animal age. Geochimica et Cosmochimica Acta 48:1135-1140

MIYAJIMA T., YAMADA Y., HANBA Y.T., YOSHII K., KOITABASHI T. AND WADA E. (1995) Determining the stable-isotope ratio of total dissolved inorganic carbon in lake water by GC/C/IRMS. Limnology and Oceanography 40:994-1000

MONTOYA J.P., HORRIGAN S.G. AND MCCARTHY J.J. (1990) Natural abundance of ^{15}N in particulate nitrogen and zooplankton in the Chesapeake Bay. Marine Ecology Progress Series 65:35-61

MONTOYA J.P., HORRIGAN S.G. AND MCCARTHY J.J. (1991) Rapid, storm-induced changes in the natural abundance of ^{15}N in a planktonic ecosystem, Chesapeake Bay, USA. Geochimica et Cosmochimica Acta 55:3627-3638

MONTOYA J.P., WIEBE P.H. AND MCCARTHY J.J. (1992) Natural abundance of ^{15}N in particulate nitrogen and zooplankton in the Gulf Stream region and warm-core ring 86A. Deep-Sea Research 39(suppl.1): S363-S392

MONTOYA J.P. AND MCCARTHY J.J. (1995) Isotopic fractionation during nitrate uptake by phytoplankton grown in continuous culture. Journal of Plankton Research 17:439-464

MUYLAERT K., VAN KERCKVOORDE A., VYVERMAN W. AND SABBE K. (1997) Structural characteristics of phytoplankton assemblages in tidal and non-tidal freshwater systems: a case study from the Schelde basin, Belgium. Freshwater Biology 38:263-276

MUYLAERT K. (1999) Distribution and dynamics of protist communities in a freshwater tidal estuary. Ph. D. Thesis, Universiteit Gent, Belgium

MUYLAERT K. AND SABBE K. (1999) Spring phytoplankton assemblages in and around the maximum turbidity zone of the estuaries of the Elbe (Germany), the Schelde (Belgium/The Netherlands) and the Gironde (France). Journal of Marine Systems 22:133-149

MUYLAERT K., SABBE K. AND VYVERMAN W. (2000a) Spatial and temporal dynamics of phytoplankton communities in a freshwater tidal estuary (Schelde, Belgium). Estuarine, Coastal and Shelf Science 50:673-687

MUYLAERT K., VAN MIEGHEM R., SABBE K., TACKX M. AND VYVERMAN W. (2000b) Dynamics and trophic roles of heterotrophic protists in the plankton of a freshwater tidal estuary. Hydrobiologia 432:25-36

MUYLAERT K., VAN WICHELEN J., SABBE K. AND VYVERMAN W. (2001) Effects of freshets on phytoplankton dynamics in a freshwater tidal estuary (Schelde, Belgium). Archiv fur Hydrobiologie 150:269-288

NEEDOBA J.A., WASER N.A., HARRISON P.J. AND CALVERT S.E. (2003) Nitrogen isotope fractionation in 12 species of marine phytoplankton during growth on nitrate. Marine Ecology Progress Series 255:81-91

NIEUWENHUIZE J., MAAS Y.E.M AND MIDDELBURG J.J. (1994) Rapid analysis of organic carbon and nitrogen in particulate materials. Marine Chemistry 45:217-224

O'LEARY M.H. (1981) Carbon isotope fractionation in plants. Biogeochemistry 20:553-567

O'LEARY M.H., MADHAVAN S. AND PANETH P. (1992) Physical and chemical basis of carbon isotope fractionation in plants. Plant, Cell and Environment 15:1099-1104

OSMOND C.B., VALAANE N., HASLAM S.M., UOTILA P. AND ROKSANDIC Z. (1981) Comparisons of $\delta^{13}C$ values in leaves of aquatic macrophytes from different habitats in Britain and Finland, some implications for photosynthetic processes in aquatic plants. Oecologia 50:117-124

OWENS N.J.P. (1985) Variations in the natural abundance of ^{15}N in estuarine suspended particulate matter: a specific indicator of biological processing. Estuarine, Coastal and Shelf Science 20:505-510

OWENS N.J.P. (1987) Natural variations in ^{15}N in the marine environment Advances in Marine Biology. Academic Press, Inc, Ltd., London, pp 389-451

PAGE H.M. AND LASTRA M. (2003) Diet of intertidal bivalves in the Ria de Arosa (NW Spain): evidence from stable C and N isotope analysis. Marine Biology 143(3):519-532

PEL R., HOOGVELD H. AND FLORIS V. (2003) Using the hidden isotopic heterogeneity in phyto- and zooplankton to unmask disparity in trophic carbon transfer. Limnology and Oceanography 48(6):2200-2207

PELZ O., CIFUENTES L.A., HAMMER B.T., KELLEY C.A. AND COFFIN R.B. (1998) Tracing the assimilation of organic compounds using delta ^{13}C analysis of unique amino acids in the bacterial peptidoglycan cell wall. Fems Microbiology Ecology 25(3):229-240

PENNOCK J.R., VELINSKY D.J., LUDLAM J.M., SHARP J.H. AND FOGEL M.L. (1996) Isotopic fractionation of ammonium and nitrate during uptake by *Skeletonema costatum*: Implications for $\delta^{15}N$ dynamics under bloom conditions. Limnology and Oceanography 41(3):451-459

PETERSON B.J. AND FRY B. (1987) Stable isotopes in ecosystem studies. Annual Review of Ecology and Systematics 18:293-320

PHILLIPS D.L. AND KOCH P.L. (2002) Incorporating concentration dependence in stable isotope mixing models. Oecologia 130:114-125

PONSARD S. AND AVERBUCH P. (1999) Should growing and adult animals fed on the same diet show different $\delta^{15}N$ values? Rapid Communications in Mass Spectrometry 13:1305-1310

POST D.M. (2002) Using stable isotopes to estimate trophic position: Models, methods, and assumptions. Ecology 83(3):703-718

RAU G.H., MEARNS A.J., YOUNG D.R., OLSON R.J., SCHAFER H.A. AND KAPLAN I.R. (1983) Animal $^{13}C/^{12}C$ correlates with trophic level in pelagic food webs. Ecology 64:1314-1318

RAU G.H., RIEBESELL U. AND WOLF-GLADROW D. (1996) A model of photosynthetic ^{13}C fractionation by marine phytoplankton based on diffusive molecular CO_2 uptake. Marine Ecology Progress Series 133:275-285

RAU G.H., RIEBESELL U. AND WOLF-GLADROW D. (1997) $CO_{2(aq)}$-dependent photosynthetic ^{13}C fractionation in the ocean: A model versus measurements. Global Biogeochemical Cycles 11:267-278

REGNIER P., WOLLAST R. AND STEEFEL C.I. (1997) Long-term fluxes of reactive species in macrotidal estuaries: Estimates from a fully transient, multicomponent reaction-transport model. Marine Chemistry 58:127-145

REGNIER P., MOUCHET A., WOLLAST R. AND RONDAY F. (1998) A discussion of methods for estimating residual fluxes in strong tidal estuaries. Continental Shelf Research 18:1543-1571

REGNIER P. AND STEEFEL C.I. (1999) A high resolution of the inorganic nitrogen flux from the Scheldt estuary to the coastal North Sea during a nitrogen-limited algal bloom, spring 1995. Geochimica et Cosmochimica Acta 63(9):1359-1374

REINFELDER J.R., KRAEPIEL A.M.L. AND MOREL F.M.M. (2000) Unicellular C_4 photosynthesis in a marine diatom. Nature 407:996-999

RIEBESELL U. AND WOLF-GLADROW D. (1995) Growth limits on phytoplankton. Nature 373:28

RIEBESELL U., BURKHARDT S., DAUELSBERG A. AND KROON B. (2000) Carbon isotope fractionation by a marine diatom: dependence on the growth-rate-limiting resource. Marine Ecology Progress Series 193:295-303

RIEBESELL U. (2000) Photosynthesis - Carbon fix for a diatom. Nature 407:959-960

RIERA P. AND RICHARD P. (1997) Temporal variation of the $\delta^{13}C$ in particulate organic matter and oyster *Crassostrea gigas* in Marennes-Oléron Bay (France): effect of freshwater inflow. Marine Ecology Progress Series 147:105-115

RIU J. AND RIUS F.X. (1996) Assessing the accuracy of analytical methods using linear regression with errors in both axes. Analytical Chemistry 68:1851-1857

ROESKE C.A. AND O'LEARY M.H. (1984) Carbon isotope effects on the enzyme-catalyzed carboxylation of ribulose biphosphate. Biochemistry 23:6275-6284

ROLLWAGEN BOLLENS G.C. AND PENRY D.L. (2003) Feeding dynamics of *Acartia* spp. copepods in a large, temperate estuary (San Francisco Bay, CA). Marine Ecology Progress Series 257:139-158

ROUNICK J.S. AND WINTERBOURN M.J. (1986) Stable carbon isotopes and carbon flow in ecosystems. Bioscience 36:171-177

SANZONE D.M., TANK J.L., MEYER J.L., MULHOLLAND P.J. AND FINDLAY S.E.G. (2001) Microbial incorporation of nitrogen in stream detritus. Hydrobiologia 464:27-35

SAVOYE N., AMINOT A., TREGUER P., FONTUGNE M., NAULET N. AND KEROUEL R. (2003) Dynamics of particulate organic matter $\delta^{15}N$ and $\delta^{13}C$ during spring phytoplankton blooms in a macrotidal ecosystem (Bay of Seine, France). Marine Ecology Progress Series 255:27-41

SCHMIDT H.L. (1999) Isotope discriminations upon biosynthesis in natural systems: General causes and individual factors of the different bioelements. Isotopes in Environmental and Health Studies 35:11-18

SHARKEY T.D. AND BERRY J.A. (1985) Carbon isotope fractionation of algae as influenced by an inducible CO_2 concentrating mechanism. In: Lucas W.J. and Berry J.A. (eds) Inorganic carbon uptake by aquatic photosynthetic organisms pp .389-401

SILFER J.A., ENGEL M.H. AND MACKO S.A. (1992) Kinetic fractionation of stable carbon and nitrogen isotopes during peptide-bond hydrolysis - Experimental-evidence and geochemical implications. Chemical Geology(3-4):211-221

SIMON M., GROSSART H.P., SCHWEITZER B. AND PLOUG H. (2002) Microbial ecology of organic aggregates in aquatic ecosystems. Aquatic Microbial Ecology 28:175-211

SMITH R.L., HOWES B.L. AND DUFF J.H. (1991) Denitrification in nitrate-contaminate groundwater: Occurrence in steep vertical geochemical gradients. Geochimica et Cosmochimica Acta 55:1815-1825

SOETAERT K. AND VAN RIJSWIJK P. (1993) Spatial and temporal patterns of the zooplankton in the Westerschelde estuary. Marine Ecology Progress Series 97:47-59

SOETAERT K., HERMAN P.M.J. AND KROMKAMP J. (1994) Living in the twilight - estimating net phytoplankton growth in the Westerschelde Estuary (The Netherlands) by means of an ecosystem model (MOSES). Journal of Plankton Research 16:1277-1301

SOETAERT K. AND HERMAN P.M.J. (1994) One foot in the grave - Zooplankton drift into the Westerschelde Estuary (The Netherlands). Marine Ecology Progress Series 105:19-29

SOETAERT K. AND HERMAN P.M.J. (1995a) Estimating estuarine residence times in the Westerschelde (The Netherlands) using a box model with fixed dispersion coefficients. Hydrobiologia 311:215-224

SOETAERT K. AND HERMAN P.M.J. (1995b) Carbon flows in the Westerschelde estuary (The Netherlands) evaluated by means of an ecosystem model (MOSES). Hydrobiologia 311:247-266

SOETAERT K. AND HERMAN P.M.J. (1995c) Nitrogen dynamics in the Westerschelde estuary (SW Netherlands) estimated by means of the ecosystem model MOSES. Hydrobiologia 311:225-246

STEPHENSON R.L. AND LYON G.L. (1982) ^{13}C depletion in an estuarine bivalve - Detection of marine and terrestrial food sources. Oecologia 55(1):110-113

SUBERKROPP K. AND CHAUVET E. (1995) Regulation of leaf breakdown by fungi in streams - influences of water chemistry. Ecology 76:1433-1445

SUBERKROPP K. (1998) Effect of dissolved nutrients on two aquatic hyphomycetes growing on leaf litter. Mycological Research 102:998-1002

TACKX M., IRIGOIEN X., DARO N., CASTEL J., ZHU L., ZHANG X. AND NIJS J. (1995) Copepod feeding in the Westerschelde and the Gironde. Hydrobiologia 311:71-83

TACKX M.L.M., HERMAN P.J.M., GASPARINI S., IRIGOIEN X., BILLIONES R. AND DARO M.H. (2003) Selective feeding of *Eurytemora affinis* (Copepoda, Calanoida) in temperate estuaries: model and field observations. Estuarine Coastal and Shelf Science 56:305-311

TACKX M.L.M., DE PAUW N., VAN MIEGHEM R., AZEMAR F., HANNOUTI A., VAN DAMME S., FIERS F., DARO N. AND MEIRE P. (2004) Zooplankton in the Schelde estuary, Belgium and the Netherlands. Spatial and temporal patterns. Journal of Plankton Research 26(2):133-141

TACKX M., AZEMAR F., BOULÊTREAU S., DE PAUW N., BAKKER K., SAUTOUR B., GASPARINI S., SOETAERT K., VAN DAMME S. AND MEIRE P. Zooplankton in the Schelde estuary, Belgium and the Netherlands. Long term trends in spring populations. Hydrobiologia (in press)

TAVERNIERS E. (1999) Zeescheldebekken: de afvoer van de Schelde in 1999. Report AMS-01/02. Ministerie van de Vlaamse Gemeenschap, Departement Leefmilieu en Infrastructuur, Afdeling Maritieme Schelde, Antwerp, Belgium

TAVERNIERS E. (2000). Zeescheldebekken: de afvoer van de Schelde in 2000. Report AMS-01/02. Ministerie van de Vlaamse Gemeenschap, Departement Leefmilieu en Infrastructuur, Afdeling Maritieme Schelde, Antwerp, Belgium

TAVERNIERS E. (2001) Zeescheldebekken: de afvoer van de Schelde in 2001. Report AMS-01/02. Ministerie van de Vlaamse Gemeenschap, Departement Leefmilieu en Infrastructuur, Afdeling Maritieme Schelde, Antwerp, Belgium

TAVERNIERS E. (2002) Zeescheldebekken: de afvoer van de Schelde in 2002. Report AMS-01/02. Ministerie van de Vlaamse Gemeenschap, Departement Leefmilieu en Infrastructuur, Afdeling Maritieme Schelde, Antwerp, Belgium

TAVERNIERS E. (2003) Zeescheldebekken: de afvoer van de Schelde in 2003. Report AMS-01/02. Ministerie van de Vlaamse Gemeenschap, Departement Leefmilieu en Infrastructuur, Afdeling Maritieme Schelde, Antwerp, Belgium

THORNTON S.F. AND MCMANUS J. (1994) Application of organic-carbon and nitrogen stable-isotope and C/N ratios as source indicators of organic-matter provenance in estuarine systems - evidence from the Tay Estuary, Scotland. Estuarine, Coastal and Shelf Science 38:219-233

THORP J.H. AND DELONG A.D. (2002) Dominance of autochthonous autotrophic carbon in food webs of heterotrophic rivers. Oikos 96(3):543-550

TURPIN D.H., VANLERBERGHE G.C., AMORY A.M. AND GUY R.D. (1991) The inorganic carbon requirements for nitrogen assimilation. Canadian Journal of Botany 69:1139-1145

VAN DAMME S., YSEBAERT T., MEIRE P. AND VAN DEN BERGH E. (1999) Habitatstructuren, waterkwaliteit en leefgemeenschappen in het Schelde Estuarium. Rapport IN99/24

VAN DE GRAAF A.A., MULDER A., DEBRUIJN P., JETTEN M.S.M., ROBERTSON L.A. AND KUENEN J.G. (1995) Anaerobic oxidation of ammonium is a biologically mediated process. Applied and Environmental Microbiology 61:1246-1251

Van den Meersche K., Middelburg J.J., Soetaert K., van Rijswijk P., Boschker H.T.S. and Help C.H.R. (2004) Carbon-nitrogen coupling and algal-bacterial interactions during an experimental bloom: Modeling a ^{13}C tracer experiment. Limnology and Oceanography 49(3):862-878

VAN SPAENDONK J.C.M., KROMKAMP J.C. AND DEVISSCHER P.R.M. (1993) Primary production of phytoplankton in a turbid coastal-plain estuary, the Westerschelde (The Netherlands). Netherlands Journal of Sea Research 31:267-279

VANDER ZANDEN M.J. AND RASMUSSEN J.B. (2001) Variation in $\delta^{15}N$ and $\delta^{13}C$ trophic fractionation: Implications for aquatic food web studies. Limnology and Oceanography 46:2061-2066

VANDERBORGHT J.P., WOLLAST R., LOIJENS M. AND REGNIER P. (2002) Application of a transport-reaction model to the estimation of biogas fluxes in the Scheldt estuary. Biogeochemistry 59:207-237

VELINSKY D.J., PENNOCK J.R., SHARP J.H., CIFUENTES L.A. AND FOGEL M.L. (1989) Determination of the isotopic composition of ammonium nitrogen at the natural abundance level from estuarine waters. Marine Chemistry 26(4):351-361

VELINSKY D.J., FOGEL M.L., TODD J.F. AND TEBO B.M. (1991) Isotopic fractionation of dissolved ammonium at the oxygen-hydrogen sulfide interface in anoxic waters. Geophysical Research Letters 18:649-652

VERLAAN P.A.J., DONZE M. AND KUIK P. (1998) Marine vs fluvial suspended matter in the Scheldt Estuary. Estuarine, Coastal and Shelf Science 46:873-883

VERLAAN P.A.J. (2000) Marine vs fluvial bottom mud in the Scheldt Estuary. Estuarine, Coastal and Shelf Science 50:627-638

VERLINDEN N. (2002) Stikstofdynamiek en nitrificatie in het estuarium van de Schelde. Master thesis, Vrije Universiteit Brussel, Belgium

VIZZINI S. AND MAZZOLA A. (2003) Seasonal variations in the stable carbon and nitrogen isotope ratios ($^{13}C/^{12}C$ and $^{15}N/^{14}N$) of primary producers and consumers in a western Mediterranean coastal lagoon. Marine Biology 142(5):1009-1018

WADA E. AND HATTORI A. (1978) Nitrogen isotope effects in the assimilation of inorganic nitrogenous compounds by marine diatoms. Geomicrobiology 1:85-101

WADA E. (1980) Nitrogen isotope fractionation and its significance in biogeochemical processes occurring in marine environments. In: Goldberg E.D., Horibe Y., Saruhashi K. (eds) Isotope Marine Chemistry. Uchida Rokakuho Publishing Co Ltd., Tokyo, pp 375-398

WASER N.A.D., HARRISON P.J., NIELSEN B. AND CALVERT S.E. (1998) Nitrogen isotope fractionation during uptake and assimilation of nitrate, nitrite, ammonium, and urea by a marine diatom. Limnology and Oceanography 43:215-224

WERNER R.A. AND SCHMIDT H.L. (2002) The in vivo nitrogen isotope discrimination among organic plant compounds. Phytochemistry 61:465-484

WOLLAST R. (1973) Origine et mecanisme de l'envasement de l'estuaire de l'Escaut. Rapport de synthèse

WOLLAST R. (1982) Behaviour of organic carbon, nitrogen and phosphorus in the Scheldt estuary. Thalassia Jugoslavica 18:11-34

WONG W.W. AND SACKETT W.M. (1978) Fractionation of stable carbon isotopes by marine phytoplankton. Geochimica et Cosmochimica Acta 42:1809-1815

WU J.P., CALVERT S.E. AND WONG C.S. (1997) Nitrogen isotope variations in the subarctic northeast Pacific: Relationships to nitrate utilization and trophic structure. Deep-Sea Research Part I-Oceanographic Research Papers 44(2):287-314

YONEYAMA T., OMATA T., NAKATA S. AND YAZAKI J. (1991) Fractionation of nitrogen isotopes during the uptake and assimilation of ammonia by plants. Plant and Cell Physiology 32:1211-1217

YONEYAMA T., KAMACHI K., YAMAYA T. AND MAE T. (1993) Fractionation of nitrogen isotopes by glutamine-synthetase isolated from spinach leaves. Plant and Cell Physiology 34:489-491

YONEYAMA T. AND TANAKA F. (1999) Natural abundance of ^{15}N in nitrate, ureides, and amino acids from plant tissues. Soil Science and Plant Nutrition 45:751-755

YONEYAMA T., MATSUMARU T., USUI K. AND ENGELAAR W.M.H.G. (2001) Discrimination of nitrogen isotopes during absorption of ammonium and nitrate at different nitrogen concentrations by rice (*Oryza sativa* L.) plants. Plant Cell and Environment 24:133-139

YOSHIDA N., HAJIME M., MITSUHIRO H., ISAO K., SADAO M., EITARO W., TOSHIRO S. AND AKIHIKO H. (1989) Nitrification rates and ^{15}N abundances of NO_2 and NO_3^- in the western North Pacific. Nature 342:895-897

ZEEBE R.E., WOLF-GLADROW D.A. AND JANSEN H. (1999) On the time required to establish chemical and isotopic equilibrium in the carbon dioxide system in seawater. Marine Chemistry 65:135-153

ZIEMAN J.C., MACKO S.A. AND MILLS A.L. (1984) Role of seagrasses and mangroves in estuarine food webs: temporal and spatial changes in stable isotope composition and amino acid content during decomposition. Bulletin of Marine Science 35(3):380-3920